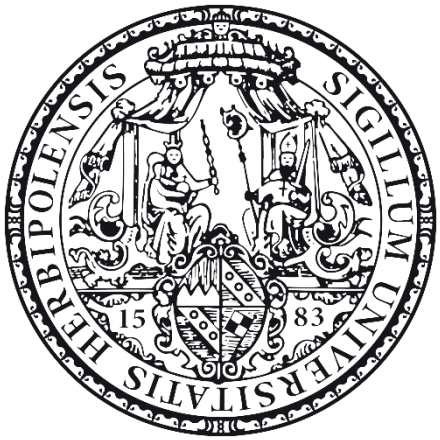

The influence of N-terminal peptides of G-protein coupled receptor kinase (GRK) 2, 3 and 5 on β-adrenergic signaling

Der Einfluss von N-terminalen Peptiden der G-Protein gekoppelten Rezeptorkinasen (GRK) 2, 3 und 5 in der β-adrenergen Signaltransduktion

Doctoral thesis for a doctoral degree

at the Graduate School of Life Sciences,

Julius-Maximilians-Universität Würzburg,

Section Biomedicine

submitted by

Theopisti Maimari

from

Lemesos, Cyprus

Würzburg 2019

Submitted on: ……..

Office stamp

Members of the *Promotionskomitee*:

Chairperson: Prof. Dr. Manfred Gessler

Primary Supervisor: Prof. Dr. Kristina Lorenz

Supervisor (Second): Prof. Dr. Andreas Schlosser

Supervisor (Third): Prof. Dr. Karoline Kisker

Date of Public Defence: ……

Date of Receipt of Certificates: ……..

Affidavit

I hereby confirm that my thesis entitled *'The influence of N-terminal peptides of G-protein coupled receptor kinase (GRK) 2, 3 and 5 on β-adrenergic signaling'* is the result of my own work. I did not receive any help or support from commercial consultants. All sources and / or materials applied are listed and specified in the thesis.

Furthermore, I confirm that this thesis has not yet been submitted as part of another examination process neither in identical nor in similar form.

Place, Date Signature

Eidesstattliche Erklärung

Hiermit erkläre ich an Eides statt, die Dissertation ‚*Der Einfluss von N-terminalen Peptiden der G-Protein gekoppelten Rezeptorkinasen (GRK) 2, 3 und 5 in der β-adrenergen Signaltransduktion'* eigenständig, d.h. insbesondere selbständig und ohne Hilfe eines kommerziellen Promotionsberaters, angefertigt und keine anderen als die von mir angegebenen Quellen und Hilfsmittel verwendet zu haben.

Ich erkläre außerdem, dass die Dissertation weder in gleicher noch in ähnlicher Form bereits in einem anderen Prüfungsverfahren vorgelegen hat.

Ort, Datum Unterschrift

Contents

List of figures:

I. Introduction

1. G-Protein Coupled Receptors

G-Protein Coupled Receptors (GPCR) are members of a family of membrane proteins which are encoded by more than 800 genes in the human genome[1]. They are integral proteins characterized by an extracellular N-terminus, an intracellular C-terminus and seven transmembrane α-helices connected by three intracellular and three extracellular loops[2]. GPCRs are widely classified using the A-F system which identifies six classes (A-F) mainly based on their functional similarities and on their amino acid sequences[3]. Class A is known as the 'rhodopsin-like family', class B is also called the 'secretin receptor family', class C consists of the GABA receptors, taste receptors, calcium-sensing receptors and the metabotropic glutamate family. To class D belong the fungal mating pheromone receptors, to class E the cAMP receptors and class F consists of frizzled/smoothened receptors[2–4]. The GPCR family includes receptors that can selectively mediate cellular responses to hormones, chemokines, neurotransmitters and calcium ions as well as sensory receptors for taste, photons and odorants. In humans, they are the largest family of cell surface receptor[5–9]. GPCRs are involved in the regulation of several physiological processes including growth, differentiation, proliferation and death. This renders GPCRs one of the most important targets for therapeutic drug development; 60% of all drugs in clinical use, target GPCRs[10] either by hampering ligand access to the receptor, by mimicking endogenous ligands or by altering ligand production. The majority (94%) of FDA approved drugs target class A – rhodopsin like receptors[11].

1.1 Regulation of GPCRs

Ligand binding to GPCRs induces G-Protein signaling through certain effector proteins and desensitization is introduced by phosphorylation of activated receptors by G-protein coupled receptor kinases (GRKs) and by subsequent binding of arrestin. This event cascade constitutes the classical model of GPCR regulation and is interpreted as a two-state model: GPCRs exist in two distinct conformations, active and inactive. However, the rapid development of innovative methods with increased power and resolution enabled the identification of multiple conformations which indicates the dynamic behavior of GPCRs [12–14].

1.1.1 G-proteins

As the name indicates, GPCR signaling is initiated by the activation of heterotrimeric G-proteins. They consist of three subunits: *alpha* (α), *beta* (β) and *gamma* (γ); eighteen Gα, five Gβ and twelve Gγ

proteins have been cloned [15–17]. The Gα subunit is composed of a helical domain and a GTPase domain which serves guanosine triphosphate (GTP) and guanosine diphosphate (GDP) binding and GTP hydrolysis[18]. In the inactive state, the Gα subunit is bound to GDP and in a complex with Gβγ. The Gβ and γ subunit build a heterodimer, a tightly associated complex[19], which can only be dissociated under denaturing conditions[20]. Two regions of Gαβγ, the C- terminal region of Gα and the C-terminal region of Gγ[21] play a role in the interaction with the receptor. Moreover, the Gα N-terminal domain is involved in the interaction with the Gβγ subunit[18,22,23]. Lipid modifications, which act as membrane anchors regulate Gα and Gγ subcellular localization. Covalent modification of Gα subunits at the N-terminus via attachment of the lipids palmitate and/or myristate and prenylation at the C-terminus of Gγ contribute to membrane association of the respective G-protein subunit[24].

Coupling to the receptor as well as coupling to effector proteins is defined by four main families of Gα subunits: Gi/Go, Gq, Gs, and G12. Gi proteins inhibit adenylyl cyclase, open K^+ channels and close Ca^{2+} channels, whereas Gs couples to activate adenylyl cyclase, which leads to increased cAMP production; Gq proteins couple to phospholipase Cβ; G12 proteins couple the Rho family of GTPases[16,19,25]. The M1 muscarinic acetylcholine receptor (M_1AChR) and the platelet-activating factor receptor (PAFR), which both belong to the GPCR family, mediate via the $G\alpha_o$ subunit the activation of the MAPK signaling[26].

The Gβγ subunit complex is also involved in various signaling pathways such as in the activation of muscarinic K^+ channels[27], induction of voltage-dependent modulation of N-type calcium channels[28] and the activation of phospholipase C[29] (Figure 1). Furthermore, the interaction of Gβγ with G-protein coupled receptor kinases (GRK) i.e. GRK2 and GRK3, leads to the translocation of this class of GRKs to the plasma membrane[30] enabling them to phosphorylate and therefore desensitize the receptors.

1.1.2 Receptor activation

Agonist binding and subsequent receptor activation, exert conformational changes of the receptor involving rearrangements of transmembrane segments 3 and 6, which leads to the formation of a transient high affinity complex, consisting of the activated receptor, the agonist and the heterotrimeric G protein[12,31,32]. GDP bound G-protein heterotrimer is inactive. The activated receptor acts as a guanine nucleotide exchange factor (GEF) causing GDP dissociation and the association of GTP with the Gα subunit. This destabilizes the G-protein complex and leads to the dissociation of α and βγ subunits, which both signal through several effectors that generate second messengers (Fig.1)[19,33,34].

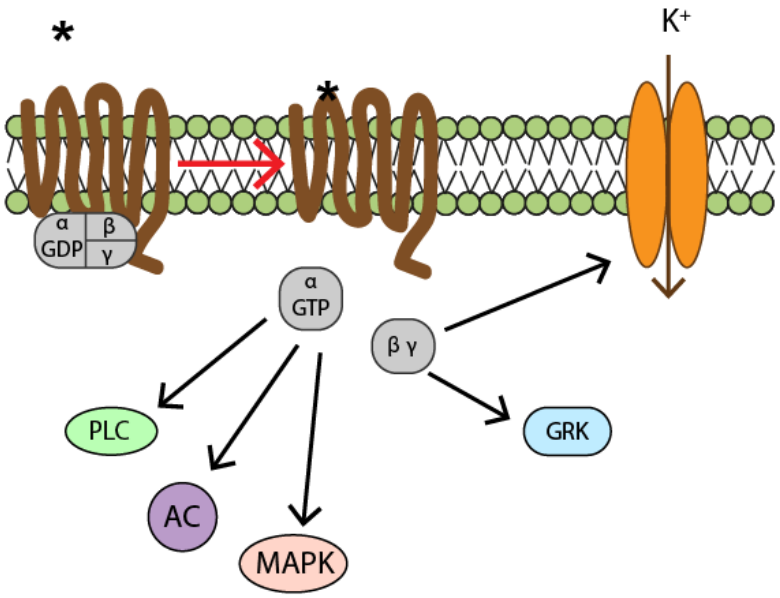

Figure 1: G-protein signaling upon receptor activation. Agonist binding (asterisk*) to the receptor leads to receptor activation and G-protein dissociation into α and βγ subunits. Both the α subunits and βγ subunits can signal through further proteins such as phospholipase C (PLC), adenylate cyclase (AC), mitogen-activated protein kinase (MAPK) and G-protein coupled receptor kinase (GRK) or certain ion channels such e.g. the potassium channel GIRK (G-protein coupled inwardly rectifying K^+).

In an effort to decipher the structural basis or GPCR activation, *Rasmussen et al.* revealed the crystal structure of the ternary complex consisting of the ligand-bound β_2 adrenergic receptor (β_2-AR) and the nucleotide free Gs protein heterotrimer[35]. A subsequent study showed that nucleotide exchange is catalyzed by GPCR structural changes, which cause destabilization of the GDP-bound state. When GDP is then released, an empty nucleotide-binding pocket (nucleotide free structure) occurs[36]. In a more recent study, hydrogen/deuterium exchange mass spectrometry (HDX-MS) and hydroxyl radical mediated protein footprinting mass spectrometry (HRF-MS) were used in a time resolved manner to investigate the formation of the GPCR-G protein complex and G-protein activation. As model GPCRs, the β_2 adrenergic receptor and the A_{2A} were used, and as model heterotrimeric G-protein the $G\alpha s\beta_1\gamma_2$. Conformational changes at the end of the α5 helix C-terminus, in the proximal α5 helix and the β3 strand of Gs were observed. These changes would facilitate GDP release by altering the GDP-binding pocket. This study also proposed that the conformation of the first β_2-AR-Gs complex they observed differs from the crystal structure of the nucleotide-free β_2-AR-Gs reported by *Rasmussen et al.*[35], suggesting the existence of intermediate transient states prior to the formation of the nucleotide-free β_2-AR-Gs complex[37]. At about the same time, the crystal structure of the complex of β_2-AR with the C- terminus of Gs was revealed and validated the existence of the intermediate state, suggested previously[38].

1.2 Desensitization of G-protein coupled receptors

Desensitization is the process by which GPCRs are regulated and lose their ability to respond to stimuli[39]. There are two mechanisms of GPCR desensitization, homologous (agonist-dependent) and heterologous (agonist–independent). Homologous desensitization occurs when the receptor response to a specific agonist at high concentration is decreased. Alternatively, GPCR desensitization may be engendered by heterologous desensitization, a process in which GPCRs are phosphorylated by second-messenger-dependent kinases such as protein kinase A or protein kinase C, regardless of whether they are activated or not[25,40,41]. GPCR desensitization involves a combination of events: receptor phosphorylation, which leads to uncoupling of the receptor from its G-protein, the internalization of plasma membrane receptors, and their downregulation; is mediated by three protein families: GRKs, arrestins and second-messenger-dependent protein kinases [42,43].

Phosphorylation is achieved rapidly, within seconds to minutes, after agonist stimulation by two classes of serine/threonine (Ser/Thr) protein kinases: the G-protein-coupled receptor kinases (GRKs) and the second messenger activated protein kinases, protein kinase A (PKA) and protein kinase C (PKC)[44]. Both classes of protein kinases can contribute to homologous desensitization depending on agonist concentration, cell type and the type of GPCR under investigation[45].

GRK-mediated receptor phosphorylation is a well-characterized mechanism for GPCR desensitization. Upon agonist binding, conformational changes are triggered which serve to unmask phosphorylation sites[46]. GRK can phosphorylate Ser/Thr residues in the third intracellular loop and/or carboxyl terminal tail of the receptor[47]. Conformational changes in combination with post-translational modifications enable the binding of β-arrestins to the receptor which in turn facilitates homologous desensitization by disabling its coupling to G proteins[48,49].

In addition to receptor desensitization, β-arrestin targets the receptor to clathrin coated pits via association with the b2-adaptin subunit of the AP-2 adaptor complex, which leads to receptor internalization-endocytosis[50], a process that serves resensitization of the receptor or its targeting to lysosomes for degradation[51,52] (Fig.2). Resensitization is the process by which the receptor is dephosphorylated and recycled back to the cell membrane.

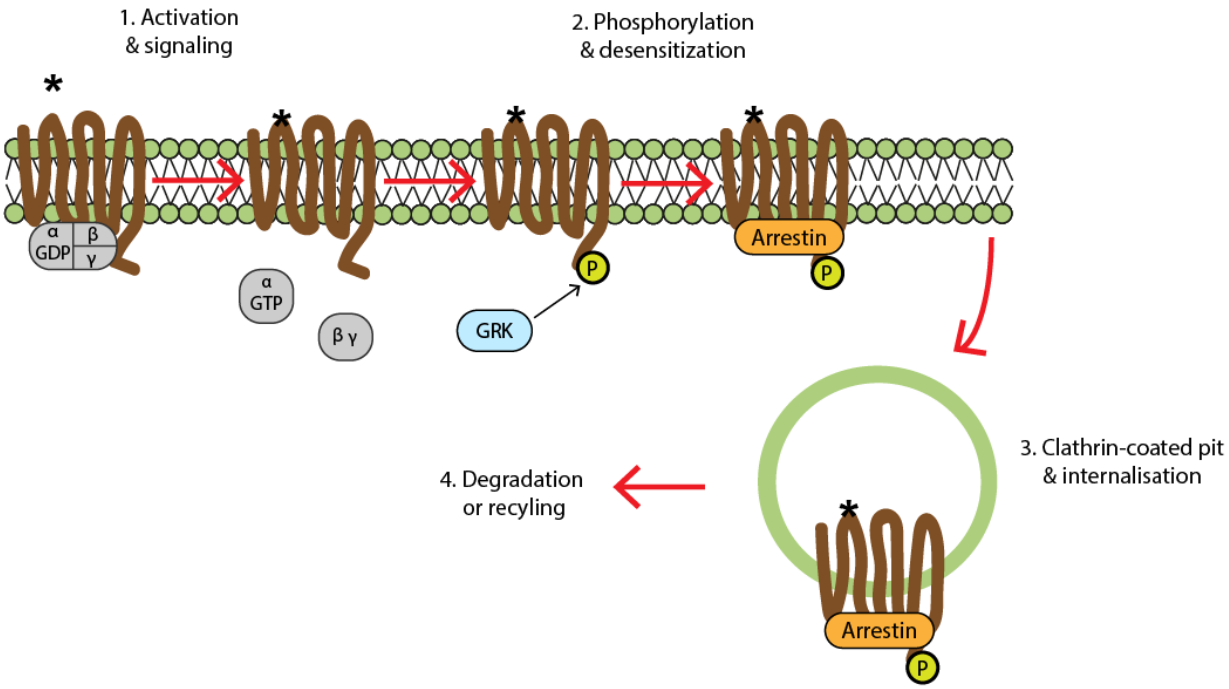

Figure 2: Regulation of G protein–coupled receptor (GPCR) trafficking by G protein–coupled receptor kinases (GRKs) and arrestins. (1) Agonist (asterisk *) binding to GPCRs leads to receptor activation (2) GRKs can phosphorylate the agonist-activated GPCR on intracellular domains, which in turn, initiates arrestin recruitment. Arrestin binding to the receptor interferes with G protein/receptor coupling and terminates receptor signaling (desensitization). (3) Receptor/arrestin complexes are then targeted to clathrin-coated pits resulting in receptor internalization. (4) Internalized GPCRs are either recycled to the plasma membrane or sorted to lysosomes for degradation.

2. The GRK family

G-protein coupled receptor kinases (GRKs) are serine/threonine kinases and belong to the family of the cAMP-dependent protein kinase (PKA), the cGMP-dependent protein kinase (PKG) and the protein kinase C (PKC), termed as AGC kinases. The GRK family consists of seven isoforms (GRK1-GRK7) which are further divided into three subfamilies: visual or rhodopsin kinases (GRK1 and GRK7), β-AR kinases (GRK2 and GRK3) and the GRK4 subfamily (GRK4, GRK5 and GRK6). The individual GRKs have some common structural features, but differential localization and expression pattern[53,54].

In addition to the canonical activity of these kinases, namely the phosphorylation of GPCRs, it has been demonstrated, that GRKs can also regulate these receptors in a phosphorylation independent manner, particularly by suppressing their interaction with G proteins. For example, the RH domain of GRK2 and GRK3 was reported to be able to inhibit Gαq-mediated activation of phospholipase C[52,55,56].

Another non-canonical function of GRKs is the phosphorylation of non-GPCR substrates such as tubulin and ezrin[57]. Moreover, GRKs seem to be important modulators of various signaling pathways in a phosphorylation-independent manner, since they are able to interact with other proteins involved in diverse molecular processes such as tubulin, caveolin, RKIP, Gαq, clathrin and phosducin[54,58–61].

GRKs are due to their canonical and non-canonical functions, important regulators of diverse signaling pathways involved in various physiological and pathological responses. GRK2, GRK3 and GRK5 are some of the best studied isoforms in regard to their effects and function under pathological conditions.

GRK2 is the best investigated GRK and its expression has been shown to be increased in cardiovascular diseases[62–64] and in Alzheimer's[65]. GRK2 levels were also increased in the livers of patients with non-alcoholic steatosis and simple steatosis[66]. Decreased GRK2 expression was observed in leukocytes from patients with multiple sclerosis and in peripheral blood mononuclear cells of patients with rheumatoid arthritis[60].

GRK3 is overexpressed in human prostate metastatic tumors[67] and decreased expression correlates with basal-breast cancer and liver metastasis[68]. Overexpression of GRK3 in the striatum attenuated L-DOPA-induced dyskinesia (LID) whereas GRK3 knockdown exacerbated it[69]. Moreover, in volume overload patients, it was observed that GRK3 expression was slightly increased[70].

GRK5 was observed to be up-regulated in heart failure[71] and its deficiency contributes to the pathogenesis of Alzheimer's disease[72]. Additionally, non-small-cell lung cancer patients with high expression of GRK5 had a worse overall survival rate than patients with lower expression levels[73].

2.1 GRKs domain organization

GRKs consist of three main structural and functional regions, which are highly conserved throughout the species[53]: a short N-terminal α-helical domain, a regulator of G protein signaling (RGS) homology domain (RH)[74] followed by a kinase domain and a variable C-terminal lipid-binding region[75](Fig.3).

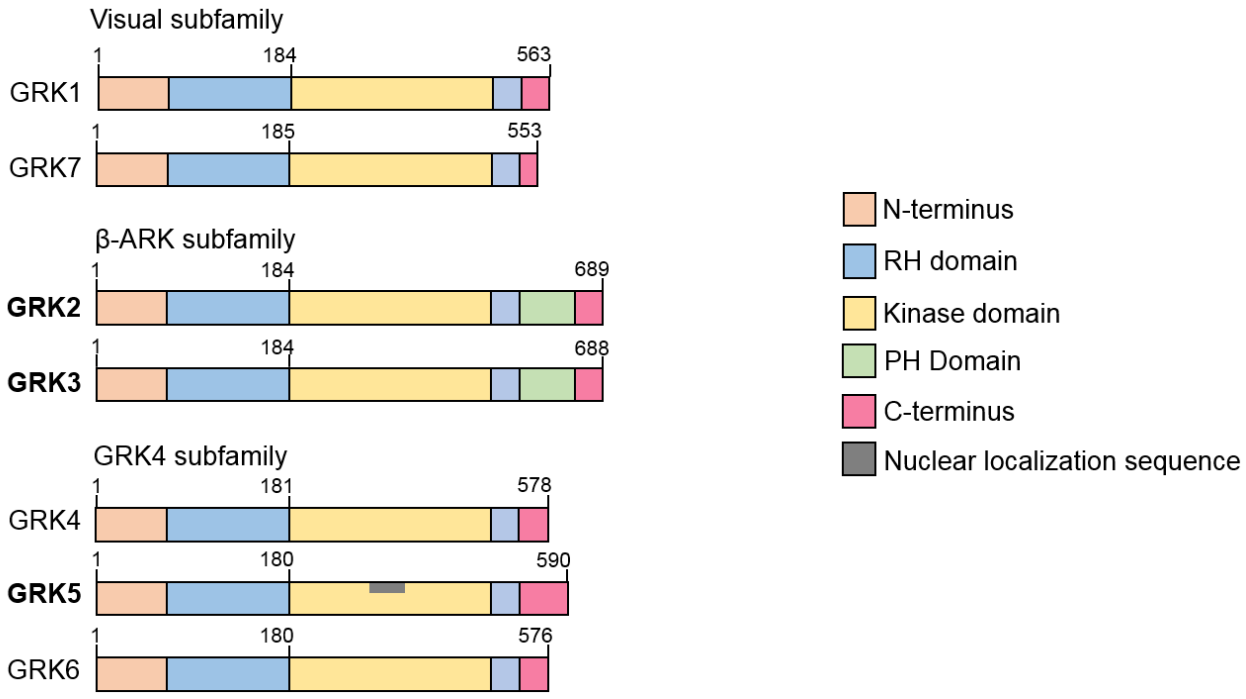

Figure 3: GRK subfamily distribution. GRKs consist of three subfamilies: Visual or rhodopsin kinases (GRK1 and GRK7), β-AR kinases (GRK2 and GRK3) and the GRK4 subfamily (GRK4, GRK5 and GRK6). They all share a NH_2-terminal region (orange), an RGS homology domain (blue), a kinase domain (yellow) and a C-terminus (pink). The β-ARK subfamily also has a pleckstrin homology (PH) domain. GRK5 has a unique attribute among the GRKs, a nuclear localization sequence (NLS).

2.1.1 N-terminus

The N-terminus of GRKs is composed of two regions: the extreme N-terminal region and the regulator of G protein signaling (RGS) homology domain (RH), which is followed by a Ser/Thr kinase domain.

The extreme N-terminal region of GRKs, which consists of approximately 20 amino acids is highly conserved and unique in this group of kinases[54]. Furthermore, it is involved in a direct interaction with GPCRs[76] and is necessary for receptor recognition[64]. Mutations and truncations (GRK1:Δ15, Δ30, E7A; GRK5: Δ2-14, L3Q/K113R, T10P; GRK2: D3K, L4A, D10A) in this N-terminal region diminished receptor

phosphorylation, but did not affect phosphorylation of soluble substrates[75,77–79]. Moreover, studies with GRK1 and GRK6 revealed that the GRK extreme N-terminal region forms a single α-helix that interacts with the kinase domain to activate the kinase. This interaction leads to stabilization of the GRK active conformation and enhancement of GRK activity and it is suggested that is promoted by receptor binding[76,80,81]. Of note, the N-terminus of GRK5 and in specific, a lipid binding domain, is implicated in the interaction of GRK5 with the cell membrane, via phosphatidylinositol 4,5-bis-phosphate (PIP2) binding[82,83].

The N-terminal domains of all GRKs have a domain following the aforementioned extreme N-terminal region, which is homologous to the regulator of G-protein signaling (RGS) family of proteins and is therefore termed as RGS homology (RH) domain[84]. RGS protein domains bind directly to activated Gα subunits and act as GTPase-activating proteins (GAPs) to regulate receptor-initiated signaling[85]. Although, it has been demonstrated that GRK2 and GRK3 interact with Gαq subunits, this is not the case for GRK5 and GRK6[64]. The GRK RH domains can be distinguished from other RH domains through their distinct Gα-binding surface[86], through their ability to bind active GTP-liganded Gαq subunits[69] and through their preference to bind Gαq but not Gαs or Gαi[59,87]. Furthermore, canonical RGS proteins increase Gα-GTPase activity, while GRK2 RGS is characterized by low activity as a Gαq GTPase-activating protein[88]. Altogether, the GRK RH domain is a Gα-binding domain that likely functions in mediating GRK targeting to specific Gα or GPCR/Gα protein complexes[59,69,87]. In addition to its Gα-binding function, the GRK RH domain forms a bipartite interaction with either the small lobe or the large lobe of the kinase domain. The interaction with the small lobe is likely involved in kinase stabilization, while the interaction with the large lobe may facilitate the arrangement of the kinase domain in an open, rather inactive state in the presence of a non-activated GPCR[89]. Moreover, the RH domain also interacts with the pleckstrin homology (PH) domain, which is localized at the C-terminal region of GRK2 and GRK3. Point mutations in the GRK2 PH domain interface caused reduced expression and kinase activity, indicating that the RH-PH domain interface presumably enables the interaction of the RH domain with the kinase domain[89]. Regarding GRK5, recent data indicate that the regulator of G-protein signaling (RGS) domain-mediated GRK5 dimerization contributes to its localization to the plasma membrane[83].

Moreover, it has been demonstrated that the GRK N-terminus can interact with other proteins. The best investigated GRK regarding interactions with other proteins is GRK2, which has several binding partners, such as caveolin, calmodulin, RKIP (Raf kinase inhibitor protein) and Gβγ. Caveolin, calmodulin and RKIP binding lead to GRK inhibition; Gβγ scavenging is involved in membrane targeting[52].

Taken together, the N-terminal region of GRKs plays an important role in facilitating GRK/receptor interaction, receptor recognition and phosphorylation, but is also implicated in interactions with other proteins.

2.1.2 C-terminus

The C-terminal regions of GRKs vary amongst the subfamilies and have little to no sequence homology; however, its main function is mediating membrane localization, which is required for full kinase activity.

In GRK1 and GRK7 this is achieved via prenylation, a post-translational modification of cysteine directed by the terminal CAAX motif and in GRK4 and 6 via palmitoylation, another post-translational modification of cysteine at the C-terminus[82,90]. These lipid groups are responsible for interacting with the plasma membrane. GRK5 is associated with the cell membrane via a polybasic/hydrophobic domain localized in a C-terminal amphipathic helix that is proposed to interact with acidic membrane lipid headgroups[91].

GRK2 and GRK3 have in contrast to the other GRKs a PH domain at their C-terminus, which mediates membrane localization via direct lipid binding (PIP_2 or other acidic phospholipids) or via an interaction with G protein βγ subunits (Fig.4) that enable the anchoring of the kinases on the plasma membrane after receptor activation[63,92,93].

In addition to its function as a mediator of membrane targeting, the C-terminus of GRK2 can interact with various proteins such as clathrin, calmodulin, caveolin, Akt and phosphoinositide 3-kinase (PI3K). The interaction with clathrin is involved in GPCR internalization; interaction with calmodulin or caveolin leads to inhibition of GRK activity; binding Akt kinase inhibits Akt's activity and the interaction with PI3K is involved in β-adrenoceptor internalization[52].

2.1.3 Other distinct GRK domains

GRK5 contains a DNA-binding nuclear localization sequence in its catalytic domain which enables its translocation to the nucleus[94,95]. It has been suggested that the splice variants of GRK4 and GRK6, GRK4α and GRK6A respectively, also contain an NLS[94,96,97].

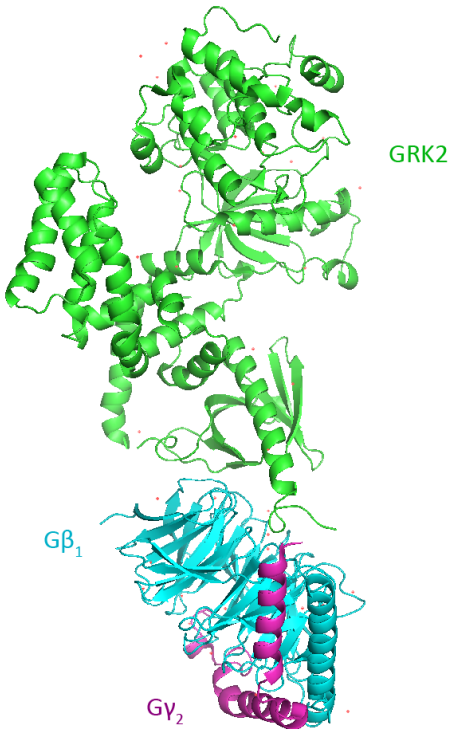

Figure 4: Human GRK2 in complex with bovine G beta gamma subunits and CCG257142. Structure was resolved via X-ray diffraction[98]. GRK2 is illustrated in green, $G\beta_1$ in turquoise and $G\gamma_1$ in magenta. (PDB ID: 6C2Y; adapted using Pymol and Adobe Illustrator)

2.2 GRK tissue localization

Most GRKs are ubiquitously expressed[54]. The rhodopsin-kinase subfamily members GRK1 (rhodopsin kinase) and GRK7 (cone opsin kinase) are mostly restricted to the retina, in rods and cones[99]. The β-ARK subfamily, i.e. GRK2 and GRK3, is ubiquitously expressed[100], but GRK2 expression is higher compared to GRK3[101]. GRK4 is highly expressed in the testes[102]; it has also been found in thyroid nodules[103] and in the kidneys, brain and uterus myometrium. GRK5 is ubiquitously expressed[54].

GRKs target a variety of receptors; for example, GRK2 mainly targets GPCRs such as angiotensin II type 1 and β-ARs, but can also phosphorylate non-GPCR substrates and associate with other proteins[60]. GRK3 phosphorylates α-ARs[104], kappa-opioid CRF1[105], olfactory receptors and thrombin receptors[54]. GRK5 targets β-ARs[106], M2 muscarinic receptors[107] and adenosine receptors[54]. GRK6 is also ubiquitously expressed[108] and phosphorylates GPCRs such as β-ARs and M2 muscarinic receptors[69]. GRK5 and GRK6, in contrast to GRK2 and GRK3 can effectively phosphorylate active as well as inactive GPCRs[109]. GRK2, GRK3, GRK5 and GRK6 have been reported to be expressed in the heart with GRK2 and GRK5 being the predominant cardiac isoforms[110,111].

2.3 GRK regulation

2.3.1 Regulation of activity

GPCR agonist-stimulation induces GRK activation, however, other regulatory mechanisms, individual to each GRK do exist.

GRK1 can regulate its activity by autophosphorylation[112]. Recoverin, a calcium binding protein can inhibit GRK1 and GRK7 depending on calcium levels within the cell[113,114]. Furthermore, PKA phosphorylates *in vitro* GRK1 and GRK7 in the N-terminus at Ser21 and Ser36 respectively, thereby reducing their activity towards rhodopsin[99].

PKA also phosphorylates GRK2 at Ser685 enhancing Gβγ binding and leading to translocation to the membrane[115]. GRK2 is furthermore regulated by cSrc phosphorylation at Tyr13, Tyr86 and Tyr92 and by PKC phosphorylation at Ser29[52]. PKC phosphorylation leads to higher activity of GRK2 towards rhodopsin[116]; cSrc phosphorylation leads to increased activity towards its substrates[117] and promotes the interaction with Gαq[118]. In addition, after GPCR stimulation, PKC phosphorylation of Raf-Kinase Inhibitor Protein (RKIP) at Ser153 leads to its dissociation from Raf-1 and promotes binding to the N-terminus of GRK2, thereby preventing it from phosphorylating the receptor[58].

GRK5 is regulated by autophosphorylation and by PKC. Autophosphorylation enables receptor phosphorylation at Thr384, Thr393, Ser396, Ser401, Ser407, and Ser411[119] and PKC phosphorylation at amino acids 565-572 leads to inhibition of its activity. Calmodulin can also modulate GRK5 activity through a calmodulin-binding domain, found both in the N- and C-terminus[54,120,121].

2.3.2 Degradation

Altered expression of GRKs, mostly GRK2 and GRK5, is observed during pathological conditions such as cardiovascular disease, cancer and inflammation, and leads to impaired GPCR signaling. Upon GPCR chronic stimulation under physiological conditions, ubiquitin-proteasome mediated degradation of GRK2 occurs[122]. Ubiquitination is a post-translational modification that tags a protein for degradation and is regulated by three types of enzymes: ubiquitin-activating enzymes (E1), ubiquitin conjugating enzymes (E2) and ubiquitin ligases (E3). The enzyme E1 activates ubiquitin by binding to it along with ATP; E2 binds to the ubiquitin-E1 complex and E3 ligates the target protein substrate to the ubiquitin complex. The ubiquitin marked protein is targeted to the proteasome for degradation[123]. The best investigated GRK to date regarding proteolysis is GRK2.

Penela et al. reported that activation of β_2-adrenergic receptors (a GPCR) increases GRK2 degradation via ubiquitination and that the blockade of GRK2 degradation has an influence on β_2- adrenergic

receptor (β_2AR) signaling and downregulation[124]. Furthermore, a subsequent study demonstrated that the β-arrestin mediated cSrc kinase recruitment and the phosphorylation of GRK2 are two events necessary for degradation initiation[125]. Later on, another study showed that activation of β_2AR in synergy with β-arrestin, increase the association of GRK2 with Mdm2 (Mouse double minute 2 homolog), which is an E3 ligase, therefore facilitating degradation[126]. However, various studies revealed that under specific pathological conditions characterized by increased GPCR activity, GRK2 activity was also increased, indicating that the interplay between GRCR and GRK2 in matters of GRK2 degradation is much more complex[127,128].

Although GRKs are being intensively studied, there are still many aspects of their regulation and function to be elucidated. Deciphering their role in physiological and pathological signaling is of great importance since they are involved in GPCR signaling and their expression is altered in various diseases.

2.4 GRKs in cardiovascular disease

In the heart the most abundant GRKs are GRK2, GRK3 and GRK5[129] and they are differentially expressed depending on the cause of heart failure. In the left ventricle (LV) of dilated cardiomyopathy (DC) and non-ischemic non-dilated cardiomyopathy (NINDC) patients, the mRNA and protein expression of GRK2 was significantly increased, in comparison to non-failing hearts (NFH). GRK3 mRNA and protein expression were also increased in those patients, but not significantly. In ischemic cardiomyopathy (IC) patients, neither the expression of mRNA nor the protein expression of GRK2, GRK3 and GRK5 was statistically significant in comparison to NFH. GRK5 mRNA and protein expression in the left and right ventricles of NINDC patients[130]. These results underline the critical role of GRKs in the regulation of cardiac function.

2.4.1 GRK2

GRK2 is an important modulator of various signal transduction pathways. It can phosphorylate different effectors involved in signal transduction. These attributes in combination with its altered expression and/or function in different pathological conditions have initiated a series of studies, in order to determine the molecular mechanisms determining its function.

Studies in mice demonstrated that globally homozygous GRK2−/− embryos die during gestation; anatomical examinations revealed that they show myocardial hypoplasia and that they die from heart failure. This led to the conclusion that GRK2 not only is required for cardiac development and function but also, that the other GRKs cannot compensate its absence[131]. It was shown that upon GPCR stimulation by angiotensin II and phenylephrine, GRK2 expression increased and initiated the prohypertrophic pathway Akt-GSK3β-NFAT. NFAT (Nuclear factor of activated T-cells) is a transcription

factor involved in the prohypertrophic and fetal gene program. In cardiac specific conditional GRK2 knockout mice it was observed that NFAT nuclear accumulation is diminished and that pressure overload induced cardiac hypertrophy was prevented[132]. Mice overexpressing GRK2 in the heart showed decreased β-AR signaling and attenuated cardiac contractility in the presence of the β-AR agonist isoproterenol; the inhibition of cardiac GRK2 increased the survival rate and improved β-blocker therapy[133,134].

These observations led to the necessity of interfering in GRK2 signaling in order to modulate its function in regard to the heart[135]. Taking into consideration that GRK2 is targeted by Gβγ to the cell membrane, where it subsequently leads to the phosphorylation of GPCRs, a GRK2 inhibitor named βARKct was tested, which consists of the GRK2 C- terminal Gβγ binding domain (residues 495-689) [136]. *Koch et al.* demonstrated that βARKct overexpression in mice leads to enhanced cardiac contractility in the presence or absence of isoproterenol. To analyze myocardial function, they measured heart rate, left ventricular pressures and aortic pressure via cardiac catherisation[136]. Furthermore, a peptide of the RGS domain of GRK2 was used as an approach to prevent hypertrophy due to its ability to bind $G\alpha_q$ which is an initiator of pathological cardiac hypertrophy[137]. Moreover, *Lorenz et al.* identified an endogenous inhibitor of GRK2, RKIP[58] which leads to increased cardiac contractility via the activation of β-AR and leads to selective inhibition of GRK2 mediated receptor –but not cytosolic–substrates[138].

Over the years, GRK2 inhibition was characterized as a valid strategy for treating various diseases, which led to the development of several inhibitors such as polyanions and polycations, balanol, Takeda inhibitors, RNA-Aptamers, paroxetine and peptides. Polyanions and polycations cannot cross the plasma membrane and often unspecific. Balanol is unspecific since it can also inhibit GRK3 and PKA. The Takeda inhibitors (Compound 2a and 2b) are more selective towards GRK2 in comparison to balanol. RNA-Aptamers are not very stable in biological media; they have low bioavailability and off-target effects. Paroxetine and its derivatives have IC_{50} values in the micro molar range and are less potent, compared to the Takeda inhibitors and to RNA-Aptamers. βARKct is a peptide that seems to be very selective; however, scavenging Gβγ subunits could have unwanted off-target effects. Furthermore, it is a rather big molecule (194 amino acids) and therefore it is not appropriate for clinical use[139].

Several attempts have been made to create a suitable inhibitor but it was not yet possible to develop one that only has beneficial effects and no side effects. It is undisputed that GRK2 is an appropriate target for disease treatment, since as described above, it is involved in the development of various diseases. Thus, additional studies are needed to identify suitable candidates for GRK2 inhibition.

2.4.2 GRK3

GRK3 is also expressed in the heart but in a lesser extent than GRK2 and GRK5[70]. The role of GRK3 in cardiac disease seems to depend on heart failure etiology.

A clinical study indicated that in patients with advanced heart failure, GRK3 expression remained unchanged in the left ventricular myocardium[140] whereas another clinical study showed that the expression of GRK3 inversely correlates with cardiac performance , suggesting a protective role for GRK3[130]. A study performed in order to identify susceptibility genes that are involved in left ventricular contractile impairment identified the GRK3 gene as a potential candidate on a chromosome associated with left ventricular function[141]. Furthermore, it was observed that GRK3 levels were unaffected in dilated cardiomyopathy but slightly increased in the right ventricle of volume overload patients[70]. In contrast to GRK2 knock-out mice which die *in utero*, GRK3 knock-out mice develop normally, although they present impairment of odorant receptor desensitization[142]. In addition, GRK3 myocardial overexpression did not alter β-AR signaling neither biochemically nor functionally[101].

GRK3 and GRK2 are highly homologous to each other and Gβγ binding plays an important role in their regulation[129]. Therefore, an analogous inhibitor to βARKct, GRK3ct was developed to investigate cardiac GRK3 function. Studies suggested that GRK3 inhibition in mice with cardiac-restricted expression of GRK3ct causes hypertension and increased cardiac output due to α_1-AR hyper-responsiveness[104]. In another study, it was observed that in GRK3ct transgenic mice, after chronic pressure overload caused by abdominal aortic binding, cardiac dysfunction was attenuated. In addition, hypertrophy in the GRK3ct mice was at similar levels as in control animals [143].

Although GRK3 is less abundant in the heart than GRK2, it also seems to play an important role in cardiomyocyte function. A study has shown that the preferred substrates of GRK3 in cardiomyocytes are the endothelin and α_1-adrenergic receptors at which it is more potent than at β_1AR[144]. It is evident that GRK3 should be taken into consideration when investigating the role of GRKs in cardiovascular disease.

2.4.3 GRK5

GRK5 is like GRK2 an abundant GRK subtype in the myocardium and are both overexpressed in heart failure[71,145]. Homozygous GRK5 knockout mice are viable but present cholinergic supersensitivity and defective muscarinic receptor desensitization[146].

Mice with increased expression levels of GRK5 showed pronounced β-AR desensitization, whilst the angiotensin II receptor mediated cardiac contractility remained stable[133]. A study with mice

overexpressing GRK5 in the heart showed that elevated GRK5 levels cause increased hypertrophy and early progression to heart failure. This was shown to be due to nuclear translocation of GRK5 and increased $G\alpha_q$ activity since the overexpression of a GRK5 nuclear deficient mutant did not lead to the same detrimental effects[147].

It has been shown that in cardiomyocytes after aortic binding *in vivo* but also *in vitro* in cardiomyocytes with increased $G\alpha_q$ activity, the nuclear accumulation of GRK5 is increased. In the nucleus, GRK5 acts as a histone deacetylase 5 (HDAC5) kinase; it upregulates the transcription of cardiac hypertrophy genes i.e via activation of myocyte enhancer factor 2 (MEF2)[147]. A following study showed that the global GRK5 deletion in mice subjected to transverse aortic constriction, attenuated pressure-overload-induced hypertrophy. In addition, this study demonstrated that also a cardiac specific deletion of GRK5 leads to hypertrophy attenuation after transverse aortic constriction, which indicates that cardiomyocyte GRK5 is required for cardiac hypertrophic responses[148].

NF-κB is a family of transcription factors involved in inflammation, immunity and cancer; in the inactive state is found in the cytoplasm, associated with IκB (inhibitory κB). NIK (NFκB inducing kinase) and TAK1 (transforming growth factor beta (TGFB)-activated kinase 1) activate IKK (IκB kinase), which phosphorylates IκB and induces its degradation. Upon degradation of IκB, NF-κB dissociates and translocates to the nucleus, where it regulates transcription of anti-apoptotic genes, immunoregulatory and inflammatory genes, genes that positively regulate cell proliferation and genes encoding negative regulators of NF-κB[149–151]. *Sorriento et al.*, reported that full-length GRK5 leads to inhibition of NF-κB transcriptional activity via a direct interaction with IκBα, an inhibitor of NF-κB. GRK5-IκBα interaction leads to IκBα nuclear accumulation and subsequently to NF-κB inhibition. The RH-domain of GRK5 facilitates this action[152]. NF- κB is a transcription factor which is ubiquitously expressed and modulates genes implicated in several cell functions; it has been shown to mediate cardiomyocyte hypertrophy[153]. A subsequent study of the same group using the amino-terminus of GRK5 including the RH domain (GRK5-NT) reported, that this segment of GRK5 can prevent the development of left ventricular hypertrophy *in vitro* as well as *in vivo*, based on NF-κB inhibition[154]. A further study from *Sorriento et al.*, has validated the inhibitory effect of GRK5-NT in left ventricular hypertrophy and showed that it affects transcription factor regulation. Namely, GRK5-NT was shown to regulate the activity of calcium-calmodulin dependent transcription factors such as nuclear factor of activated T- cells (NFAT)[155].

However, this activity of nuclear GRK5 is not induced during hypertrophy caused under physiological conditions, indicating a dependency on the hypertrophy model[156].

3. Raf-Kinase Inhibitor Protein (RKIP)

RKIP belongs to phosphatidylethanolamine-binding protein family (PEBP) and it is referred to as PEBP1. The *PEBP1* gene is evolutionary highly conserved and has homologues ubiquitously expressed in bacteria, plants and animals[157]. In humans, it is a 23 kDa protein and consists of two mains domains, which facilitate regulation of various pathways that monitor differentiation and cell proliferation: the ligand binding pocket and a globular structure that enables protein-protein interactions. RKIP is expressed in all tissues but mostly in the nervous system, thyroid and adrenals[158–160].

RKIP is involved in various signaling cascades such as the Raf-MEK-ERK pathway and GPCR signaling, and is also implicated in the regulation of nuclear factor κB (NF-κB) signaling pathway and glycogen synthase kinase-3 (GSK3) proteins[161].

It has been reported to interact with multiple components of the NF-κB signaling pathway and to inhibit NF-κB signaling in various ways, for example by directly inhibiting NIK, TAK1 and IKK [160,162]. Inhibition of these kinases prevents the NF-κB translocation to the nucleus and the regulation of the transcription of genes involved in inflammatory, immunoregulatory, apoptotic, and proliferation processes.

GSK3 is a serine/threonine kinase found in eukaryotes which is implicated in the regulation of receptor tyrosine kinases and GPCRs; additionally, it acts as a tumor suppressor that downregulates oncogenic pathways such as Wnt signaling. It is involved in diseases such as diabetes, cancer and neurodegeneration[163,164]. RKIP binds GSK3 proteins and regulates GSK3β and its substrates by controlling oxidative stress, namely through reactive oxygen species (ROS)-activated p38 MAPK, leading to increased GSK3β activity. Thus, it is suggested, that the RKIP/GSK3 interaction could serve as a predictor of cancer progression and as a therapeutic target as well[165].

3.1 RKIP's function in the Raf-MEK-MAPK pathway

Upon binding of a growth factor to the transmembrane receptor tyrosine kinases (RTKs), the Raf-MEK-MAPK signaling pathway conveys signals from the cell membrane to the nucleus through a series of activation and phosphorylation steps and is involved in cell processes such as differentiation, proliferation, apoptosis and migration[166–168]. Deregulation of the Raf-MEK-MAPK pathway is crucial in disease manifestation. For instance, uncontrolled cell growth caused by a defect in the signaling cascade is the main characteristic of cancer development[169].

RKIP was identified as a Raf-1 (Rapidly accelerated fibrosarcoma) binding protein which can suppress the phosphorylation and activation of MAPK/ERK kinase (MEK) by Raf-1[170]. Further studies demonstrated that RKIP can form complexes with Raf-1, MEK and ERK. The phosphorylation and

activation of MAPK/ERK kinase (MEK) by Raf-1 requires direct association of these two proteins. Upon RKIP binding to either Raf-1 or MEK, the aforementioned association is disrupted leading to interruption of MEK activation and thus of downstream signaling[171].

3.2 RKIP's function in GPCR signaling

RKIP phosphorylation by protein kinase C (PKC) at serine 153[58] leads to its dissociation from Raf-1 and triggers RKIP dimerization through an interaction interface, in close proximity to the PKC phosphorylation site and that consists of a loop structure[172]. RKIP then binds GRK2 at its N- terminus, which as mentioned previously is important for the interaction with GPCR, and prevents the phosphorylation and desensitization of the receptor (Fig.5). GRK2 retains its catalytic activity [58] and the phosphorylation of its cytosolic substrates remains unaffected[138]. GRK2 inhibition by RKIP prevents GPCR desensitization and internalization and leads to increased GPCR signaling which can have multiple beneficial effects, such as enhanced contraction and relaxation in the heart[58,138].

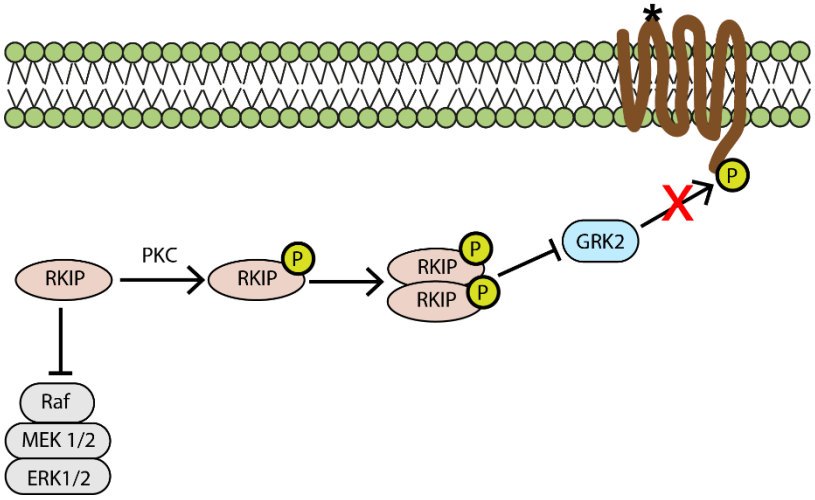

Figure 5: RKIP signaling. RKIP is phosphorylated by protein kinase C (PKC). This leads to its dissociation from Raf- 1 (Raf), dimer formation and binding to GRK2. Thereby, GRK2 is inhibited and prevented from phosphorylating the receptor. Unphosphorylated RKIP inhibits Raf and thereby inhibits the activation of extracellular signal–regulated kinases ERK1 and ERK2 (ERK1/2).

3.2.1 β-adrenergic receptors

β-adrenergic receptors (β-ARs) belong to the superfamily of GPCRs. Their primary agonists are catecholamines such as epinephrine and norepinephrine and they are involved in the regulation of several cellular processes such as myocardial contractility and relaxation, smooth muscle tone, and glucose and lipid metabolism. There are four subtypes: β_1-ARs which are mainly localized in the heart

and kidney; β_2-ARs are localized in the heart but also in lungs and blood vessels; β_3- ARs are mainly found in the adipose tissue; β_4-ARs have not been thoroughly investigated yet[40– 42].

As mentioned previously, β-ARs are important regulators of myocardial function. The dysregulation of β-ARs has been characterized as a precursor for the development of heart failure[176,177]. Heart failure is the end stage of many cardiovascular diseases and remains one of the most common causes of death worldwide. The main characteristic of heart failure is increased activation of the sympathetic nervous system (SNS) and of the renin angiotensin aldosterone system (RAAS) due to increased load or stress on the heart, which results in elevated catecholamine release. Catecholamine levels regulate cardiac contractility. At the molecular level, this causes stimulation and increased activation of β-ARs in the heart, which initially serves as a compensatory mechanism in order to increase cardiac output (Fig.6). Upon stimulation, cardiomyocyte β_1-AR primarily binds to the Gs protein, which leads to activation of AC, which in turn generates the second messenger cyclic adenosine monophosphate (cAMP); increased levels of cAMP lead to cAMP-dependent protein kinase A (PKA) activation. Activated PKA phosphorylates troponin I, the L-type Ca2+ channel and phospholamban (PLB), resulting in greater contractility (Figure 6). In addition to Gs, β_2-AR can couple to Gi protein. Gi coupling releases the activated Giα and the Giβγ subunits. Giα inhibits AC activity and activates the cytosolic effector molecule phospholipase A2 (cPLA2), which leads to cAMP-independent increase of calcium signaling and therefore cardiac contraction. Giβγ activates the mitogen-activated protein kinases (MAPK)[173,176,178].

However, the survival of HF patients treated with β-AR agonists is reduced, although a temporary beneficial effect is observed[179]. Activation of β-ARs initiates their phosphorylation by GRKs, leading to receptor desensitization and downregulation. GRKs phosphorylate β_2-ARs at the C-terminus at Thr360, Ser364, Ser396, Ser401, Ser407, Ser411, Ser355 and Ser356 [180,181]. This is initially considered a protective mechanism; however, chronic receptor activation has deleterious effects on the heart. Nevertheless, in the failing heart this triggers a vicious cycle of persistent SNS activation and subsequent desensitization and downregulation of the receptor[182]. A probable mechanistic link between SNS hyperactivation and β-AR dysregulation is increased GRK2, and likely also GRK5, expression[70]. This vicious cycle leads eventually to the attenuation of contractility and progressive cardiac remodeling. Cardiac remodeling is defined as a group of changes at molecular, cellular and interstitial level, which cause changes in size and function of the heart[183]. β-adrenergic receptor blocking agents are a class of drugs widely used for heart failure treatment. However, their administration has certain limitations such as contraindications and lack of responsiveness to the medication[184].

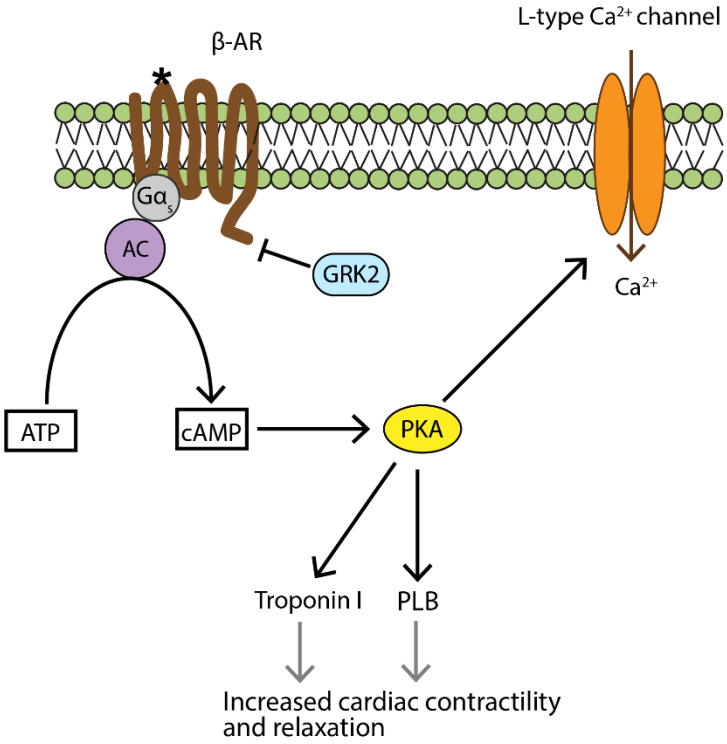

Figure 6: β-AR-mediated cardiomyocyte contractility. Upon ligand binding (asterisk), cardiomyocyte β-AR binds to Gαs, which leads to activation of adenylate cyclase (AC), which in turn generates from ATP the second messenger cyclic adenosine monophosphate (cAMP); increased levels of cAMP lead to protein kinase A (PKA) activation. Activated PKA phosphorylates troponin I, the L-type Ca^{2+} channel and phospholamban (PLB), resulting in increased contractility and relaxation.

RKIP was shown to enhance GPCR signaling via GRK inhibition and subsequent investigations, revealed a link between RKIP and β-AR signaling in heart failure. Cardiac RKIP expression is increased in heart failure patients and in mice with pressure overload-induced heart failure. It was shown that in mice with pressure overload-induced heart failure, cardiac RKIP overexpression had a protective effect. On the other hand, RKIP depletion in the same model exaggerated heart failure. RKIP knockout mice treated with RKIP via AAV9-mediated gene transfer were protected against pressure overload-induced heart failure. RKIP stimulates β_1-AR-G_s signaling, which leads to enhanced cardiac contractility and it acts cardioprotective under sympathetic stress by activating β_2- AR and by mediating anti-apoptotic effects through stimulation of the Akt kinase. However, RKIP is not only implicated in GPCR signaling, but also in MAPK signaling. Whether RKIP is phosphorylated or not, determines it mode of action. When RKIP is phosphorylated at serine 153 it acts as a GRK2 inhibitor and when it is unphosphorylated it acts as a Raf-1 inhibitor. As a Raf-1 inhibitor it could potentially increase cardiomyocyte death due to inhibition of the Raf-MEK-MAPK signaling cascade which facilitates cardiomyocyte survival[138,161].

Although heart failure is a highly prevalent disease, efficient medication is not yet available, therefore, therapeutic targets involved in the β-adrenergic signaling cascade (besides β-ARs) are being widely investigated.

3.3 RKIP implications in disease

RKIP is a protein of interest in many cancer types such as prostate, breast, liver, lung and melanoma. It was shown to be low expressed in several cancer types and even absent in metastasis. Downregulation of RKIP was shown to correlate with metastatic phenotype in a wide variety of cancers, whereas increased RKIP levels block invasion and metastatic progression indicating that RKIP functions as a metastatic suppressor. Although RKIP's role in cancer has been extensively studied, the mechanism by which the cells achieve its downregulation in the metastatic process remains to be elucidated, since genetic deletions or mutations were rarely observed in patient samples. It has been suggested that the RKIP downregulation is due to hypermethylation of its promoter[185,186].

Alzheimer's is a chronic neurodegenerative disease that manifests clinically through a slow and gradual impairment of cognitive functions due to the progressive dysfunction and death of nerve cells[187]. There are two forms of the disease based on the onset time point: early onset patients are younger than 65 years old and late onset patients are older than 65 years old. Downregulation of RKIP mRNA was observed in brains of patients with late onset of Alzheimer's. In a mouse model for Alzheimer's it was shown that RKIP levels were decreased in hippocampal formations. Additionally, RKIP knockout mice displayed at an age older than four months a decline in olfactory perception, a typical feature of patients suffering from Alzheimer's[188]. The hippocampus is a brain part that is of great significance for memory function, which gradually declines during the Alzheimer's disease. RKIP is the precursor of the hippocampal cholinergic neurostimulating peptide (HCNP), which stimulates cholinergic activity in septal nuclei[189,190]. HCNP is located N-terminally on its precursor protein from where it is cleaved by an enzyme in the hippocampus[191]. It was observed that HCNP expression in the CA1 (*cornu Ammonis*) field of the hippocampus of Alzheimer's late onset patients was decreased, suggesting that the downregulation of cholinergic neurons in these patients could be due to decreased levels of HCNP, highlighting its role in the hippocampus[192,193].

The role of RKIP, both under physiological and pathological conditions constitutes a challenge for modern medicine that needs to be studied further, in order to reveal the mechanism behind its effects and to determine potential therapeutic interventions by targeting RKIP or other molecules involved in its signaling network.

4. Aim

GPCRs are one of the most important targets for therapeutic drug development. G protein coupled receptor kinases (GRK) phosphorylate and thereby desensitize GPCR. GRK are serine/threonine kinases and belong to the family of AGC kinases. The GRK family consists of seven isoforms (GRK1-GRK7) which are further divided into three subfamilies: visual or rhodopsin kinases (GRK1 and GRK7), β- adrenergic receptor kinases (GRK2 and GRK3) and the GRK4 subfamily (GRK4, GRK5 and GRK6). Individual GRK show a differential localization and expression pattern[54]. They target various types of GPCR. GRK2 phosphorylates for example β-ARs that are critical regulators of cardiac function. An endogenous inhibitor of GRK2 was identified, which leads to increased cardiac contractility via the activation of β- AR: the Raf kinase inhibitor protein (RKIP)[58]. It inhibits GRK2 but not GRK5 and it has been revealed to bind to the N-terminus (1-185) of GRK2, which is important for the GRK2/receptor interaction[194]; it leads to selective inhibition of GRK2 receptor –but not cytosolic–substrates[138].

The aim of this thesis was firstly to further investigate the RKIP/GRK interaction interface and the distinct protein-interacting domains of the GRKs localized in the heart, using N-terminal peptides of GRK2, GRK3 and GRK5 and performing protein interaction assays such as co-immunoprecipitations and pull-down assays. Three N-terminal peptides were used for the protein interaction assays consisting of amino acids 1-53 or 54-185 or 1-185 and were either expressed in HEK cells carrying a myc-tag or they were GST-tagged and were purified from *E.coli*. These domains of GRK play an important role in receptor recognition, membrane localization and receptor interaction. After analyzing the interaction interface and revealing at which N-terminal region of the investigated GRKs RKIP binds, it should be examined whether these regions (peptides) can simulate RKIP's function in β-adrenergic signaling. In particular, whether they show a similar effect on β-AR phosphorylation, internalization and downstream signaling like RKIP. Subsequently, it should be also examined whether they have a physiological effect on cardiomyocytes in terms of contractility and hypertrophy that mimics RKIP's effects in the heart using adenoviral constructs of the peptides in order to transduce them into neonatal mouse cardiomyocytes. Finally, the potential mechanism of action of the peptides should be investigated. The information retrieved from these experiments should contribute to the development of novel therapeutic targeting strategies for heart failure that simulate RKIP's beneficial effects in the heart.

II. Material

1. Substances

1.1 General chemicals

Chemical	**Vendor**
2-Mercaptoethanol	AppliChem
Acetic acid	Carl Roth
Agar agar	AppliChem
Agarose	AppliChem
Alexa Fluor 488	Molecular Probes
Ammonium persulfate (APS)	Carl Roth
Benzamidine	Sigma Aldrich
BES PUFFERAN® ≥ 99%	Carl Roth
Bovine Serum Albumin Fraction V (BSA)	AppliChem
Brilliant Blue G	Sigma Aldrich
Bromophenol blue indicator ACS	Merck
Developer	Sigma Aldrich
Dimethyl sulfoxide (DMSO)	AppliChem
Di-Sodiumhydrogenphosphate (Na_2HPO_4)	AppliChem
Dithiothreitol (DTT)	AppliChem
DNA Ladder	NEB
Ethanol	Carl Roth
Ethylene glycol-bis(β-aminoethyl ether)-N,N,N',N'-tetraacetic acid (EGTA)	AppliChem
Ethylenediaminetetraacetic acid (EDTA)	AppliChem
Fixer	Sigma Aldrich
Gelatin from bovine skin	Sigma Aldrich
Glycerol	Carl Roth
Glycine	AppliChem
HCl 37%	Carl Roth
Hoechst 33258	Sigma Aldrich
Isopropanol	Carl Roth
Isoproterenol Hydrochloride	Sigma Aldrich
Magnesium chloride	AppliChem

Methanol	Carl Roth
Monopotassium phosphate (KH_2PO_4)	AppliChem
Nonfat dried milk	AppliChem
Nonidet P-40	AppliChem
Norepinephrine	Sigma Aldrich
Paraformaldehyde	Sigma Aldrich
Peptone ex meat	Carl Roth
Phenylephrine hydrochloride	Sigma Aldrich
Phenylmethylsulfonyl fluoride (PMSF)	Sigma Aldrich
Potassium Chloride (KCl)	AppliChem
Rotiphorese Gel®30	Carl Roth
Rotiszint eco plus	Carl Roth
Sodium azide (NaN_3)	Serva
Sodium bicarbonate ($NaHCO_3$)	AppliChem
Sodium chloride (NaCl)	AppliChem
Sodium dodecyl sulfate (SDS)	AppliChem
Sodium fluoride (NaF)	Merck
Sodium phosphate	AppliChem
Tetramethylethylendiamine (TEMED)	AppliChem
Tris(hydroxymethyl)-aminomethane	AppliChem
Triton X-100	AppliChem
Trypsin inhibitor soybean	Sigma Aldrich
Tween-20	AppliChem
Urea	AppliChem
Yeast extract	Carl Roth

1.2 Cell culture chemicals

Chemical	**Vendor**
Claycomb Medium	Sigma Aldrich
Dulbecco's Modified Eagle's Medium (DMEM)	PAN-Biotech
Dulbecco's PBS (with Ca^{2+} and Mg^{2+})	Life Technologies
Dulbecco's PBS (without Ca^{2+} and Mg^{2+})	Life Technologies
Fetal Calf Serum (FCS)	Merck

Fetal Calf Serum (FCS)	Sigma Aldrich
Fibronectin	Sigma Aldrich
L-Ascorbic Acid	PAN-Biotech
L-Glutamine	PAN-Biotech
Penicillin/Streptomycin	PAN-Biotech
Poly-D-lysine hydrobromide	Sigma Aldrich
Trypsin/EDTA	PAN-Biotech
Vitamin B12	Sigma Aldrich
Isoproterenol	Sigma Aldrich
Phorbol 12-myristate 13-acetate	Sigma Aldrich

2. Kits

Kits	**Vendor**
Pierce® BCA Protein Assay Kit	Thermo Scientific
Pierce® ECL Plus Western Blotting Substrate	Thermo Scientific
Plasmid Plus Midi Kit®	Qiagen
Gel Extraction Kit®	Qiagen
Effectene Transfection Reagent	Qiagen
QIAquick Gel Extraction Kit	Qiagen
Pierce™ Coomassie (Bradford) Protein Assay Kit	Thermo Scientific
Trans-Blot Turbo Starter Kit	BIORAD
KAPA HiFi PCR Kit	Roche
PCR Mycoplasma Test Kit	AppliChem
Neonatal Heart Dissociation Kit	MACS, Miltenyi Biotec

3. Enzymes

Enzymes	**Vendor**
Gateway™ LR Clonase™ Enzyme mix	Thermo Scientific
Gateway™ BP Clonase™ Enzyme Mix	Thermo Scientific
Thrombin	GE Healthcare
Restriction enzymes	New England Biolabs
T4-DNA-Ligase	New England Biolabs

BamHI	New England Biolabs
HindIII	New England Biolabs
XbaI	New England Biolabs
Lysozyme	Sigma Aldrich

4. Antibodies

4.1 Primary antibodies

Primary antibodies	**Species**	**Dilution**	**Vendor**	**Nr**
Phospho p44/42 MAPK (Erk1/2)	rabbit	1:1000	Cell Signaling	9101
Phospho PKA Substrate	rabbit	1:2000	Cell Signaling	9624
Phospho PKA Substrate	rabbit	1:2000	Cell Signaling	9621
Phospho PKA Substrate	rabbit	1:2000	Cell Signaling	2261
Phospho PKC Substrate	rabbit	1:1000	Cell Signaling	2261
Phospho β_2-AR	rabbit	1:2000	Santa Cruz	sc-22191
myc-tag	mouse	1:4000	Cell Signaling	2276
GFP	rabbit	1:2000	Sigma Aldrich	G 1544
GRK2 C-15	rabbit	1:2000	Santa Cruz	sc-562
FLAG M2	mouse	1:5000	Sigma Aldrich	F1804
Phosucin	mouse	1:1000	Santa Cruz	sc-398752
Phosucin	mouse	1:1000	Santa Cruz	sc-271769
HA	mouse	1:5000	Covance	MMS-101R
GRK3	rabbit	1:2000	Santa Cruz	sc-563
GRK5	rabbit	1:2000	Santa Cruz	sc-565
his-tag	mouse	1:3000	Cell Signaling	2366
GST-tag	mouse	1:2000	Santa Cruz	sc-138
c-Myc	rabbit	1:1000	Santa Cruz	sc-378
Gβ	rabbit	1:2000	Santa Cruz	sc-790
β-actin	mouse	1:5000	Sigma Aldrich	A5441

4.2 Secondary antibodies

Secondary Antibodies	Species	Dilution	Vendor	Nr
Rabbit Peroxidase conjugated IgG	goat	1:10000	Dianova	111-035-144
Mouse Peroxidase conjugated IgG	goat	1:10000	Dianova	115-035-003
Goat Peroxidase conjugated IgG	donkey	1:5000	Santa Cruz	sc-2020
IRDye® 800CW anti-Mouse IgG	goat	1:10000	Li-Cor	P/N 925-32210
IRDye® 800CW anti-Rabbit IgG	goat	1:10001	Li-Cor	P/N 925-32211

5. Plasmid vectors

Vector	Species	Remark	Reference
$pcDNA_3$	-	-	Invitrogen
pET-3c-His_6-RKIP	rat	N-terminal His-tag	K.Lorenz
pGEX-GST-GRK2 1-53	bovine	N-terminal GST-tag	K.Lorenz
pGEX-GST-GRK2 54-185	bovine	N-terminal GST-tag	K.Lorenz
pGEX-GST-GRK2 1-185	bovine	N-terminal GST-tag	K.Lorenz
pGEX-GST-GRK3 1-53	bovine	N-terminal GST-tag	K.Lorenz
pGEX-GST-GRK3 54-185	bovine	N-terminal GST-tag	K.Lorenz
pGEX-GST-GRK3 1-185	bovine	N-terminal GST-tag	K.Lorenz
pGEX-GST-GRK5 1-53	bovine	N-terminal GST-tag	K.Lorenz
pGEX-GST-GRK5 54-185	bovine	N-terminal GST-tag	K.Lorenz
pGEX-GST-GRK5 1-185	bovine	N-terminal GST-tag	K.Lorenz
$pcDNA_3$-myc-GRK2 1-53	bovine	N-terminal myc-tag	K.Lorenz
$pcDNA_3$-myc-GRK2 54-185	bovine	N-terminal myc-tag	K.Lorenz
$pcDNA_3$-myc-GRK2 1-185	bovine	N-terminal myc-tag	K.Lorenz
$pcDNA_3$-myc-GRK3 1-53	bovine	N-terminal myc-tag	K.Lorenz
$pcDNA_3$-myc-GRK3 54-185	bovine	N-terminal myc-tag	K.Lorenz
$pcDNA_3$-myc-GRK3 1-185	bovine	N-terminal myc-tag	K.Lorenz
$pcDNA_3$-myc-GRK5 1-53	bovine	N-terminal myc-tag	K.Lorenz
$pcDNA_3$-myc-GRK5 54-185	bovine	N-terminal myc-tag	K.Lorenz
$pcDNA_3$-myc-GRK5 1-185	bovine	N-terminal myc-tag	K.Lorenz
$pcDNA_3$-Flag-RKIP	rat	N-terminal Flag-tag	K.Lorenz
$pcDNA_3$-β-Arrestin2-SYFP	bovine	C-terminal SYFP-tag	C. Krasel
$pcDNA_3$-β-Arrestin2-mCherry	bovine	C-terminal mCherry-tag	C. Krasel

pcDNA$_3$-YFP-ERK2	mouse	N-terminal YFP-tag	K.Lorenz
pcDNA$_3$-YFP-GRK2_1-185	bovine	N-terminal YFP-tag	T. Maimari
pcDNA$_3$-YFP-GRK3_1-185	bovine	N-terminal YFP-tag	T. Maimari
pcDNA$_3$-YFP-GRK5_1-185	bovine	N-terminal YFP-tag	T. Maimari
pcDNA$_3$-GRK2_1-185_SYFP	bovine	C-terminal YFP-tag	T. Maimari
pcDNA$_3$-GRK3_1-185_SYFP	bovine	C-terminal YFP-tag	T. Maimari
pcDNA$_3$-GRK5_1-185_SYFP	bovine	C-terminal YFP-tag	T. Maimari
pcDNA$_3$-GRK2_1-185_mCherry	bovine	C-terminal mCherry-tag	T. Maimari
pcDNA$_3$-GRK3_1-185_mCherry	bovine	C-terminal mCherry-tag	T. Maimari
pcDNA$_3$-GRK5_1-185_mCherry	bovine	C-terminal mCherry-tag	T. Maimari
pcDNA$_3$-Phosducin		-	K.Lorenz
pAD/CMV/V5-myc_GRK2_1-185	bovine	N-terminal myc-tag	K.Lorenz
pAD/CMV/V5-myc_GRK3_1-185	bovine	N-terminal myc-tag	T.Maimari
pAD/CMV/V5-myc_GRK5_1-185	bovine	N-terminal myc-tag	T.Maimari
pcDNA$_3$-Flag β_2AR	human	N-terminal Flag-tag	K.Lorenz
pcDNA$_3$-Flag β_2AR_330-413	human	N-terminal Flag-tag	T.Maimari

6. Purified proteins

Purified Protein	**Origin**
His$_6$-RKIP	this project
GST-GRK2 1-53	this project
GST-GRK2 54-185	this project
GST-GRK2 1-185	this project
GST-GRK3 1-53	this project
GST-GRK3 54-185	this project
GST-GRK3 1-185	this project
GST-GRK5 1-53	this project
GST-GRK5 54-185	this project
GST-GRK5 1-185	this project

7. Biological material

7.1 Prokaryotic cells

Bacterial cells	**Origin**
E.coli Bl21 pLysS	Novagen
E.coli XL1-Blue	Stratagene
E.coli ElectroMAX™ DH10B™ Cells	Thermo Scientific

7.2 Eukaryotic cells

Cell line	**Description**	**Origin**
HEK293	Human embryonic kidney cells transformed with Adenovirus Type 5 (Ad5)	Pharmacology, Würzburg (Graham et al., 1977)
GFP-β_2AR HEK293	Human embryonic kidney cells transformed with Adenovirus Type 5 (Ad5) with stable expression of GFP-β2AR	C. Krasel, Pharmacology, Würzburg

7.3 Adenoviruses

Adenovirus	Species	Remark	Reference
AdV lacZ	*E.coli*	-	K.Lorenz
AdV-myc-GRK2 1-185	bovine	N-terminal myc-tag	K.Lorenz
AdV-myc-GRK3 1-185	bovine	N-terminal myc-tag	T.Maimari
AdV-myc-GRK5 1-185	bovine	N-terminal myc-tag	T.Maimari

8. Oligonucleotides

Primers Cloning	**Sequence**
GRK2_1-185 HindIII forward	5'TCC CTC TAG aag ctt ATG GCG GAC CTG GAG GCG GTG 3'
GRK2_1-185 XbaI reverse	5' TGC TGA ATT tct aga GTG GAT GTT GAG CTC CAC ACC 3'
GRK3_1-185 HindIII forward	5' TCC CTC TAG aag ctt ATG GCG GAC CTG GAG GCC GTG 3'
GRK3_1-185 XbaI reverse	5' TGC TGA ATT tct aga ATG GAT ATT TAA TTC CAC GTT 3'
GRK5_1-185 HindIII forward	5' TCC CTC TAG aag ctt ATG GAG CTG GAA AAC ATC GTG 3'

GRK5_1-185 XbaI reverse	5' TGC TGA ATT tct aga AGT GTT TTT GGT CAC CGG TTG 3'
GRK2_1-185 BamHI forward	5' TCC CTC TAG gga tcc GCG GAC CTG GAG GCG GTG CTG 3'
GRK2_1-185 XbaI reverse	5' TGC TGA ATT tct aga CTA GTG GAT GTT GAG CTC CAC 3'
GRK3_1-185 BamHI forward	5' TCC CTC TAG gga tcc GCG GAC CTG GAG GCC GTG CTG 3'
GRK3_1-185 XbaI reverse	5' TGC TGA ATT tct aga ATG GAT ATT TAA TTC CAC GTT 3'
GRK5_1-185 BamHI forward	5' TCC CTC TAG gga tcc GAG CTG GAA AAC ATC GTG GCC 3'
GRK5_1-185 XbaI reverse	5' TGC TGA ATT tct aga CTA AGT GTT TTT GGT CAC CGG '
Flag β_2AR_330-413 BamHI forward	5'TCC CTC TAG gga tcc ATG GAC TAC AAA GAC GAT GAC GAC AAG CCC AGA TTT CAG GAT TGC 3'
Flag β_2AR_330-413 XBaI reverse	5'TGC TGA ATT tct aga TTA CAG CAG TGA GTC ATT TGT ACT 3'

Primers Gateway Cloning	**Sequence**
myc-tag forward	**5'GGGG ACA AGT TTG TAC AAA AAA GCA GGC T**AT GGA GCA GAA GCT GAT CTC CGA GGA GGA CCT G 3'
myc-GRK5 1-185 reverse	**5' GGGG AC CAC TTT GTA CAA GAA AGC TGG GT**C TAA GTG TTT TTG GTC ACC GGT TGC CT 3'
myc-GRK3 1-185 reverse	**5' GGGG AC CAC TTT GTA CAA GAA AGC TGG GT**A TGG ATA TTT AAT TCC ACG TTT TTC CA 3'
myc-GRK2 1-185 reverse	**5' GGGG AC CAC TTT GTA CAA GAA AGC TGG GT**A AGA ATG TGG AGC TCA ACA TCC ACT AG 3'

9. Consumables

Consumables	**Vendor**
Amicon® Ultra centrifugal filter units	Millipore
Medical X-ray Film	Fuji Film
Cell culture plates/flasks	Sarstedt
Chromatography columns	Biorad
Protein A Sepharose	GE Healthcare
Glutathione Sepharose 4B	GE Healthcare
NiNTA Agarose	Qiagen
HisTrap FF crude	GE Healthcare
GSTrap HP	GE Healthcare
Slides	Thermo Scientific
Coverslips	Marienfeld, Sarstedt

Cryotubes	Sarstedt
Syringes	BD Discardit
0.2 µm sterile filters	Sartorius
Serological pipettes	Sarstedt
Chameleon Duo	Li-Cor
Precision Plus Protein™ Dual Color Standards	Biorad
nProtein A Sepharose® 4 Fast Flow	GE Healthcare
NSP96-2,0 CardioExcyte96 Sensorplate	Nanion Technologies
NSP96-0,6 CardioExcyte96 Sensorplate	Nanion Technologies
GelRed Nucleic Acid Gel Stain	VWR
Quick-Load 1 kb DNA Ladder	New England Biolabs
Quick-Load 100 bp DNA Ladder	New England Biolabs

10. Radioactive material

Substance	**Vendor**
^{3}H-CGP 12177	Hartmann

III. Methods

1. Molecular methods

1.1 Gateway cloning system

Gateway Cloning Technology facilitates the transfer of DNA segments between vectors using site-specific recombination, instead of restriction endonucleases and ligases that were classically used for cloning. It is based on the site-specific recombination system of bacteriophage lambda (λ) and its integration into the *E.coli* chromosome through lysogenisation. Upon integration, the phage genome is transmitted to the following generations until its excision is triggered, whereby the virus enters the lytic pathway. Lambda recombination occurs between specific attachment (*att*) sites on the interacting DNA molecules: *att*B on the *E.coli* chromosome and *att*P on the lambda chromosome. The so-called 'BP' and the so-called 'LR' recombination reactions *in vitro* constitute the basis of the Gateway Technology: The BP reaction is catalyzed by BP Clonase enzyme mix and facilitates the recombination of an *att*B substrate with an *att*P substrate (donor vector) to create an *att*L containing entry clone. The LR reaction, catalyzed by the LR Clonase enzyme mix, facilitates recombination of the entry clone (*att*L substrate), created with the BP reaction, with an *att*R substrate (destination vector) in order to create an *att*B expression clone. This method involved a PCR for creation and amplification of the *att*B substrate, agarose gel electrophoresis, DNA gel extraction, BP reaction, transformation, LR reaction, Pac I digestion, sodium acetate precipitation, transfection of the Pac I digestion product and virus amplification in HEK293 cells.

1.2 Polymerase Chain Reaction

PCR is a technique developed by Kary Mullis in the 1980s[195]. It utilizes the ability of DNA polymerase to synthesize the complementary DNA of a given template strand. PCR enables exponential amplification of a nucleic acid sequence *in vitro*, alterations of sequences and addition of new sequence information e.g. so-called 'tags'. Necessary for a PCR are oligonucleotides (primers) that are synthesized with regard to 5' and 3' ends of the sequence of interest. They will hybridize and thereby facilitate the initiation of the reaction. Repeated cycles of DNA denaturation, primer annealing to their complementary sequences and extension of the sequence by DNA polymerase facilitate the amplification of nucleotide sequences. During heat denaturation at 94-98°C the hydrogen bonds between complementary bases break, yielding two single DNA strands. In the annealing phase the temperature is lowered to enable primer binding to single DNA strands. It is crucial to apply the

appropriate annealing temperature depending on the length of the sequence and on the melting point of the primers. In case, the annealing temperature is too high, it can hamper the primers from binding to the DNA; on the other hand if it is too low the primer might bind incorrectly. During extension/elongation, the last phase of the cycle, free dNTPs from the reaction mixture are used by the DNA polymerase to synthesize a DNA strand complementary to the DNA template strand. The extension temperature depends on the optimum activity temperature of the polymerase used.

For the purposes of Gateway cloning the primers were designed to include the *att* recombination sites necessary for the BP reaction (see Materials p.10).

Listed below are the PCR components and conditions for obtaining the *att*B-flanked PCR product.

Components	
5x KAPA HiFi	10µl
10 mM KAPA dNTP Mix	0.3 mM
10 µM forward primer	0.3 µM
10 µM reverse primer	0.3 µM
Template DNA	0.2 µg
1 U/µl KAPA HiFi DNA Polymerase	1 U
PCR grade water	up to 50 µl

Step	**T[°C]**	**t[min]**	
Initial denaturation	95°C	3 min	x 1 cycle
Denaturation	98°C	20 sec	
Annealing	65°C	15 sec	x 25 cycles
Extension	72°C	15 sec	
Final Extension	72°C	1 min	x1 cycle

For performing the aforementioned PCR the thermocycler S1000 Thermal Cycler (Biorad) was used.

1.3 Agarose gel electrophoresis

Agarose gel electrophoresis is the standard technique for separating DNA fragments by size. DNA fragments are negatively charged, so when an electrical field is applied they migrate through the agarose gel matrix toward a positive electrode. By adjusting the agarose concentration the size of the gel pores changes, thus allowing the separation of a wide range of different-size nucleic acids.

Agarose gels were prepared using TAE (Tris base, acetic acid and EDTA) buffer. The myc-tagged peptides were approximately 600 bp long. For these constructs a 1% gel was used. A DNA-binding dye (GelRed Nucleic Acid Gel Stain) was added to the agarose gel to enable the visualization of bands, which represent DNA fragments. Loading buffer was added to the samples. A DNA ladder (a collection of DNA fragments of known lengths) is used to estimate the size of the DNA fragment (100 bp- or 1 kb-Ladder, New England Biolabs). The separation was performed at 100 V. After separation, DNA molecules were visualized under UV light using INTAS Gel iX Imager. For DNA extraction from the gel, the band was excised and the DNA was purified using the QIAquick Gel Extraction Kit® from Qiagen.

50x TAE buffer

2 M	Tris-HCl
6% (m/v)	Acetic acid
50 mM	EDTA

5x DNA loading buffer

100 mM	EDTA
50% (v/v)	Glycerin
0.1% (m/v)	Bromphenol blue

1.4 BP-Reaction

For performing the BP Reaction (Fig.7) the components listed below were mixed together and then incubated for 2 hours at 25°C in order to yield a sufficient number of entry clones. The PCR product flanked with *att*B recombination sites was transferred through the BP reaction in a donor vector (Fig.8) resulting in an entry clone with kanamycin resistance and a by-product containing the *ccd*B gene which yields no colonies when using standard strains of *E.coli.*

Proteinase K solution was added to stop the reaction and the samples were incubated at 37°C for 10 minutes.

Components	
attB-PCR product	100 fmol
pDONRTM vector	100 fmol
5x BP Clonase Reaction Buffer	4 µl
TE Buffer, pH 8.0	to 16 µl
BP Clonase	4 µl

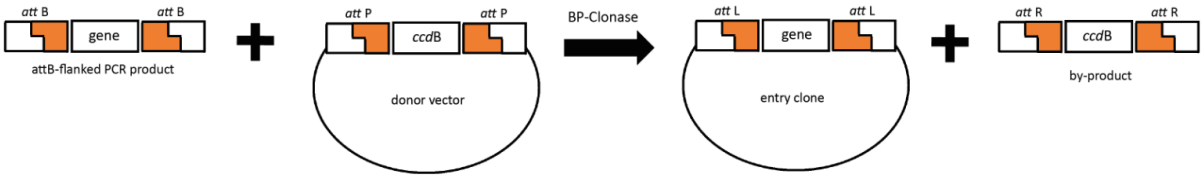

Figure 7: BP-Reaction catalyzed by BP-Clonase. The BP-Reaction facilitates the recombination of an attB-flanked PCR product (attB substrate) with a donor vector (attP substrate) to create an attL-containing entry clone[196].

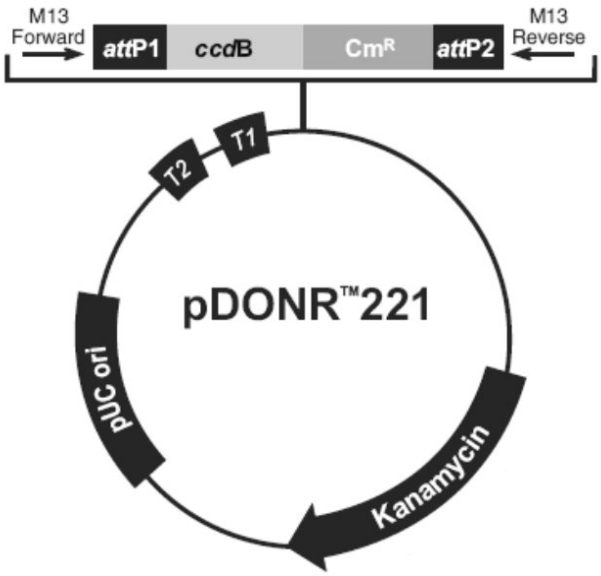

Figure 8: Plasmid vector map of pDONR™221 used in the BP-Reaction as donor vector. Modified from Gateway® Technology, life technologies, invitrogen [196].

1.5 Transformation of *E.coli*

Transformation is the uptake and incorporation of exogenous genetic material by competent bacteria. Competence was artificially induced by creating cells which are passively permeable to DNA under non physiological conditions, such as electric shock[197], heat shock and incubation in appropriate buffers[198].

1.5.1 Transformation by electric shock

DNA was added in an appropriate cuvette containing the electrocompetent bacteria. The sample was then placed in the electroporator for the electric shock. Subsequently, the bacteria were added to LB-medium and incubated at 37°C to allow expression of the antibiotic resistance marker.

LB (lysogeny broth)-Medium:

1,6 % (m/V)	Pepton ex meat
1 % (m/V)	Yeast extract
0,5 % (m/V)	NaCl

1 µl of the BP-Reaction sample was transformed in 50 µl electrocompetent *E.coli* DH10B (Thermo Fisher Scientific) using the MicroPulser Electroporator (Biorad) and 0.1 cm cuvettes at 1.8 kV. Following incubation with LB-medium (1 h; 37°C) a part of the transformation mix was spread on a prewarmed kanamycin LB agar plate and placed in the incubator at 37°C overnight.

LB Agar plates (Petri dishes)

1.2% (m/v)	Agar
0.1 mg/ ml	Ampicillin
or 0.05 mg/ml	Kanamycin

1.5.2 Transformation by heat shock

Through a sudden increase in temperature, pores are created in the plasma membrane of the bacteria allowing plasmid DNA to enter the bacterial cell.

Bacterial cells were thawed on ice and 100 µl were incubated with 1 µg plasmid DNA on ice for 15 to 20 min. The heat shock was applied by incubation at 42°C and then for 50 seconds an immediate incubation on ice for 1 minute followed. 900 µl LB-medium was added and the transformation mix was

incubated for 50 minutes at 37°C. Finally, part of the transformation mix (50 µl or the pellet) is plated on appropriate selective agar plates. The plates were incubated overnight at 37°C.

1.5.3 Chemical transformation

Chemical transformation uses a positive ions rich environment provided by calcium, magnesium and potassium to counteract the electrostatic repulsion between the negative charged plasmid DNA and bacterial cellular membrane, thus allowing the plasmid DNA to enter the cell. This transformation method was used for transforming the ligation reaction into *E.coli* XL-1 Blue.

5x KCM buffer	
500 mM	KCl
150 mM	$CaCl_2$
250 mM	$MgCl_2$

The transformation mix consisted of the following components:

Transformation mix	
10 µl	ligation sample
90 µl	5x KCM buffer
100 µl	chemically competent bacteria

The mix was incubated for 20 minutes on ice followed by 10 minutes at room temperature (RT). Subsequently, 1 ml LB-medium was added to the ligation reaction and the transformation mix was incubated for 50 minutes at 37°C. The mix was then centrifuged at 2655 g for 3 minutes (Eppendorf 5427R) and the supernatant was discarded. The pellet was resuspended in 50 µl supernatant and plated on a selective agar plate which was then incubated at 37°C overnight.

1.6 Verification of positive clones

To verify the clones that have successfully incorporated the plasmid of interest, a control PCR was performed. For this, colonies were picked, inoculated in 3 ml LB-medium with antibiotic and incubated overnight at 37°C. 3 µl of the culture were used as template for the PCR.

Example for a control- PCR

Components	
5x KAPA HiFi Buffer	10 µl
10 mM KAPA dNTP Mix	0.3 mM
10 µM forward primer	0.3 µM
10 µM reverse primer	0.3 µM
Template DNA	3 µl
1 U/µl KAPA HiFi DNA Polymerase	1 U
PCR grade water	ad 50 µl

Example PCR cycle

Step	T[°C]	t[min]	
Initial denaturation	95°C	3 min	x 1 cycle
Denaturation	98°C	20 sec	
Annealing	65°C	15 sec	x 25 cycle
Extension	72°C	15 sec	
Final Extension	72°C	1 min	x1 cycle

The samples were then analyzed using agarose gel electrophoresis.

1.7 Plasmid DNA Purification

The 3 ml cultures of positive clones were inoculated in 100 ml selective LB-medium and incubated overnight at 37°C. After centrifugation (Beckman Coulter Allegra X-15R) for 10 minutes, at 5250 g at 4°C, the cells were harvested and the plasmid DNA was purified using the Plasmid Plus Midi Kit® from Qiagen. DNA concentrations were determined spectrophotometrically at 260 nm using NanoDrop One^{c} (Thermo Scientific). The A_{260}/A_{280} purity ratio should be above 1.6. The A_{260}/A_{230} purity ratio should be above 2. Lower values are an indication of sample contamination[199]. In order to verify that the sequence of the purified plasmid DNA corresponds to the sequence of interest, plasmid DNA from positive clones was sent for sequencing (Eurofins).

1.8 LR-Reaction

The entry clone successfully purified after the BP reaction (Fig.9) recombines with a destination vector (pAd/CMV/V5-DEST; Fig.10) to yield an ampicillin resistant expression clone and a by-product plasmid,

which contains the *ccd*B gene and is therefore unable to give rise to colonies when standard *E.coli* strains are used. For performing the LR Reaction, the components listed below were mixed together and then incubated for at least 2 hours at 25°C in order to yield a sufficient number of expression clones.

Components	
pAdCMV	75 ng
Entry clone	150 ng
5x LR Clonase Reaction Buffer	2 µl
TE-Buffer, pH 8.0	to 8 µl
LR-Clonase	2 µl

Proteinase K solution was added to stop the reaction and the samples were incubated at 37°C for 10 minutes.

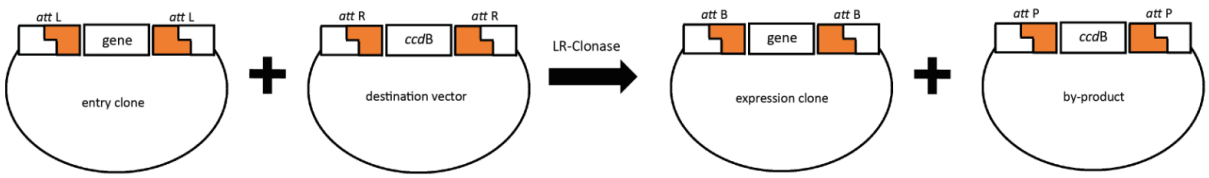

Figure 9: LR-Reaction catalyzed by LR-Clonase. Facilitates recombination of an entry clone (attL substrate) with a destination vector (attR substrate) to create an attB-containing expression clone[196].

The same procedure was then followed as after the BP reaction: transformation by electric shock and verification of the positive clones.

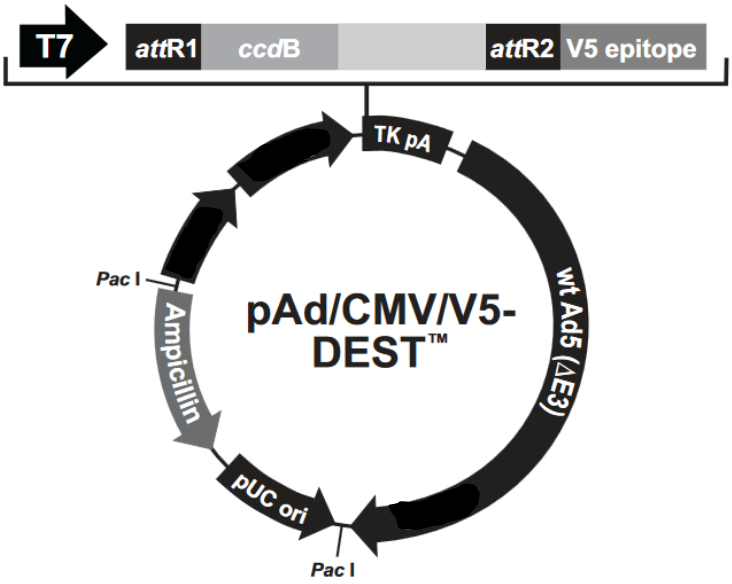

Figure 10: Plasmid vector map of pAd/CMV/V5-DEST™ used in the LR-Reaction as destination vector. Modified from Gateway ® Technology, life technologies, invitrogen [283].

1.9 PacI digestion and DNA precipitation

In order to remove from pAd/CMV/V5-DEST™ the sequence which allows high-copy replication and maintenance in *E.coli* (pUC ori) and to allow exposure of the inverted terminal repeats (ITRs) which are required for viral replication and packaging, the expression vector was digested with PacI (New England Biolabs). The PacI digestion components are listed below:

PacI digestion	
DANN	5 µg
Smart-Cut Buffer	5 µl
PacI	2 µl
H2O	to 50 µl

The reaction was incubated at 37°C overnight.

For DNA precipitation, the digestion reaction was incubated with 5 µl 3M sodium acetate and 275 µl 100 % ethanol at -80 °C overnight. The sample was then centrifuged at 20817 g, 4°C for 15 minutes and the supernatant was discarded. The pellet was washed once with 300 µl 70% ethanol and was centrifuged at 20817 g, 4°C for 3 minutes. Finally the pellet was resolved in 20 µl H_2O.

2. Cell biology methods

2.1 Virus amplification

The adenoviral vector (Ad5) purified after PacI digestion and DNA precipitation is replication deficient. The genome is deleted in the early region (E) 1 often in combination with the E3 region to provide space for alternate gene expression cassettes. The E1 region encodes proteins necessary for the viral life cycle; thus, it is necessary to use a cell line that complements this non-replicating adenoviral vector to produce the adeno-E1 proteins. The E3 region encodes proteins that function in counteracting the immune system and they are not necessary for adenovirus replication in cultured cells[200].

The adenoviral vector was transfected into HEK293 cells using the Effectene Kit (Qiagen) according to instructions of the manufacturer. The cells were adherent and approximately 70% confluent. EC buffer and enhancer were added to the aforementioned (1.9) resolved pellet and the mixture was vortexed and incubated for 5 minutes at RT. Subsequently, effectene (Qiagen) was added, the mixture was again vortexed and incubated for 10 minutes at RT. The exact composition of the effectene transfection complex is listed below. 500 µl growth medium (DMEM, 4.5g/l glucose) was added to the transfection mixture and immediately added to the cells.

Components	
adenoviral vector	20 µl
EC buffer	130 µl
Enhancer	8 µl
Effectene	20 µl

The cells were incubated at 37°C, 5% CO_2 until they were detached due to structural changes caused by viral invasion (cytopathic effect). The cells were then carefully scraped and centrifuged for 10 minutes at 850g and 4°C. The supernatant was aspirated and the pellet was resolved in 1 ml 10 mM Tris, pH 8.0. The cell debris and virus stock contained in the pellet were frozen in liquid nitrogen and thawed in a water bath at 37°C. This procedure was repeated three times. 500 µl were added to cells in a 10 cm plate and the plate was incubated at 37°C. When about 80 % of the cells detached, the cells were centrifuged for 10 minutes at 850 g and 4°C. The supernatant was aspirated and the pellet was resolved in 2 ml 10 mM Tris, pH 8.0. The freeze/thaw cycle mentioned above was repeated three times. 100 µl of the virus stock was added to cells in a 15 cm plate and the rest was stored at -80°C. When the cells detached from the plate the same centrifugation step followed as described above and the pellet was resolved in 3 ml 10 mM Tris, pH 8.0. After three freeze/thaw cycles the virus stock was stored in aliquots at -80°C.

2.2 Primary cells

Neonatal mouse cardiomyocytes (NMCMs) from FVB-N mice were isolated at postnatal day 0-3 using the neonatal heart dissociation kit for mouse and rat from MACS, Miltenyi Biotec. The manufacturer's protocol was used. The neonatal mouse hearts were harvested and transferred into a 10 cm dish containing PBS. Utilizing forceps, the remaining blood was removed as well as the vessels and the remaining connective tissue. Enzyme mix 1 was preheated for 5 minutes at 37°C and 2362.5 µl of the mix were added to 137.5 µl of enzyme mix 2.

Enzyme mix 1	
62.5 µl	Enzyme P
2300 µl	Buffer X

Enzyme mix 2	
25 µl	Buffer Y
12.5 µl	Enzyme A
100 µl	Enzyme D

Enzyme mix 2	
25 µl	Buffer Y
12.5 µl	Enzyme A
100 µl	Enzyme D

The harvested tissue was transferred into the gentleMACS C Tube and 2.5 ml of enzyme mix was added. The C tube was closed, inverted and placed with the cap down. Program 37C_mr_NHDK_1 was started; after termination of the program the C-tube was detached from the gentleMACS Dissociator and 7.5 ml of cell culture medium with FBS were added.

NMCMs medium (pH 7.3)	
5.77 g	MEM
192.5 mg	$NaHCO_3$
0.1%	Vitamin B_{12}
1%	Pencillin/Streptomycin
1%	L-Glutamine
Ad 550 ml	H_2O

The sample was resuspended and strained through a MACS SmartStrainer 70 µm and the strainer was washed with 3 ml of cell culture medium with FBS. Cell suspension was centrifuged at 600 g for 5 minutes and the supernatant was completely aspirated. The pellet was resuspended in 30 ml NMCM medium, the cells were seeded on a 10 cm plate (7.5 ml per plate) and incubated for 1 hour at 37°C (1% CO_2). Finally, the cells were counted using 0.4% (m/v) trypan blue, a stain used in microscopy for

assessment of cell viability, with a Neubauer cell counting chamber. Trypan blue is a vital stain that is not absorbed by healthy viable cells, but stains cells with a damaged cell membrane. Therefore stained cells are considered non-viable and are not taken into consideration for cell counting[201]. When the cell number was determined, the cells were seeded accordingly.

2.3 Cell culture

2.3.1 Subculture

Confluent cells (HEK293, GFP-β_2-AR-HEK293) were passaged as follows. The growth medium was aspirated and the cells were then carefully washed with DPBS. The cells were incubated with Trypsin-EDTA (0.05/0.02 % in PBS-buffer) to induce detaching. Trypsin is a proteolytic enzyme and EDTA chelates ions such as magnesium and calcium, which stabilize adhesion proteins leading to disruption of cell-cell interactions, thus causing the cells to detach from the vessel surface. After aspiration of trypsin, the reaction was stopped by adding growth medium. The cells were resuspended and passaged accordingly.

HEK293 were cultivated at 37°C, 7% CO_2 with the below listed complete medium. The stably transfected cell line GFP-β_2-AR-HEK293 was cultivated at 37°C, 7% CO_2 also with the below listed complete medium with addition of 0.45 mM geneticin (selective antibiotic).

Complete Medium DMEM (4.5 g glucose)	
10% (v/v)	Fetal Calf Serum (FCS)
2 mM	L-Glutamine
100U/ml	Penicillin
100µg/ml	Streptomycin

2.3.2 Cryoconservation of cells

For long term storage, cells were frozen and stored in liquid nitrogen. A freezing medium which contains a cryoprotectant such as DMSO is required in order to avoid freezing damage[202].

The cells were washed with DPBS and detached from the plate surface with Trypsin-EDTA. They were then resuspended with growth medium and centrifuged for 5 minutes, at 200g, at RT (Eppendorf 5702). The supernatant was aspirated and discarded. The pellet was resuspended in cold freezing medium (composition see below) and 1 ml was added to each CryoPure tube (Sarstedt). The CryoPure tubes were placed in Nalgene® Mr. Frosty Cryo Freezing Container which was filled with isopropanol. It enables a gentle 1°C/minute rate of cooling when placed at -80°C. After at least four hours the tubes with the cells were placed in the liquid nitrogen container.

Freezing medium

70%	DMEM (4.5 g glucose)
10%	DMSO
20%	FCS

2.3.3 Thawing of cells

The tube with the cells was removed from the liquid nitrogen container and held under running warm water or shortly placed in a water bath at 37°C until the cells were thawed. The cells were carefully aspirated, transferred into a 15 ml tube with warm growth medium and centrifuged for 5 minutes at 200 g at RT. The supernatant was discarded since it contained DMSO which is toxic for the cells, the pellet was resuspended in growth medium and added to a culture plate with growth medium.

2.3.4 Cell counting with the Neubauer chamber

The Neubauer chamber (Fig.11) is a thick glass plate with the size of a glass slide. Neubauer chamber's counting grid is 3 mm^2 and is divided into 9 large squares. The large central square is divided into 25 medium squares with double or triple lines. Each of these 25 squares are again divided into 16 small squares (*Figure 2.3.4.1*). The glass cover is a square glass slide which is placed on the top of the Neubauer chamber, covering the central area.

With a pipette, 20 µl of the cell suspension were drawn up carefully. The pipette tip was placed against the edge of the cover glass and the liquid was slowly expelled until the counting chamber was full due to capillary action. The cells located in the large corner squares (*Figure 2.3.4.1* -marked in red) were counted and multiplied by 10^4 in order to obtain the amount of cells in 1 ml.

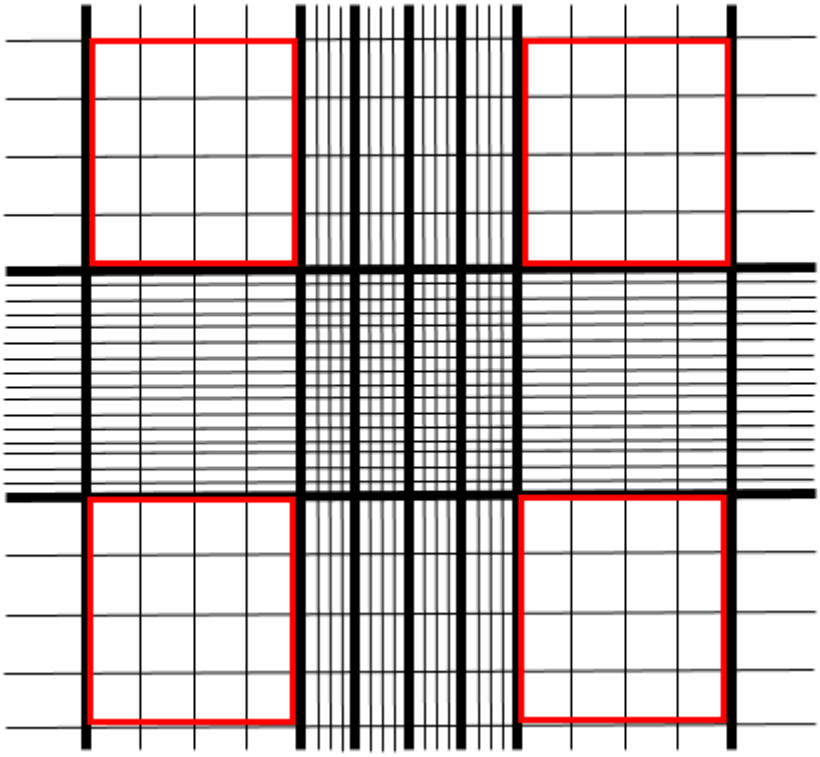

Figure 11: Neubauer cell counting chamber. Corner squares marked in red are used for cell counting.

2.3.5 Coating of plates and coverslips

The glass coverslips (Marienfeld 24 mm) used for confocal microscopy and life cell imaging were coated with sterile poly-d-lysine (0.1 mg/ml in DPBS). The coverslips were placed in the wells of a 6-well plate, were covered with poly-d-lysine and incubated in the dark at RT for at least 30 minutes. Poly-d-lysine was then aspirated and the coverslips were washed with DPBS prior to the cell suspension addition. Poly-d-lysine is a positively charged polymer and through its interaction with negatively charged cells or proteins it improves cell adherence. Furthermore, Poly-D-lysine as an artificial product, can be resistant to enzymatic degradation and therefore prolong cell adherence. [203]

The 96-well plate used for the CardioExcyte96 (Nanion) experiments was coated with sterile fibronectin (1:100 in DPBS). The coated plate was placed in the incubator at 37°C, 5% CO_2 for at least one hour. Fibronectin is a glycoprotein which promotes cell adhesion and attachment through its central cell-binding domain, an Arg-Gly-Asp amino acid sequence[204].

2.4 Transfection methods

2.4.1 Calcium phosphate precipitation

The principle of calcium phosphate co-precipitation involves mixing DNA with 2.5 M calcium chloride in a 2xBBS buffer solution to generate a calcium-phosphate–DNA co-precipitate, which is then dispersed onto cultured cells. The DNA co-precipitate binds to the cell surface, and the DNA enters the cell through endocytosis.

2xBBS-Buffer (pH 6.95)

50 mM	N,N-Bis(2-hydroxyethyl)-2-aminoethanesulfonic acid
280 mM	NaCl
1.5 mM	Na_2HPO_4

DNA was diluted in water. $CaCl_2$ and 2xBBS were added, the mixture was vortexed to induce the complex formation and then incubated for 10 minutes at RT. An example for a calcium phosphate transfection mix is listed below. After incubation the complex was added onto the cells drop-wise, the cells were gently swirled to disperse the transfection complex into the media and were then incubated for 48 hours at 37°C, 5%CO_2.

Calcium phosphate transfection complex

Transfection mix	
450 µl	H_2O
50 µl	$CaCl_2$
0.5 -10 µg	DNA
500 µl	2xBBS Buffer

2.4.2 Adenoviral transduction

Transduction is the gene transfer into a cell by a virus or a viral vector. Here, the adenoviral vector pAd/CMV/V5 was used to transduce neonatal mouse cardiomyocytes (NMCM).

The cells were transduced 24 hours after they were isolated using a stock solution of the virus at a 1:2000 dilution in cardiomyocyte medium without FCS. The appropriate volume of the virus stock solution to achieve adequate expression was directly introduced to the cells. All the experiments took place approximately 48 hours after transduction to allow protein expression.

2.5 Protein biochemistry methods

2.5.1 Cell lysates

2.5.1.1 Chemical disruption with detergents

Depending on the experiment to be performed, the appropriate lysis buffer was selected. For phosphorylation assays, the growth medium was aspirated and 1 ml for a 10 cm plate cold RIPA (Radioimmunoprecipitation assay) buffer containing protease and phosphatase inhibitors (1% PI, 1% PMSF and 10% IBX) was added. RIPA buffer contains sodium deoxycholate and sodium dodecyl sulfate (SDS) which are anionic detergents effective in disrupting all membranes and denaturing proteins, therefore dissociating protein-protein interactions. Furthermore, it contains Nonidet P-40, a milder nonionic detergent. The plate was placed on ice and the cells were scraped off with a cell scraper. The cell suspension was centrifuged (Eppendorf 5427R) for 15 minutes at 20817 g at 4°C to enable the removal of cell debris. The supernatant was transferred to a clean tube and 4x Laemmli loading buffer was added.

RIPA buffer

50 mM	Tris (pH 7.4)
150 mM	NaCl
1% (v/v)	Nonidet P-40
0.5% (m/v)	Sodium deoxycholate
0.1% (m/v)	Sodium dodecyl sulfate (SDS)
1 mM	EDTA

100x Protease inhibitor mix (PI)

0.1% (m/v)	Trypsin inhibitor soybean
25 mM	Benzamidine
50 mM	Tris (pH 7.4)

100x PMSF

100 mM	Phenylmethylsulfonyl fluoride (PMSF)

10x IBX

500 mM	NaF
50 mM	$Na_4P_2O_7$
1 mM	Na_3VO_4
0.02% (v/v)	NaN_3

4x loading buffer

200 mM	Tris-HCl (pH 6.8)
8% (m/v)	SDS
40% (m/v)	Glycerin
20% (v/v)	2-mercaptoethanol
0.05% (m/v)	Bromophenol blue

For co-immunoprecipitation of Flag-β_2AR in HEK293 cells, triton lysis buffer supplemented with protease inhibitors (1% PI, 1% PMSF) was used. Triton X-100 is a not denaturing, nonionic detergent, which has a polar group head that disrupts the hydrogen bonding in lipid bilayers and ultimately demolishes the integrity of the lipid membrane at the critical micelle concentration. Thus, the integrity of the membrane is destroyed releasing the cellular contents. Triton X-100 is appropriate for solubilizing membrane proteins and for isolating cytoplasmic proteins. Thereby, proteins retain their native state and protein-protein interactions can be preserved enabling co-immunoprecipitations. The cells were scraped off with a cell scraper and incubated with ice-cold triton lysis buffer for 1 hour, with end-over-end agitation at 4°C. The cell suspension was centrifuged (Eppendorf 5427R) for 15 minutes, at 20817 g, at 4°C to enable the removal of cell debris. The supernatant was used for performing co-immunoprecipitations.

Triton lysis buffer

50% (v/v)	2x TSE
10% (v/v)	10x IBX
1% (v/v)	Triton-X
1% (v/v)	PI
1% (v/v)	PMSF

2.5.1.2 Mechanical cell disruption

For investigating protein-protein interactions with RKIP by co-immunoprecipitation, the cells were lysed by sonication and a detergent free buffer.

The growth medium was aspirated and 1 ml for a 10 cm plate cold DPBS buffer containing protease and phosphatase inhibitors (1% PI, 1% PMSF, 10% IBX) was added. The plate was placed on ice and the cells were scraped off with a cell scraper. The cell suspension was sonicated with SONOPULS HD 4100, sonotrode BR30, amplitude 51% (Bandelin) for 2 seconds and was centrifuged (Eppendorf 5427R) for 15 minutes, at 20817 g, at 4°C to enable the removal of cell debris. The supernatant was transferred to a clean tube and 4x Laemmli loading buffer was added.

2.5.2 Analysis of protein concentration

The protein concentration of cell lysates was determined with the Pierce™ Coomassie Plus (Bradford) Assay Kit. A colorimetric reagent with Coomassie G-250 facilitates the detection and quantitation of total protein. A spectral shift from the brown form of the dye (absorbance at 465nm) to the blue form of the dye (absorbance at 610nm) is achieved when protein binds to the Coomassie dye in the reagent acidic environment. The optimal wavelength to measure the blue color from the Coomassie dye-protein complex is 595 nm[205].

The lysates, blank and standard solutions were pipetted into the wells of a 96-well plate. After addition of the colorimetric reagent, the plate was shortly shaken (Eppendorf ThermoMixer C) and incubated for 10 minutes at RT. The absorption was measured at 595nm (Tecan Spark 20M) and the concentration was calculated using a standard curve.

2.5.3 SDS-Polyacrylamide gel electrophoresis (SDS- PAGE)

Proteins are denatured by the negative charges of SDS (sodium dodecyl sulfate,) which is a major constituent of the Laemmli loading buffer. The samples are loaded onto a polyacrylamide gel which consists of a stacking and separating part. The stacking part of the gel is necessary for concentrating all proteins in one band; the separating gel allows separating of proteins based on their molecular weight. The gel is placed in an electrophoresis running buffer and a voltage is applied (200 V). These negatively charged molecules are migrating toward the anode and since the charge-to-mass ratio is nearly the same among SDS-denatured proteins, the separation depends entirely on molecular mass. As the gel acts like a sieve, large proteins migrate slowly through the gel and small proteins faster.[206] The Mini-PROTEAN® Tetra Cell Electrophoresis-System from BioRad was used.

Stacking gel (4% acrylamide)	
1.5 ml	Rotiphorese Gel®30
3 ml	4x stacking gel buffer
7.5 ml	H_2O
120 µl	ammonium persulfate
12 µl	TEMED

4x stacking gel buffer	
0.5 M	Tris pH 6.8
0.4% (m/v)	SDS

Separating gel (12% acrylamide)	
12 ml	Rotiphorese Gel®30
7.5 ml	4x separating gel buffer
10.5 ml	H2O
195 µl	ammonium persulfate
15 µl	TEMED

4x separating gel buffer	
1.5 M	Tris pH 6.8
0.4% (m/v)	SDS

10x SDS running buffer	
0.25 M	Tris-HCl
1.92 M	Glycine
1% (m/v)	SDS

2.5.3 Protein staining

Proteins are separated electrophoretically and the gel is transferred in a Coomassie Brilliant Blue R-250 staining solution. The Coomassie dye binds to proteins through Van der Waals attractions and through ionic interactions between positive protein amine groups and dye sulfonic acid groups. Coomassie R-250 can detect as little as 0.5 µg/cm^2 of protein[207].

The SDS-gel was incubated for 20 minutes in Coomassie staining solution on the shaker at RT. The gel was then washed with destaining solution until the excess on staining solution was removed and clear protein bands were visible.

Staining solution

45% (v/v)	CH_3OH
2.5 g	Brilliant Blue R250
45% (v/v)	H_2O
10% (v/v)	CH_3COOH

Destaining solution

30% (v/v)	CH_3OH
10% (v/v)	CH_3COOH
60% (v/v)	H_2O

2.5.4 Electrophoretic transfer of proteins onto membranes (Western Blot)

After gel electrophoresis, the separated proteins are transferred (blotted) onto a second matrix, usually a polyvinylidene difluoride (PVDF) or nitrocellulose membrane. This procedure is termed as Western Blot[208,209]. Through an electric field oriented perpendicular to the surface of the gel the negatively charged proteins migrate from the gel onto the binding matrix (membrane). The membrane is placed between the gel surface and the positive electrode in a sandwich. The sandwich includes filter paper at each end to protect the gel and blotting membrane placed in such a way to enable the protein transfer.

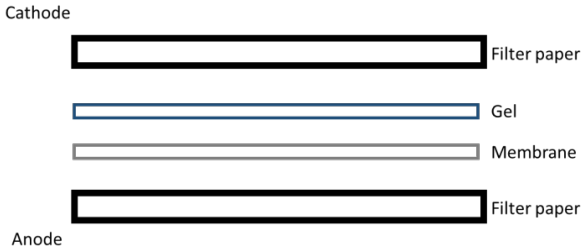

Figure 12: Sandwich assembly for western blot.

For these experiments either PVDF membrane, activated with methanol, or nitrocellulose membrane was used. The transfer was performed with the semi-dry system Trans-Blot® Turbo™ using the supplied transfer buffer and stacking paper. The programs used were the 'Mixed molecular weight' (1.3A, 25V, 7 minutes) for 1.0 mm gels and the '1.5mm Gels' for 1.5 mm gels (1.3A, 25V, 10 minutes).

2.5.5 Immunodetection

The transfer of proteins onto a membrane by western blot enables their detection via antibodies. To avoid non-specific binding of antibodies on the membrane surface, the membrane is incubated in a blocking solution. Subsequently, the membrane is probed with an antibody directed to the protein of interest (primary antibody) and thereafter another antibody specific to the host species of the primary antibody (secondary antibody). Secondary antibodies can be conjugated to an enzyme, a fluorescent dye or another molecule to enable their detection[210].

The membrane was incubated with milk blocking solution for one hour at RT. The blocking solution was removed, the membrane was washed using BSA washing buffer and was incubated with the primary antibody in an appropriate dilution either overnight at 4°C or for a few hours at RT. After the incubation time the membrane was washed with BSA washing buffer four times, for 5 minutes and was then incubated for one hour with the secondary antibody. Finally, the membrane was washed with BSA washing buffer four times, for 5 minutes. The secondary antibodies used were either conjugated with horseradish peroxidase (HRP) or they were conjugated with Infra-Red dyes. HRP was detected on films using the Pierce® ECL Plus Western Blotting Substrate Kit in a dark room; Infrared dyes were detected using Odyssey CLx from LI-COR.

Quantification of western blots was performed with ImageJ. Adobe Illustrator and Adobe Photoshop were used for creating figures.

BSA washing buffer

0.25% (m/v)	Albumin Fract. V (BSA)
150 mM	NaCl
50 mM	Tris (pH 7.4)
0.2% (v/v)	Nonidet P-40

Blocking milk

5% (m/v)	Nonfat dried milk
100 mM	NaCl
10 mM	Tris (pH 7.4)
0.1% (v/v)	Tween 20

2.5.6 Stripping of Western Blot membranes

When probing for multiple proteins of interest a single membrane may be re-probed after stripping with a low pH buffer[211].

For reprobing, the membrane was shortly washed with BSA wash buffer and was incubated in stripping buffer for 2 hours at RT. After stripping the membrane was blocked, washed and incubated with primary and secondary antibody accordingly.

Stripping buffer

100 mM	Glycine (pH 2.5)
0.1% (m/v)	SDS

2.5.7 Detection of protein-protein interactions via co-immunoprecipitation

Antibody coupled resin can be used for detecting protein-protein interactions and isolating protein complexes of interest from cellular extracts using specific antibodies under non-denaturing conditions. Bait and prey proteins interact *in vivo* and following incubation with the antibody coupled resin, the bait and therefore the formed protein complex bind to the antibody and can then be precipitated[212]. Co-precipitated proteins are analyzed by SDS-PAGE followed by western blot detection to verify the identity of interaction partners. This method was used to detect a possible interaction between RKIP and myc-GRK2/3/5 1-53, GRK2/3/5 54-185, GRK2/3/5 1-185 and between β_2AR and GRK2/3/5 1-53, GRK2/3/5 54-185, GRK2/3/5 1-185.

Protein A Sepharose beads (8 µl per sample) were incubated overnight with Flag antibody (0, 4 µg per sample) in DPBS-buffer. Flag-RKIP or Flag-β_2AR were co-transfected with the above-mentioned peptides in 10cm cell culture plates with HEK293 cells. For the immunoprecipitation with Flag-RKIP and Flag-β_2AR different protocols were followed.

Flag-RKIP expressing cells were scratched from cell culture plates using DPBS-buffer containing 10% IBX, 1% PI and 1% PMSF and lysed via sonication. The lysates were centrifuged to remove cell debris. 900 µl of the lysate was incubated with end-over-end agitation with 50 µl Flag-coupled Protein A Sepharose resin in DPBS-buffer for 1.5 hours at 4°C. After repeated cycles of washing with DPBS, Laemmli loading buffer was added to the beads.

For Flag- β_2AR expressing cells triton lysis buffer was used. The cells were homogenized and incubated with ice-cold triton lysis buffer for 1 hour, with end-over-end agitation at 4°C. Following centrifugation to remove cell debris, the lysate was incubated for 30 minutes with non-coupled beads, with end-over-

end agitation at 4°C in order to remove proteins from the sample that are prone to nonspecifically attaching to the beads (preclearing). The supernatant was removed and added to the beads probed with anti-Flag antibodies. The sample was incubated for 2 hours with end-over-end agitation at 4°C. After repeated cycles of washing with triton lysis buffer, Laemmli loading buffer was added to the beads. The samples were analyzed with gel electrophoresis and western blotting using anti-Flag and anti-myc antibodies in both protocols.

Triton Lysis buffer

50% (v/v)	2x TSE
10% (v/v)	10x IBX
1% (v/v)	Triton-X
1% (v/v)	PI
1% (v/v)	PMSF

2.5.8 In vitro detection of protein-protein interactions via pull down assays

The pull-down assay is an *in vitro* method used to analyze the existence of a protein–protein interaction where a tagged bait protein is captured on an immobilized affinity ligand specific for the tag thereby enabling the binding and purification of the prey protein[213]. This method was used to analyze the interaction between RKIP and GRK2/3/5 1-53, GRK2/3/5 54-185 and GRK2/3/5 185. Glutathione Sepharose 4 B (GS4B) beads (30 µl per sample) were incubated with 400 µmol purified GST or GST-tagged GRK2/3/5 1-53, 54-185 and 1-185 overnight with end-over-end agitation at 4°C. Subsequently, the samples were incubated for two hours with a 5% albumin solution to block unspecific binding. Flag-RKIP was transfected in a 15 cm cell culture plate per sample and the cells were lysed in DPBS-buffer containing 10% IBX, 1% PI and 1% PMSF via sonication. After the washing of the beads coupled with the purified proteins, the Flag-RKIP lysates were added and the beads were incubated overnight with end-over-end agitation at 4°C. The beads were washed five times, Laemmli loading buffer was added and the samples were analyzed with gel electrophoresis and western blotting using anti-Flag and anti-GST antibodies. Washing and incubation steps were performed with pull down assay buffer.

Pull down assay buffer (pH 7.4)

20 mM	HEPES
50 mM	NaCl
1 mM	EDTA

2.6 Protein expression and purification

2.6.1 His_6-RKIP

To express His_6-RKIP (His-RKIP) *in E.coli* the pET expression system was utilized which is based on the T7 promoter-driven system, originally developed by Studier and colleagues[214–216]. The RKIP gene from rat was cloned with an N-terminal His_6 tag in the pET-3c Vector (Agilent Technologies) and the vector was then transferred in *E.coli* BL21 DE3 via heat shock transformation. These bacteria are lysogens of bacteriophage DE3 and carry the lacI gene, the lacUV5 promoter, and the gene for T7 RNA polymerase. Once a DE3 lysogen is formed, the lacUV5 promoter, which is inducible by isopropyl-β-D-thiogalactopyranoside (IPTG), directs transcription of the T7 RNA polymerase gene, thereby initiating the transcription of the target DNA in the plasmid[217].

For the purification of polyhistidine tagged proteins, immobilized metal ion affinity chromatography (IMAC) was applied. IMAC is based on the specific covalent bond of amino acids to metals, in particular histidine, to metals. A HisTrap FF Crude column (GE Healthcare), which is a ready-to-use column in combination with the ÄKTA pure chromatography system (GE Healthcare), a fast protein liquid chromatography (FPLC) system was used. HisTrap FF Crude columns are prepacked with precharged Ni Sepharose 6 Fast Flow. Sepharose affinity resin consists of highly cross-linked agarose beads coupled with a chelating group which is precharged with nickel that selectively and reversibly retains histidine-tagged proteins. The bound protein can then be eluted by adding imidazole, a compound that acts as a metal ion ligand and thereby competitively displaces the tagged protein from the beads.

To express His-RKIP, the expression plasmid was transformed into competent *E.coli* BL21 (DE3), was plated on ampicillin selection plates and incubated overnight at 37°C. A single colony was picked and resuspended in 10 ml LB-medium supplemented with ampicillin (100 µg/ml) to produce a starter culture. Following overnight incubation at 37°C in a shaking incubator the starter culture was inoculated in 400 ml LB-medium supplemented with ampicillin (100 µg/ml) and was again incubated in the shaking incubator until OD_{600} reached 0.4. The protein expression was then induced by addition of IPTG (end concentration 200 µM) and the culture was incubated further for 4 hours at 37°C. To harvest the bacteria, the culture was centrifuged for 10 minutes at 3400 g at 4°C (Beckman Avanti J-25) and the pellet was shock frozen in liquid nitrogen and stored at -80°C. Prior purification the pellet was thawed on ice and resuspended in 15 ml buffer 1.

Buffer 1

20 mM	Tris (pH 7.4)
300 mM	NaCl
7 mM	β-mercaptoethanol

The resuspended bacteria were lysed via sonication (Bandelin Sono Puls HD 200; 3x10 bursts, Cycle 30, Power MS72/D) and centrifuged for 1 hour at 165000 g at 4 °C (Beckman Le-70). The supernatant was filtered through a 0.2 µM sterile filter (Sartorius). The system (Äkta pure) was equilibrated with His-binding buffer.

His-binding buffer (pH 7.4)

20 mM	NaH_2PO_4
500 mM	NaCl

Following equilibration, the sample was loaded onto the column at a flow rate of 0.5 ml/ minute. After sample application, the column was repeatedly washed with His-binding buffer and finally the bound protein was eluted applying His-elution buffer at a flow rate of 0.5 ml/ minute.

His-elution buffer (pH 7.4)

20 mM	NaH_2PO_4
500 mM	NaCl
150 mM	imidazole

The elution fractions containing the purified protein were identified from the chromatogram, were collected, pooled, filtered and equilibrated in His-elution buffer using Amicon® Ultra centrifugal filter units in order to minimize the imidazole concentration and concentrate the purified protein. After repeating the filtering step 6 times adding His-elution buffer (without imidazole) in each step, the remaining sample was collected and its concentration was determined using NanoDrop One^c (Thermo Scientific). The purified protein was aliquoted, shock frozen and stored at -80°C.

2.6.2 Glutathione-S-transferase (GST)-tagged peptides

To express and purify the GST-tagged peptides of GRK2, GRK3 and GRK5 consisting of either of amino acids 1 to 53, 54 to 185 or 1 to 185 the gene fragments were inserted into the MCS of the pGEX vector (performed either by Ulrike Zabel or Marketa Andrsova). The pGEX expression system is similar to the pET expression system. It contains a lacI gene that is responsible for expressing a repressor protein which binds to the operator region of the *tac* promoter and represses target protein expression[218]. When the promoter is chemically induced using IPTG, GST-tagged recombinant proteins are expressed. Furthermore, the pGEX vector used, offered the possibility of cleaving the tagged protein from GST using a site-specific protease, thrombin, whose recognition sequence is located immediately upstream from the multiple cloning site.

For purifying GST-tagged proteins, affinity chromatography was applied. Affinity chromatography is based on a specific interaction between one specific molecule in the lysate and a second molecule that is immobilized to the stationary phase. A GSTrap HP column (GE Healthcare) which is a ready-to-use column, prepacked with Glutathione Sepharose High Performance resin in combination with the ÄKTA pure chromatography system (GE Healthcare) were used for purifying GST-tagged peptides/proteins. High Performance sepharose resin contains immobilized glutathione that selectively and reversibly retains GST-tagged proteins. The bound protein can then be eluted under mild, nondenaturing conditions using reduced glutathione which displaces the tagged protein from the beads.

To express GST-tagged peptides, the expression plasmid was transformed into competent *E.coli* BL21 (DE3), was plated on ampicillin selection plates and incubated overnight at 37°C. A single colony was picked and resuspended in 10 ml LB-medium supplemented with ampicillin (100 µg/ml) to produce a starter culture. Following overnight incubation at 37°C in a shaking incubator 5 ml of the starter culture were inoculated in 400 ml LB-medium supplemented with ampicillin (100 µg/ml) and was again incubated in the shaking incubator until OD_{600} reached 0.5-0.8. The protein expression was then induced by addition of IPTG (200 µM) and the culture was incubated further overnight at 30°C. The bacteria were harvested by centrifugation for 5 minutes at 3400 g at 4°C (Beckman Avanti J-25). The pellet was resuspended in 7.5 ml disruption buffer and was centrifuged again for 5 minutes at 5250 g at 4°C (Beckman Coulter Allegra X-15R).

Disruption buffer

20 mM	Tris (pH 7.6)
100 mM	NaCl
2 mM	DTT
1 mM	EDTA

The pellet was shock frozen in liquid nitrogen and stored -80°C.

For purification, two different protocols were followed due to the insolubility and low yield expression of GST-GRK2 1-185 and GST-GRK3 1-185. For these two peptides the following 'Phosphate-BME' protocol was applied[219].

2.6.2.1 Purification using the 'Phosphate-BME' protocol

'Phosphate-BME' buffer supplemented with 0.5 mg/ ml lysozyme was used for thawing and resuspending the bacteria pellet.

Phosphate-BME buffer

0.1 M	NaH_2PO_4
0.1%	β- mercaptoethanol
12,7 mM	EDTA

The suspension was incubated on ice for 30 minutes and a freeze/thaw cycle followed, i.e. the sample was frozen in liquid nitrogen and rapidly thawed in a 65°C water bath. Solid urea was added (6 M) and the sample was inverted until urea was solubilized. Ever since the reversible denaturation of proteins by chaotropic agents such as urea were shown, these compounds are predominantly used to dissolve inclusion bodies. The sample was sonicated two to four times on ice for 30 seconds and then the volume was increased to 20 ml with 6 M urea. After centrifugation at 17,210 g for 10 minutes, the supernatant was decanted in dialysis tubing (MWCO 12,000-14,000; Fisherbrand) in order to gradually remove urea and allow the proteins to refold. The sample was dialyzed once against 1x PBS containing 3 M urea for at least three hours, following dialysis against 1x PBS containing 1 M urea for 3 hours, and three times against 1x PBS (2x 3 hours, 1x 16 hours). The contents of the dialysis tubing were transferred into a centrifuge tube and were centrifuged at 17,210 g for 10 minutes. The protein solution was collected and purified as described below.

10X PBS

1.37 M	NaCl
26.8 M	KCl
101 mM	Na_2HPO_4
15 mM	KH_2PO_4

2.6.2.2 Standard purification protocol

For the rest of the peptides, the pellet was thawed on ice and resuspended in 15 ml disruption buffer. The resuspended bacteria were lysed via sonication (Bandelin Sono Puls HD 200; 3x10 bursts, Cycle 30, Power MS72/D) and centrifuged for 1 hour at 16,5000 g at 4 °C (Beckman Le-70). The supernatant was filtered through a 0.2 µM sterile filter (Sartorius). The purification system (Äkta pure) was equilibrated with GST-binding buffer.

GST-binding buffer pH 7.3

140 mM	NaCl
2.7 mM	KCl
10 mM	Na_2HPO_4
1.8 mM	$KHPO_4$

Following equilibration, the sample was loaded onto the column at a flow rate of 0.5 ml/ minute. After sample application the column was repeatedly washed with GST-binding buffer and finally the bound protein was eluted applying GST-elution buffer freshly supplemented with reduced glutathione at a flow rate of 0.5 ml/ minute.

GST-elution buffer pH 8

50 mM	Tris-HCl
2 mM	DTT
10 mM	Reduced glutathione

The elution fractions containing the purified protein were identified via the chromatogram, were collected, pooled, filtered ans equilibrated in GST-elution buffer (without reduced glutahione) using Amicon® Ultra centrifugal filter units in order to minimize the reduced glutathione concentration and concentrate the purified protein. After repeating the filtering step 6 times adding GST-elution buffer

(without reduced glutathione) in each step, the remaining sample was collected and its concentration was determined using NanoDrop One^{c} (Thermo Scientific). The purified protein was aliquoted, shock frozen and stored at -80°C.

2.7 Methods for detecting β_2-adrenergic receptor (β_2-AR) activity

2.7.1 Analysis of β_2-AR phosphorylation in GFP-β_2-AR-HEK293 cells

To investigate whether the β_2-AR phosphorylation was affected in the presence of the peptides at a similar extent like in the presence of RKIP, GFP-β_2-AR-HEK293 cells were co-transfected with either of the peptides, stimulated with 1 µM isoproterenol for 10 minutes and lysed with RIPA buffer containing 10% IBX, 1% PI and 1% PMSF. After the addition of Laemmli, the samples were analyzed using SDS-PAGE. The proteins were then transferred onto PVDF membranes and the phosphorylation was detected using anti-phospho β_2-AR antibodies.

2.7.2 Analysis of protein kinase A (PKA) activity in GFP-β_2-AR-HEK293 cells

In order to examine whether downstream signaling of the receptor is influenced by the peptides in a similar manner as by RKIP, the phosphorylation of phosducin, a substrate of PKA, was investigated in absence as well as in presence of the peptides. GRK2 and phosducin were co-transfected with either of the peptides or RKIP. The following day the cells were treated with FCS-free medium. Two days after transfection, the cells were incubated with 100 µM 3-isobutyl-1-methylxanthine (IBMX) for 25 minutes at 37°C. IBMX is a selective phosphodiesterase inhibitor which blocks the breakdown of intracellular cAMP and thereby enhances cAMP-mediated effects such as PKA activation. Subsequently, the cells were stimulated with 1 µM isoproterenol for 10 minutes. The cells were lysed with phosphorylation assay buffer, sonicated and centrifuged at 20,817 g for 15 minutes (Eppendorf 5427R) to remove cell debris.

Phosphorylation assay buffer

20 mM	HEPES
2 mM	EDTA
10 mM	$MgCl_2$

The lysates were mixed with 4x Laemmli sample buffer and they were analyzed via SDS gel electrophoresis and immunodetection using anti-PKA-substrate antibodies.

2.8 Fluorescence based methods

2.8.1 Confocal microscopy

In order to provide insight regarding the effect of the peptides on β-AR internalization, confocal live cell imaging was performed on Leica TCS SP8 CTR advanced system using GFP-β_2-AR-HEK293 cells which constitutively overexpress GFP-tagged β_2-AR and thereby enable live imaging of the receptor in the cell membrane. Stimulation of β-ARs with isoproterenol leads to sequential recruitment of β-arrestin, AP-2 adaptor protein, clathrin, and dynamin to the receptor complex, resulting in internalization and endocytosis[220]. To investigate the effect of the peptides on receptor internalization the peptides were cloned into pmCherry1-C1 to fuse the fluorophore mCherry to the C-terminus of the respective peptides in order to facilitate the identification of peptide expressing cells via fluorescence microscopy. Cells were cultured on glass coverslips (Marienfeld), which were coated with poly-d-lysine in 6-well plates. Using the Effectene Transfection Reagent Kit (Qiagen) the cells were transfected according to the manufacturer's protocol with $pcDNA_3$ or the peptides. On the next day the medium was exchanged with FCS deprived medium (0% FCS) and two days later the measurement was performed. The coverslip was carefully removed from the well of the 6-well plate and was placed into a coverslip holder used for live cell imaging; 1 ml of FCS deprived medium was added. The microscope chamber was heated to 36°C. Confocal images were taken with a 20× objective and a scale bar is shown in each picture. Cells were stimulated with 1 µM isoproterenol and immediately a sequential recording of images was initiated. Settings for recording were kept constant at 1024 × 1024 pixel format and line average 16. Images were taken every minute for 10 minutes. GFP was excited with a diode laser at 488 nm laser line according to the manufacturer's settings and fluorescence intensities were recorded from 494 to 555 nm. Laser intensity was set to 0.1–2%. mCherry was excited at 552 nm laser line and fluorescence intensities were recorded from 555 to 693 nm. Laser intensity was set to 2–6%. For quantitative analysis of the β_2-adrenergic receptor internalization, fluorescence intensities were recorded over time in manually determined regions of interest (ROIs) which were defined including the inner cell and excluding the cell membrane using the LAS X software provided by the manufacturer (Leica). For the analysis of confocal images the Leica LAS X software was used. Adobe Illustrator and Adobe Photoshop were used for creating figures.

2.8.2 Paraffin fixation

Cell fixation serves the preservation of cellular architecture and composition of cells in biological material and therefore also analysis of cell size and protein localization. There are four types of chemical fixation: crosslinking fixatives (e.g. aldehydes), precipitating fixatives (e.g. alcohols), oxidizing agents (e.g. osmium tetroxide) and the metallic group (e.g. mercuric chloride) of fixatives. For fixing neonatal mouse cardiomyocytes (NMCM), 4% paraformaldehyde (PFA) in PBS was used. PFA facilitates cross-linking between proteins or proteins and nucleic acids through hydroxymethylene bridges[221]. This preserves the secondary structure of proteins[222].

To achieve fixation, the cells were washed twice with DPBS, incubated for 10 minutes at RT with the 4% PFA solution and were washed again with DPBS.

Procedure for preparing the 4% PFA solution:

4g PFA has to be solubilized at 60°C with continuous stirring

Then, addition of 1M NaOH until PFA is completely solubilized (pH 7.5)

The solution needs to be stirred during cool-down and aliquots can be stored at -20°C.

2.8.3 Phalloidin staining

Phalloidin belongs to phallotoxins, a group of naturally occurring bicyclic heptapeptides that bind to actin and binds to actin filaments more tightly than to actin monomers[223]. For these experiments Alexa Fluor 488-labeled phalloidin was used for F-actin labeling providing high binding selectivity and photostability. Visualization of NMCMs and their cross sectional area through fluorescently-labeled phalloidin enabled the analysis of cell size.

NMCMs were cultured on poly-d-lysine coated glass coverslips (Marienfeld) (100.000 cells/12-well). On the next day, medium was exchanged to 1% FCS-NMCM medium and cells were transduced. The following day the medium was exchanged with FCS deprived medium for 24 hours. Then the cells were treated with either 5 µM isoproterenol in medium supplemented with ascorbic acid (100 µM) or with 4 µM phenylephrine for 24 hours to induce hypertrophy and fixated using paraformaldehyde as described above. To allow the fluorophore to enter the cell, permeabilisation of the membrane is necessary. For this, the cells were incubated for 2 minutes with a cold (-20°C) aceton-methanol solution (1:1), which dissolves lipids from cell membranes leading to permeabilisation of membranes[224]. Afterwards, the cells were incubated for 30 minutes with a BSA solution (2% (m/v) in DPBS) and then incubated with Alexa Fluor 488 Phalloidin (Molecular Probes, 5U/ml) for 20 minutes at RT in the dark. The samples were washed with DPBS once, and then incubated with bisbenzimide (Hoechst) to stain

DNA (15 minutes, 700 ng/ml, RT). Bisbenzimide has the ability to preferentially bind to adenine-thymine rich regions of DNA thus leading to nuclei visualization; it is excited by ultraviolet light and emits blue fluorescence at 460–490 nm[225]. The cells were then washed three times with DPBS and were mounted with Fluoromount-G (Southern Biotech) on glass microscope slides. Images of the cells were recorded with a Leica DM6 B (20x/0.55 HC PL FLUOTAR objective) microscope. Hoechst was recorded at 435-485 nm and Alexa Fluor 488 at 520-550 nm. The area of cardiomyocytes was determined with ImageJ. Approximately 50 cells per condition and experiment were analyzed. Determination of the cross sectional area of cells stained with phalloidin was performed with ImageJ. Adobe Illustrator and Adobe Photoshop were used for creating figures.

3. Other methods

3.1 Internalization assay with ^{3}H-CGP

CGP-12177 hydrochloride is a hydrophilic substance and acts as an antagonist for β_1- and β_2-adrenoceptors[226,227]. As radioligand ^{3}[H]-CGP is frequently used for whole cell binding assays where binding of ^{3}[H]-CGP on β-receptors allows their detection and quantification. For the analysis of receptor internalization in response to isoproterenol, GFP-β_2-AR-HEK293 were cultured on poly-d-lysine coated 12-well plates and either one of the peptides or pcDNA$_3$ as negative control was transfected using the calcium phosphate precipitation assay. Two days following transfection, the culture medium was aspirated and replaced by 1 ml incubation buffer.

Incubation buffer (pH 7.4)	
137 mM	NaCl
5 mM	KCl
1 mM	$MgCl_2$
1.5 mM	$CaCl_2$
20 mM	HEPES

After 10 minutes of resting, cells were stimulated with 1 µM isoproterenol for 5 minutes to initiate internalization. Immediately afterwards the cells were placed on ice to stop the reaction and were carefully washed three times with DPBS; then, radioligand containing buffer was added to the cells and the plates were incubated for 2-3 hours at 4 °C allowing ^{3}[H]-CGP to bind the non-internalized receptors still localized in the cell membrane. 3.5 µCi ^{3}[H]-CGP in 250 µl incubation buffer were used per well. After incubation, the cells were washed three times with DPBS to remove excess ^{3}[H]-CGP

and they were then dissolved in 0.5 M NaOH at RT for 30 minutes. The cell suspension was then transferred into scintillation fluid (Rotiszint eco plus, Carl Roth) and ^{3}[H]-CGP content was analyzed using a β-counter (Tri-Carb 4910TR, Perkin Elmer).

3.2 Contractility measurements

To measure the beat rate of primary cardiomyocytes (CMs) in real time, the CardioExcyte96 system (Nanion Technologies) was used. CMs were seeded on Nanion CardioExcyte 96 Sensor Plates (NSP-96, Nanion Technologies; Figure 3.2.1) which are based on standard 96-well plates with a circular gold sensor electrode on the bottom of each well enabling up to 96 simultaneous recordings through the software CardioExcyte Control (Nanion Technologies).

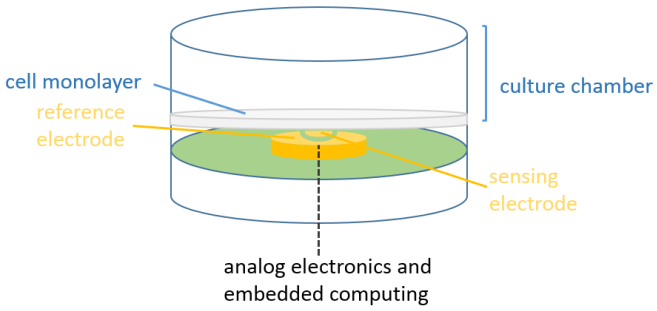

Figure 13: Schematic figure presents a zoomed view of one sensor chamber (well) with a cell monolayer. A CardioExcyte sensor plate 96 includes 96 of these chambers[228].

This hybrid instrument combines impedance readout (a correlate of cell contractility) with extracellular field potential (EFP) recordings generated by cellular action potentials of a cell monolayer[228,229]. Impedance measurements are based on the mechanical movement of the spontaneously contracting cells whereas EFP recordings display the underlying electrophysiological process. Impedance methods are routinely used to analyze biological samples for instance in regard to proliferation rates[230]. In this system, planar gold electrodes facilitate fast and frequent impedance measurements modulated by cell adhesion and cell morphology changes allowing assessment of cardiomyocyte function. Impedance is the measure of resistance to a current when voltage is applied (voltage-current ratio) at a particular frequency ω. It possesses both magnitude and phase. When the cells are seeded onto a sensor plate, they induce a higher resistance, which can then be detected. The applied frequency ω determines

whether the electrons will cross though or in between the cells, thereby enabling for instance the detection of cell morphology changes and detection of cardiomyocytes contractions. In the present study we focused on the investigation of the effect of the peptides on cardiomyocyte contractility using the impedance readout function of the CardioExcyte96 system.

A NSP-96 plate was coated prior to NMCM isolation with fibronectin (1:100 in PBS with Ca^{2+}, Mg^{2+}), and was incubated for at least 1.5 hours at 37°C. Cells (70.000 cells in 200 µl/well) were then seeded and the plate was placed in the incubator at 1% CO_2 and 37°C. On the next day, the medium was exchanged to 1% FCS NMCM medium and the plate was then placed in the CardioExcyte96. Setup and measurements were started. The CardioExcyte96 system has its own incubation system-Ibidi gas mixer (Ibidi) - where the CO_2 level is set at 1%, humidity at 80% and flow rate at 15 l/h. Cells were adjusted for 2-3 hours to the new environment and were then transduced. Approximately 24 hours after transduction the medium is exchanged to FCS deprived NMCM medium and after another 24 hours they were stimulated with 50 nM isoproterenol. Directly after stimulation, the time interval of impedance recording was set to 1-2 minutes. Data were analyzed for contractility and cell viability using the provided software. By using the online analysis (OA) tool one can export all the data collected at all-time points for specific parameters such as beat rate or base impedance. The data were normalized to control (lacZ) and to the sweep before stimulation.

3.3 Statistical analysis

All data are shown as mean ± standard error of the mean (SEM). GraphPad Prism was used for statistical analyses. One-way ANOVA and Bonferroni test for data sets with ≥3 groups or unpaired t-test for 2 groups were used for analysis of statistical significance. A confidence interval of 95% was designated. *P<0.05* is indicated with a `*´.

IV. Results

1. RKIP/GRK interaction interface

RKIP, an endogenous inhibitor of GRK2 leads to increased cardiac contractility via the activation of β-AR[58]. It is known to inhibit GRK2 but not GRK5, another predominant GRK in the heart. GRK2, GRK3, and GRK5 are the most abundant GRKs in the heart[54]. RKIP has been demonstrated to bind to the N-terminus (1-185) of GRK2, which is important for the GRK2/receptor interaction[194] leading to selective inhibition of GRK2 receptor –but not cytosolic– substrates[138]. GRK2 is highly homologous to GRK3 and they belong to the same subfamily. GRK5, in contrast to GRK3 shows only low homology to GRK2 (Fig.14).

Figure 14: Multiple sequence alignment of bovine GRK2 (689 aa), GRK3 (688 aa) and GRK5 (590 aa). Sequence homology map was created using CLUSTALW. An '*' (asterisk) indicates positions which have a single, fully conserved residue. A ':' (colon) indicates conservation between groups of strongly similar properties. A '.' (period) indicates conservation between groups of weakly similar properties. Alignment score for GRK2:GRK3 is 84.593 %, alignment score for GRK2:GRK5 is 28.1356 %, alignment score for GRK3:GRK5 is 27.4576 %.

Bovine GRK2, GRK3 and GRK5 were used for the experiments in this project. The sequence homology scores of the bovine GRK2, GRK3 and GRK5 are very similar to those of the respective human proteins, namely: for GRK2:GRK3 is 83.7209 %, for GRK2:GRK5 is 28.1356 % and for GRK3:GRK5 is 28.1356 %.

In order to validate the binding region of RKIP in GRK2 and to gain further information on the specificity of RKIP towards different GRK isoforms, the RKIP-GRK interaction interface was investigated by protein interaction assays: co-immunoprecipitation (Co-IP) and pull down assays.

1.1 RKIP binds to GRK2 and GRK3 but not GRK5

For the Co-IPs, RKIP with an N-terminal Flag-tag was used. HEK293 cells were transfected with full-length GRK2, GRK3 or GRK5 and Flag-RKIP. Cells transfected with $pcDNA_3$ instead of Flag-RKIP, served as negative control. Before the cells were lysed, they were stimulated with phorbol-12-myristate 13-acetate (PMA). PMA is employed to activate protein kinase C (PKC) which phosphorylates RKIP at Ser153 causing RKIP dimerization and dissociation from Raf1 and subsequent association to GRK2. After the cells were lysed with PBS buffer, supplemented with protease and phosphatase inhibitors, the lysates were incubated with flag antibodies coupled Protein A Sepharose beads. Finally, the beads were repeatedly washed to eliminate unspecific binding and Laemmli sample buffer was added, to enable gel electrophoresis and immunoblotting. RKIP antibodies were used to detect Flag-RKIP (IP) and GRK2, GRK3 or GRK5 specific antibodies were used to detect whether the respective GRK bound Flag-RKIP. The presence of Flag-RKIP and GRKs in the lysates (input) was controlled via immunoblotting. To exclude unspecific binding of the GRKs on the beads, $pcDNA_3$ was used instead of Flag-RKIP. To validate the effect of PMA stimulation, unstimulated control samples were also used. Intense non-specific bands at approximately 20 kDa were caused due to the immunoglobulin G (IgG) light chain that bound to Protein A, and are indicated as IgG.

These experiments validated previously published results regarding increased RKIP binding to GRK2 upon PKC stimulation in comparison to non-stimulated cells. In addition, RKIP as previously showed, did not bind to GRK5[58]. Interestingly, RKIP bound to GRK3 with increased binding levels upon PKC stimulation with PMA (Fig.15).

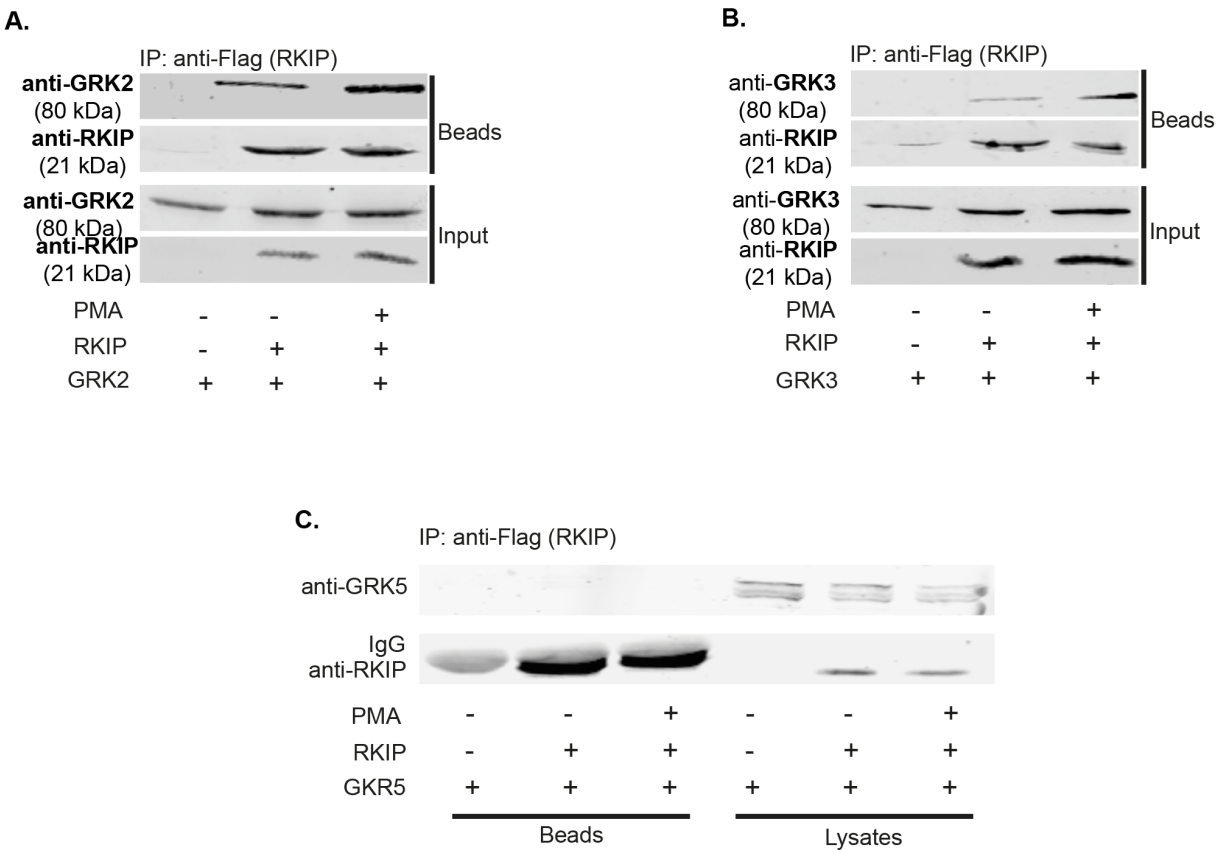

Figure 15: RKIP binds to GRK2 and GRK3 but not GRK5 upon PKC stimulation. Flag-RKIP was immunoprecipitated from HEK293 cell lysates with and without PKC stimulation. The respective co-precipitated GRK (A: GRK2, B: GRK3, C: GRK5) was detected via western blotting using antibodies directed against indicated proteins. Prior to cell lysis the cells were stimulated with phorbol 12- myristate 13-acetate (PMA; 1 µM, 5 min) to enhance PKC activity. Cell lysates were incubated with Protein A sepharose coupled with Flag-M2 antibody. IgG: immunoglobulin light chain. For the GRK2 Co- IP n=3, for the GRK3 and GRK5 Co-IPs n=5.

1.2 RKIP binds to the N-terminus of GRK2 and GRK3 (aa 54-185 and aa 1-185)

1.2.1 Co-immunoprecipitations

The extreme N-terminal region of GRKs (approximately 20 amino acids) is highly conserved[54]; it is involved in a direct interaction with GPCRs[76] and is necessary for receptor recognition[64]. Moreover, it was revealed that through a single α-helix, the GRK extreme N-terminal region interacts with the kinase domain to activate the kinase. This interaction stabilizes the GRK active conformation, enhances GRK activity and it is suggested that is promoted by receptor binding[76,80,81]. Furthermore, the RGS homology domain (RH), which is localized after the extreme N-terminal region (ca. aa 50-185), is homologous to the regulator of G-protein signaling (RGS) family of proteins and is therefore termed as RH domain[84]. The GRK RH domain is a Gα-binding domain that likely functions in mediating GRK targeting to specific

Gα or GPCR/Gα protein complexes[59,69,87]. Moreover, it has been demonstrated that the GRK N-terminus interacts with other proteins. The best investigated GRK regarding protein interactions is GRK2, which can bind several proteins, such as caveolin, calmodulin, RKIP (Raf kinase inhibitor protein) and Gβγ[52].

In order to identify the binding region of RKIP in GRK2 and GRK3, peptides of the N-terminal regions of GRK2, GRK3 and GRK5 (aa 1-53, aa 54-185 and aa 1-185) were cloned into $pcDNA_3$ vectors and a myc-tag was attached to the N-terminus to enable their detection by immunoblotting. The region consisting of the first 53 amino acids includes the extreme N-terminus, which as mentioned above is implicated in receptor recognition and interaction and it also enhances GRK activity. The second peptide consisting of amino acids 54-185 includes the RH domain, which is mainly involved in protein interactions and therefore, also in membrane targeting via interactions with the Gα and Gβγ subunits. The third peptide is the full-length N-terminus, which combines the features of the extreme N-terminal region and of the RH domain.

Flag-tagged RKIP and myc-tagged GRK peptides were then transiently transfected in HEK293 cells. To exclude unspecific binding of the GRK peptides on the beads, $pcDNA_3$ was used instead of Flag-RKIP in control samples. The cells were lysed with PBS buffer supplemented with protease and phosphatase inhibitors and the lysates were incubated with Flag antibodies-coupled Protein A Sepharose beads in order to immunoprecipitate RKIP (IP). Finally, the beads were repeatedly washed to eliminate unspecific binding and in order to enable immunoblotting, Laemmli sample buffer was added. The successful expression of Flag-RKIP and of the myc-tagged GRK peptides in the lysates (input) was controlled via immunoblotting using anti-Flag and anti-myc antibodies. Intense non-specific bands at approximately 20 kDa were caused due to the immunoglobulin G (IgG) light chain that bound to Protein A, and are indicated as IgG.

It was revealed that the peptides GRK2 and GRK3 54-185 and GRK2 and GRK3 54-185 1-185 bind to RKIP, whereas the corresponding peptides of GRK5 did not (Fig.16). The smallest peptide consisting of amino acids 1-53 could not be successfully expressed and detected in HEK293 cells for neither of the GRKs, thus it was excluded from further experiments.

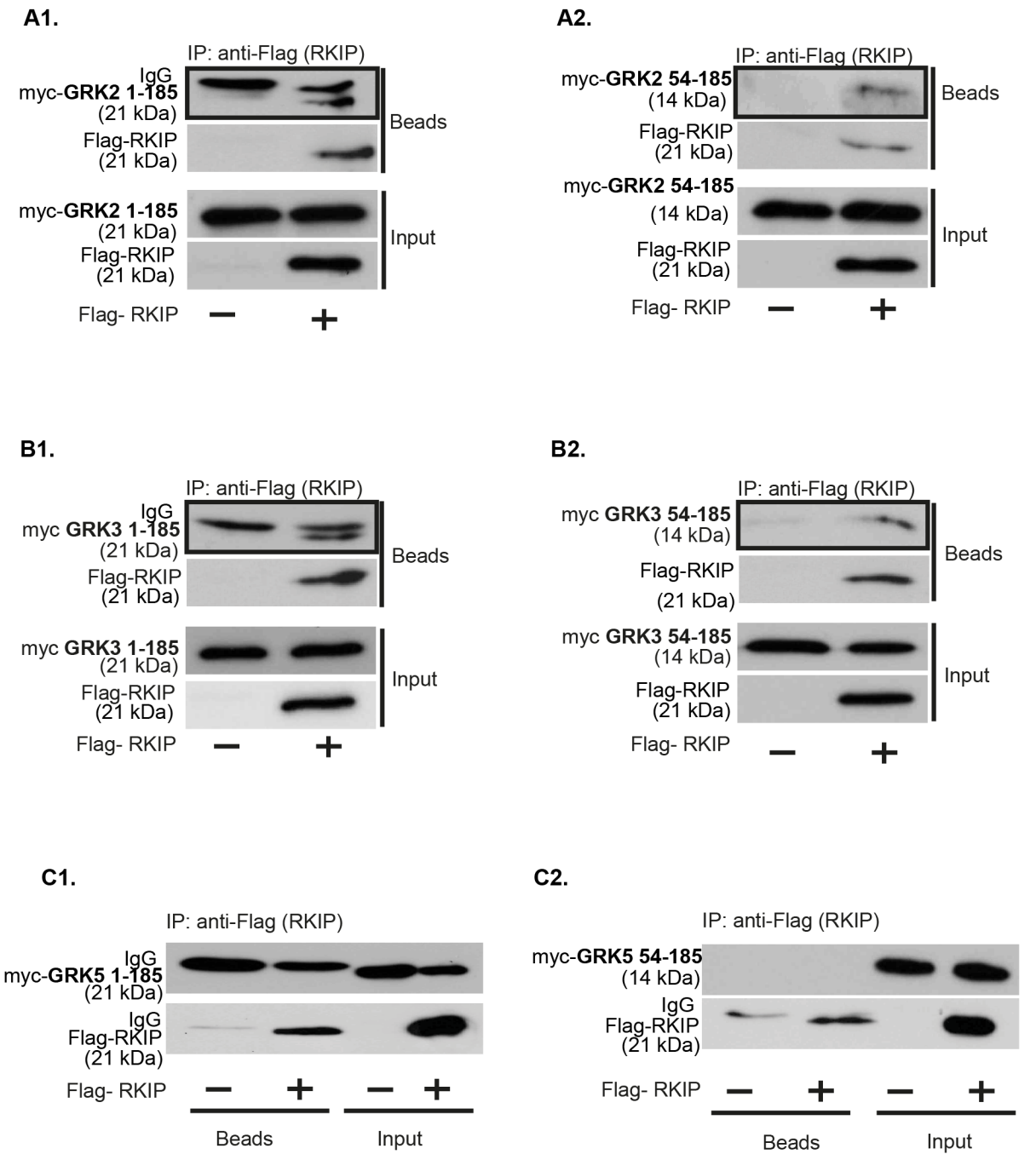

Figure 16: RKIP binds the N-terminal peptides 54-185 and 1-185 of GRK2 and GRK3 but not of GRK5. HEK293 cells were transfected with Flag-RKIP and myc-tagged peptides. Cell lysates were incubated with Protein A sepharose coupled with Flag-M2 antibodies. Flag-RKIP was immunoprecipitated and co- precipitated myc-peptides were detected via immunoblotting using antibodies directed against the myc-tag. Block A: GRK2 peptides (A1: myc-GRK2 1-185, A2: myc-GRK2 54-185). Block B: GRK3 peptides (B1: myc-GRK3 1-182, B2: myc-GRK3 54-185). Block C: GRK5 peptides (C1: myc-GRK5 1-185, C2: myc-GRK5 54-185). IgG: immunoglobulin light chain.

1.2.2 Pull down assays

The pull-down assay is an *in vitro* method used to analyze the existence of a protein-protein interaction. Pull-down assays were performed with Flag-tagged RKIP expressed in HEK293 cells and from *E.coli* purified GRK peptides. For this, 400 µM of purified GST-tagged GRK peptides and GST as control were used to assess whether the RKIP/peptide binding observed in the Co-IP assays is a direct binding and to validate the Co-IP experiments.

The purified GST-tagged peptides of GRK2, GRK3 and GRK5 (1-53, 54-185, 1-185) or GST served as bait protein, captured on an immobilized affinity ligand, in this case Glutathione sepharose 4B beads. After incubation of the beads with the bait protein to enable coupling, and washing to remove excess bait protein, the prey protein was added to beads. HEK293 cells were transfected with Flag-RKIP, which was used as prey protein. Purified GST- or His-tagged RKIP were not used due to high unspecific binding on the sepharose beads. After incubation of the bait-coupled beads with the prey protein, the beads were washed to minimize unspecific binding and Laemmli loading buffer was added. The samples were analyzed via gel electrophoresis and western blotting using anti-Flag and anti-GST antibodies. Purified Glutathione-S-Transferase (GST) and uncoupled Glutathione sepharose 4B beads served as negative controls in order to exclude unspecific binding of Flag-RKIP to the beads, from being considered as positive binding. In these experiments it was possible to also investigate the binding capacity of RKIP to the smallest GRK peptide (1-53) due to its successful purification from *E.coli*.

All the peptides of GRK2 and GRK3, including 1-53 bound to RKIP (Fig.17 A and B). However, RKIP did not bind to any of the peptides of GRK5 (Fig.17 C), which in turn underlines the specificity of RKIP for the βARK-subfamily of GRKs i.e. GRK2 and the highly homologous GRK3. Binding to GRK5 peptides could not be established through this series of experiments; this may be explained by a very weak or transient binding behavior.

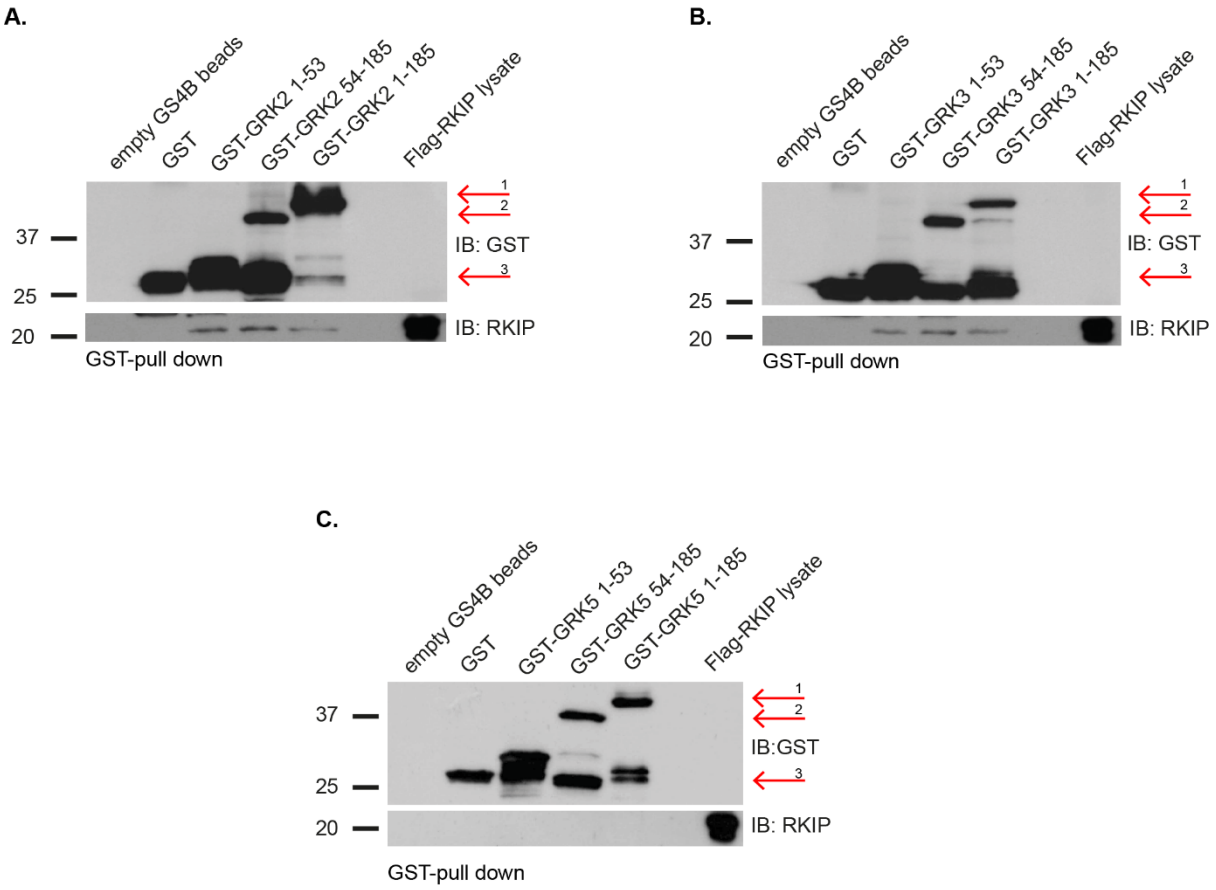

Figure 17: RKIP binds the N-terminal peptides of GRK2 and GRK3 but not GRK5. Purified GST or purified GST- tagged peptides (bait proteins) were coupled on Glutathione sepharose 4B beads. HEK293 cell lysates containing Flag-RKIP (prey protein) were incubated for 2 hours at 4°C to facilitate the pull down by bait protein coupled beads. Binding on the bait proteins and both bait and prey were detected via immunoblotting (IB) with corresponding antibodies. GST and uncoupled GS4B beads served as negative controls. A: GST-GRK2 1-53 (3), GST-GRK2 54-185 (2); GST-GRK2 1-185 (1). B: GST-GRK3 1-53 (3), GST-GRK3 54-185 (2); GST-GRK3 1-185 (1). C: GST-GRK5 1-53 (3), GST-GRK5 54-185 (2); GST-GRK5 1-185 (1). Molecular mass standards (in kDa) are shown on the left of each panel. n=3.

2. Influence of the peptides on β_2AR phosphorylation

GRK2 phosphorylates, among others, β-ARs and thereby initiates their desensitization and downregulation. RKIP has been shown to bind GRK2 (to the N-terminus 1-185) and to prevent β-AR phosphorylation. Since RKIP binds to the N-terminus of GRK2, that is known to interact with the receptor, we aimed to analyze whether the N-terminal part of GRK2, GRK3 or GRK5 would be sufficient to interfere with GRK-receptor activation and thus receptor phosphorylation.

Therefore, β_2-AR phosphorylation in the absence and presence of the respective peptides was analyzed. HEK293 cells with constitutive overexpression of GFP-tagged β_2-AR (GFP-β_2-AR-HEK293) were transfected with GRK2 and either with $pcDNA_3$ (negative control) or RKIP, or a peptide of GRK2, GRK3 or GRK5 (1-185 or 54-185). To initiate phosphorylation of the receptor, the cells were stimulated with isoproterenol (1µM, 10 min, 37°C), a non-selective β-adrenergic receptor agonist. The cells were lysed with RIPA buffer and β_2-AR phosphorylation was analyzed by antibodies directed against the phosphorylated receptor. RKIP overexpression was used as an internal positive control.

Interestingly, the N-termini of GRK2 and GRK3 1-185 reduced β_2AR phosphorylation to a comparable extent as RKIP, suggesting that the receptor signaling may be enhanced, not only by RKIP but also by the N-termini of GRK2 and GRK3. On the other hand, GRK5 1-185 had no significant influence on receptor phosphorylation (Fig.18).

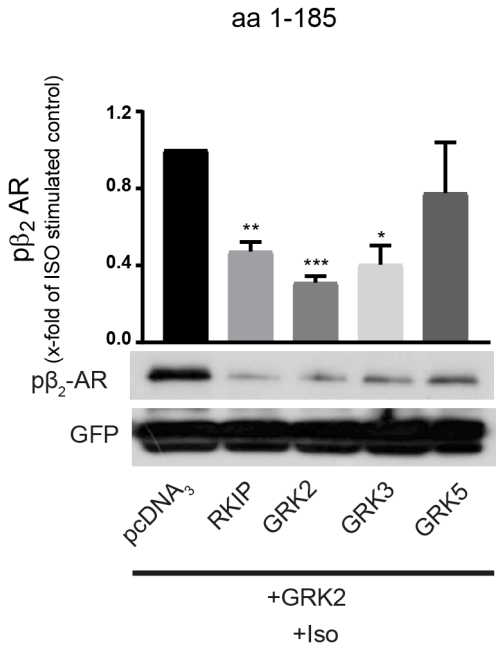

Figure 18: The N-terminal peptides of GRK2 and GRK3 (1-185) reduce β_2AR phosphorylation to a comparable extent as RKIP. HEK293 cells with constitutive overexpression of GFP-tagged β_2-AR (GFP-β_2-AR-HEK293) were transfected with GRK2 and either with $pcDNA_3$ (negative control) or RKIP, or a peptide of GRK2, GRK3 or GRK5 (1-185). Following isoproterenol stimulation (Iso; 1 µM, 10 min, 37°C), cells were lysed with RIPA buffer. RKIP served as positive control, $pcDNA_3$ as negative control and GFP as loading control. Receptor phosphorylation was detected via western blotting and anti pβ_2-AR antibodies. *, $P < 0.05$; **, $P < 0.01$; ***, $P < 0.001$ versus stimulated $pcDNA_3$ control. Shown is the isoproterenol-mediated stimulation normalized to the negative control. Results are from 5 independent experiments.

Thereafter, also the smaller peptides 54-185 of GRK2, GRK3 and GRK5 were analyzed in this experimental setting. Interestingly, among these peptides only the corresponding GRK2 peptide reduced the phosphorylation of the β_2-AR significantly. This reduction was comparable to the effect of RKIP. GRK3 54-185 and GRK5 54-185 had no effect on the β_2-AR phosphorylation (Fig.19).

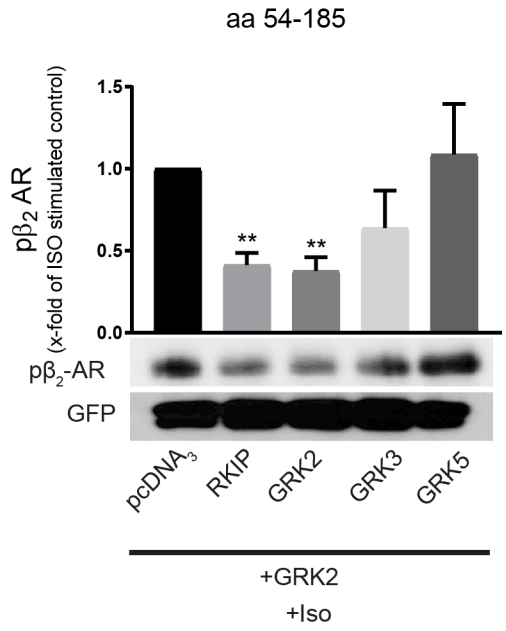

Figure 19: The N-terminus aa 54-185 of GRK2 significantly reduces β_2AR phosphorylation to a comparable extent as RKIP. GRK2 54-185, GRK3 54-185 or GRK5 54-185 or $pcDNA_3$ were transiently transfected with GRK2 in HEK293 cells with constitutive overexpression of GFP-tagged β_2-AR (GFP-β_2-AR-HEK293). Following isoproterenol stimulation (Iso; 1 µM, 10 min, 37°C), the cells were lysed with RIPA buffer. RKIP served as internal positive control, $pcDNA_3$ as negative control and GFP as loading control. Receptor phosphorylation was detected via western blotting with corresponding antibodies. *, $P < 0.05$; **, $P < 0.01$; ***, $P < 0.001$ versus stimulated $pcDNA_3$ control. Shown is the isoproterenol-mediated stimulation normalized to the negative control. n=5.

These experiments suggest that the N-terminal peptides can simulate the function of RKIP in regard to receptor phosphorylation. Since, especially the longer peptides encoding the entire N-terminus were efficient in simulating the effect of RKIP, it is likely that the peptide/receptor binding site is localized within the amino acids 1-53, which was also suggested by Homan *et al.*[75], Boguth *et al.*[76], Yu *et al.*[77] and others. However, in particular the N-terminus of GRK2 may have several relevant binding sites. In line with Co-IP and pull down experiments, GRK5 54-185 was not able to reduce β_2-AR phosphorylation, which might also be due to the receptor subtype. After this point, only the full length N-terminal peptide (amino acids 1-185) was used for further experiments.

3. The effect of the peptides on isoproterenol-induced β_2-AR internalization.

GRK-mediated receptor phosphorylation is a well-characterized mechanism for GPCR desensitization. Upon agonist binding, conformational changes and GRK-mediated phosphorylation are triggered and enable the binding of β-arrestins to the receptor, which in turn facilitates receptor desensitization by disabling its coupling to G proteins[48,49]. In addition to receptor desensitization, β-arrestin binding can also target the receptor to clathrin coated pits which leads to receptor internalization[50], a process that serves to resensitize the receptor or target it to lysosomes for degradation[52].

Since it was shown that the peptides of GRK2 and GRK3 (amino acids 1-185) were able to prevent β_2-AR phosphorylation, which is a prerequisite for receptor internalization, it is interesting to evaluate whether the presence of the peptides also prevents internalization.

To assess the impact of GRK2 1-185, GRK3 1-185 and GRK5 1-185 on receptor internalization, HEK293 cells with constitutive overexpression of GFP-tagged β_2-AR (GFP-β_2-AR-HEK293) were transfected with C-terminally mCherry-tagged GRK2 1-185, GRK3 1-185 and GRK5 1-185. The cells were stimulated with isoproterenol (1µM) for 10 min. Receptor internalization was recorded with fluorescence microscopy and live cell imaging (Fig.20).

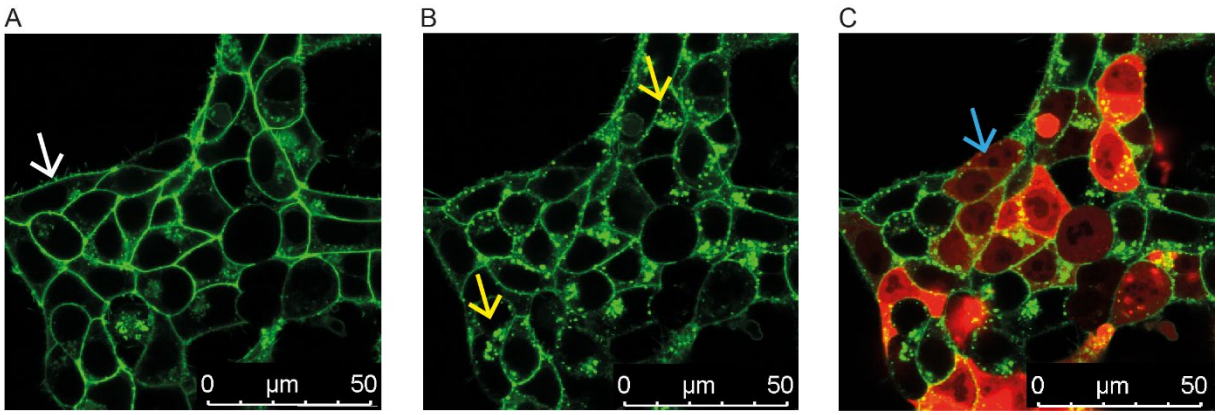

Figure 20: Representative confocal pictures of GFP-β_2-AR HEK cells transfected with GRK3 1-185_mCherry. A. HEK cells with constitutive overexpression of GFP-β_2-AR; the white arrow indicates GFP tagged- β_2- AR localized at the cell membrane; B. Receptor internalization 5 minutes after stimulation with 1 µM isoproterenol; yellow arrows indicate internalized GFP-β_2-AR. C. Overlay of GFP and mCherry pictures 5 min after stimulation; the blue arrow indicates cells transfected with GRK3 1- 185_mCherry (green: GFP-β_2-AR in cell membrane, red: GRK3 1-185_mCherry). The microscope Leica TCS SP8 CTR was used. Settings for recording: 1024 × 1024 pixel format; line average 16. Images were taken every minute for 10 minutes. GFP was excited with a diode laser at 488 nm laser line according to the manufacturer's settings and fluorescence intensities were recorded from 494

to 555 nm. Laser intensity was set to 0.1–2%. mCherry was excited at 552 nm laser line and fluorescence intensities were recorded from 555 to 693 nm. Laser intensity was set to 2–6%.

The intensity of internalized GFP in each cell, which corresponds to the internalized GFP-β_2-AR was measured after 5 minutes and was normalized against the inner cell area. The levels of receptor internalization were significantly lower in cells transfected with GRK2 1-185 (*, $P < 0.05$) and GRK3 1- 185 (***, $P < 0.001$). Cells transfected with GRK5 1- 185 did not show a significant reduction of receptor internalization (Fig.21).

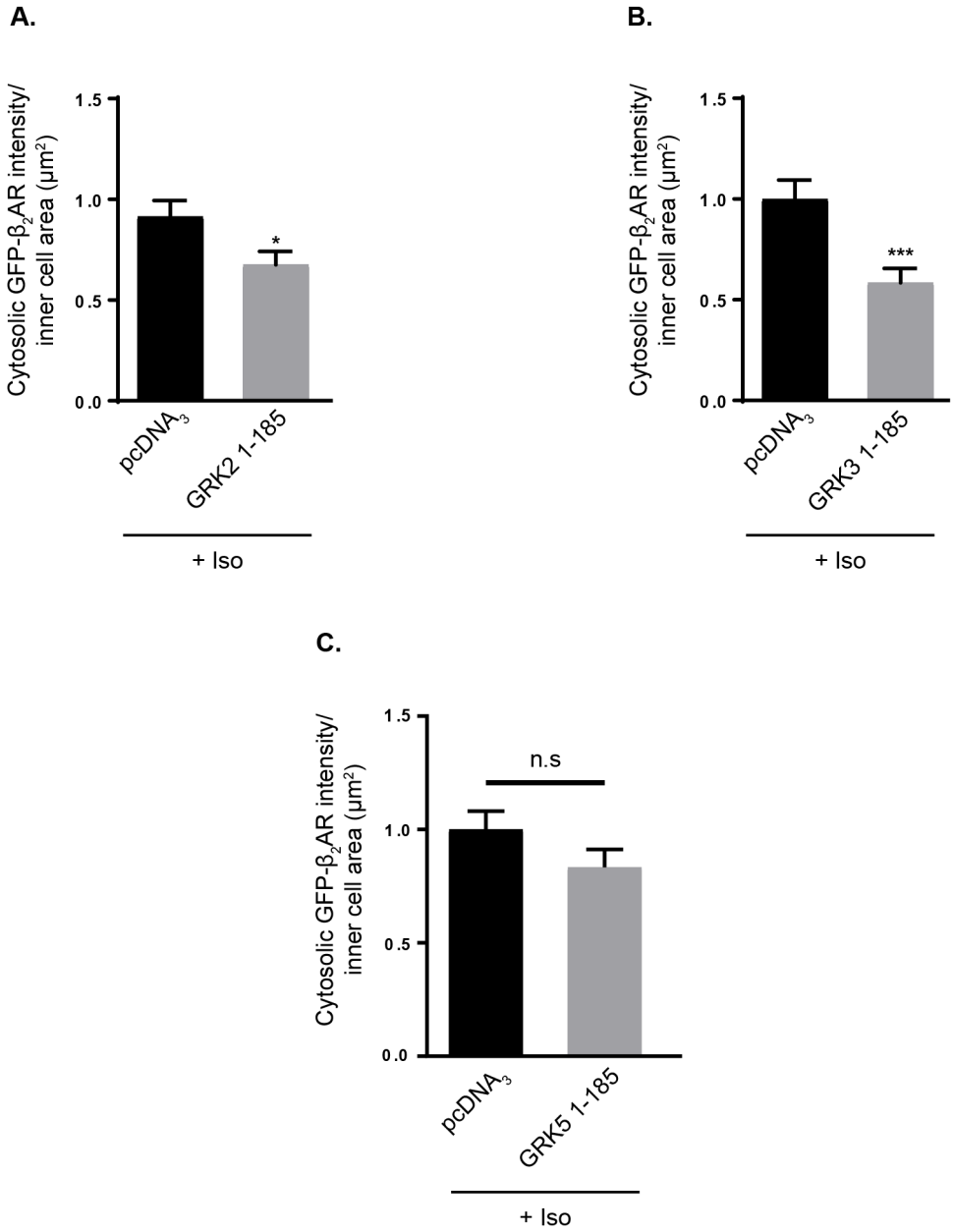

Figure 21: The N-termini of GRK2 and GRK3 (1-185) significantly reduced GFP-β_2-AR internalization as determined by confocal imaging. GFP-β_2-AR-HEK293 cells were transfected with mCherry-tagged GRK2 1-185 (A), mCherry-tagged GRK3 1-185 (B), mCherry-tagged GRK5 1-185 (C). Isoproterenol stimulated internalized GFP signal corresponds to internalized β_2-AR and was normalized to the respective inner cell area before stimulation.

Depicted is the isoproterenol stimulated internalization, which was evaluated 5 min after isoproterenol stimulation (1µM). Results were retrieved in a blinded manner. n=27-29 cells per construct of at least 3 independent experiments. *, $P < 0.05$; ***, $P < 0.001$ versus stimulated control.

To validate these results, β_2-AR internalization was also determined by a radioligand binding assay. As radioligand, [^{3}H] CGP- 12177 was used that is cell impermeable and has a high affinity to β-AR; thus it allows their ^{3}H based detection via a β-counter.

GFP-β_2-AR-HEK293 cells were transfected with GRK2 1-185, GRK3 1-185, GRK5 1-185 or pcDNA$_3$ and were stimulated for 5 min with 1 µM isoproterenol to induce internalization. The reaction was stopped and the cells were washed and incubated with [^{3}H] CGP. After several washing steps to remove unbound [^{3}H] CGP, the cells were lysed with 0.5 M NaOH and the [^{3}H] CGP that was bound to the β-ARs on the outer cell membrane was analyzed using a β-counter. The measured counts per minute (CPM), which is the measurement unit for β-radiation, allowed the calculation of the receptor internalization rate.

These experiments showed that the internalization of β-AR was significantly reduced in cells co-transfected with GRK2 1-185 or GRK3 1-185 compared to control samples (Fig.22). Whereas the internalization rate of the control was ≈ 23%, for GRK2 1-185 and GRK3 1-185 cells it was ≈ 11% and ≈ 8% respectively. The internalization rate of the isoproterenol stimulated control cells corresponds to that in the literature under similar experimental settings, which is in the range of ≈ 13- 25 %[58,180].

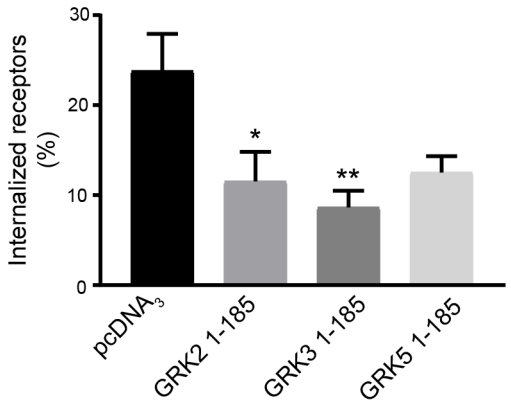

Figure 22: GRK2 1-185 and GRK3 1-185 significantly reduced β_2-AR internalization measured via radioligand binding assay. GFP-β_2-AR-HEK293 cells were transfected in triplets with myc tagged GRK2 1-185 or GRK3 1-185 or GRK5 1-185 or pcDNA$_3$. The cells were stimulated with isoproterenol for 5 min (1 µM) and afterwards they were incubated with [^{3}H] CGP for two hours. To calculate percentage of internalization for each condition, the mean counts per minute (CPM) of the unstimulated control cells was set as 100%. Percentage of the isoproterenol-stimulated signal was subtracted from 100%. Results are means ± SEM of 6 independent experiments; *, $P < 0.05$; **, $P < 0.01$ versus stimulated control.

These results suggest that the peptides of GRK2 and GRK3 are indeed able to regulate β_2-AR internalization. However, in contrast to the previous experiments performed via confocal imaging, the N-terminal peptide of GRK5 also showed an effect (non-significant; P = 0.055) on β_2-AR internalization; this may be due to the different experimental settings that were applied, since a radioligand binding assay is a more sensitive method for detecting internalized β_2-ARs.

4. The peptides' impact on PKA activity

To gain insight into the effects of the N-terminal (1-185) peptides of GRK2, GRK3 and GRK5 on β_2AR downstream signaling, PKA activation was investigated by determining the phosphorylation of phosducin, a cytosolic target of PKA. Phosducin is a 33-kDa protein and a regulator of G-protein-mediated signaling, found in the retina and also in liver, lung, heart, and brain[231]. β-AR activation stimulates $G\alpha_s$, which in turn activates adenylate cyclase (AC), which generates the second messenger cyclic adenosine monophosphate (cAMP); increased cAMP levels activate cAMP-dependent protein kinase A (PKA) which in turn can phosphorylate various substrates such as phosducin[173,232].

HEK293 cells with constitutive overexpression of GFP tagged β_2-AR (GFP-β_2-AR-HEK293) were transiently transfected with GRK2 and phosducin and $pcDNA_3$ or GRK2 1-185 or GRK3 1-185 or GRK5 1-185 or RKIP. RKIP was used as positive control and $pcDNA_3$ as negative control. The cells were treated with 3-isobutyl-1-methylxanthine (IBMX), which is a phosphodiesterase (PDE) inhibitor. Intracellular cAMP that is increased after β_2-AR stimulation and which is rapidly degraded by PDEs, cannot be degraded in the presence of IBMX and activates PKA. After 10 min of isoproterenol stimulation, the cells were lysed and phosducin phosphorylation was analyzed via gel electrophoresis and western blotting using antibodies directed against PKA substrates.

All N-terminal peptides, GRK2 1-185, GRK3 1-185 and GRK5 1-185 induced an increase of phosducin phosphorylation after isoproterenol stimulation (Fig.23). This result suggests that GRK5 1-185 is implicated in PKA signaling but probably through a non-canonical pathway since β_2-AR phosphorylation and internalization were not affected by GRK 1-185.

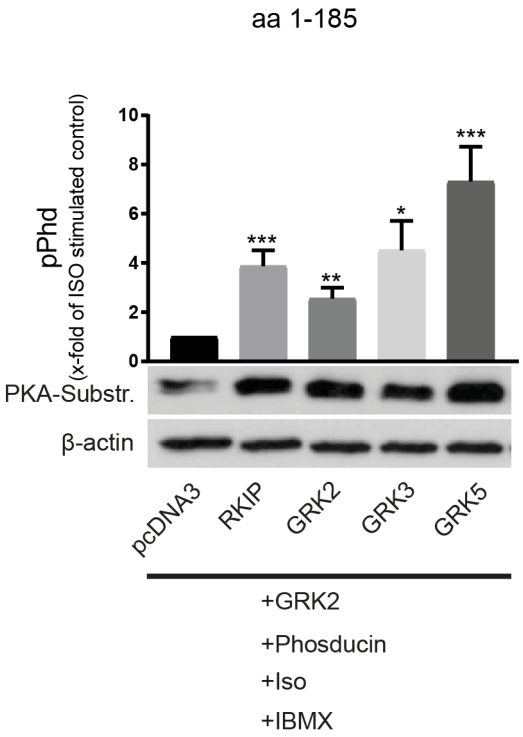

Figure 23: GRK2 1-185, GRK3 1-185 and GRK5 1-185 significantly enhance the phosphorylation of a PKA substrate. GFP-β_2-AR-HEK293 cells were transfected with GRK2 and phosducin and either pcDNA$_3$ or one of the peptides: GRK2 1-185, GRK3 1-185 or GRK5 1-185. The cells were preincubated with IBMX (100 µM, 25 min) and stimulated with isoproterenol (Iso; 1µM, 10 min). Phosducin phosphorylation (pPhd) was detected using antibodies directed against PKA-substrates. β-actin served as loading control. Results are normalized to the control. n=13 independent experiments. *, $P < 0.05$; **, $P < 0.01$; ***, $P < 0.001$ versus pcDNA$_3$ negative control.

5. Analysis of a β_2AR-peptide interaction by co-immunoprecipitations assays

It was until now shown that the N-terminal peptides (1-185) of GRK2, GRK3 or GRK5 affect β_2AR phosphorylation, β_2AR internalization and downstream signaling. One hypothesis regarding the mechanism by which these events take place, was that the respective peptides bind directly to β_2AR and hinder its phosphorylation.

To examine whether this hypothesis was valid, co-immunoprecipitation experiments to investigate the β_2AR-peptide interaction were performed. HEK293 cells were transfected with Flag-tagged β_2AR and myc-tagged GRK2 1-185, GRK3 1-185 or GRK5 1-185. Cells co-transfected with $pcDNA_3$ served as control. Cell lysates (input) were then incubated with non-coupled Protein A sepharose in order to remove proteins from the sample that are prone to nonspecifically attaching to the beads (preclearing). Subsequently, the lysates were incubated with flag antibodies coupled Protein A sepharose beads. After repeated cycles of washing, Laemmli loading buffer was added to the beads and the samples were analyzed via gel electrophoresis and immunoblotting. Flag antibodies were used to detect Flag-β_2AR and myc-tag antibodies were used to detect whether the respective GRK peptide bound Flag-β_2AR. The successful expression of Flag-β_2AR and of the myc-tagged GRK peptides in the HEK293 lysates (input) was controlled via immunoblotting using anti-Flag and anti-myc antibodies. Intense non-specific bands at approximately 20 kDa were caused due to the immunoglobulin G (IgG) light chain that bound to Protein A, and are indicated as IgG.

After gel electrophoresis and immunoblotting, GRK2 1-185 (Fig.24 A) and GRK3 1-185 (Fig.24 B) bound the receptor, suggesting that the previously observed peptide mediated effects take place due to a direct interaction between receptor and peptide. For GRK5 1-185 no consistent binding on the receptor could be observed which could be an indication for a rather weak interaction between them (Fig.24 C). GRK2 54-185 (Fig.24 D) and GRK3 54-185 (Fig.24 E) did not bind the receptor indicating that the extreme amino terminal region of GRK2 and GRK3 is necessary for the receptor interaction.

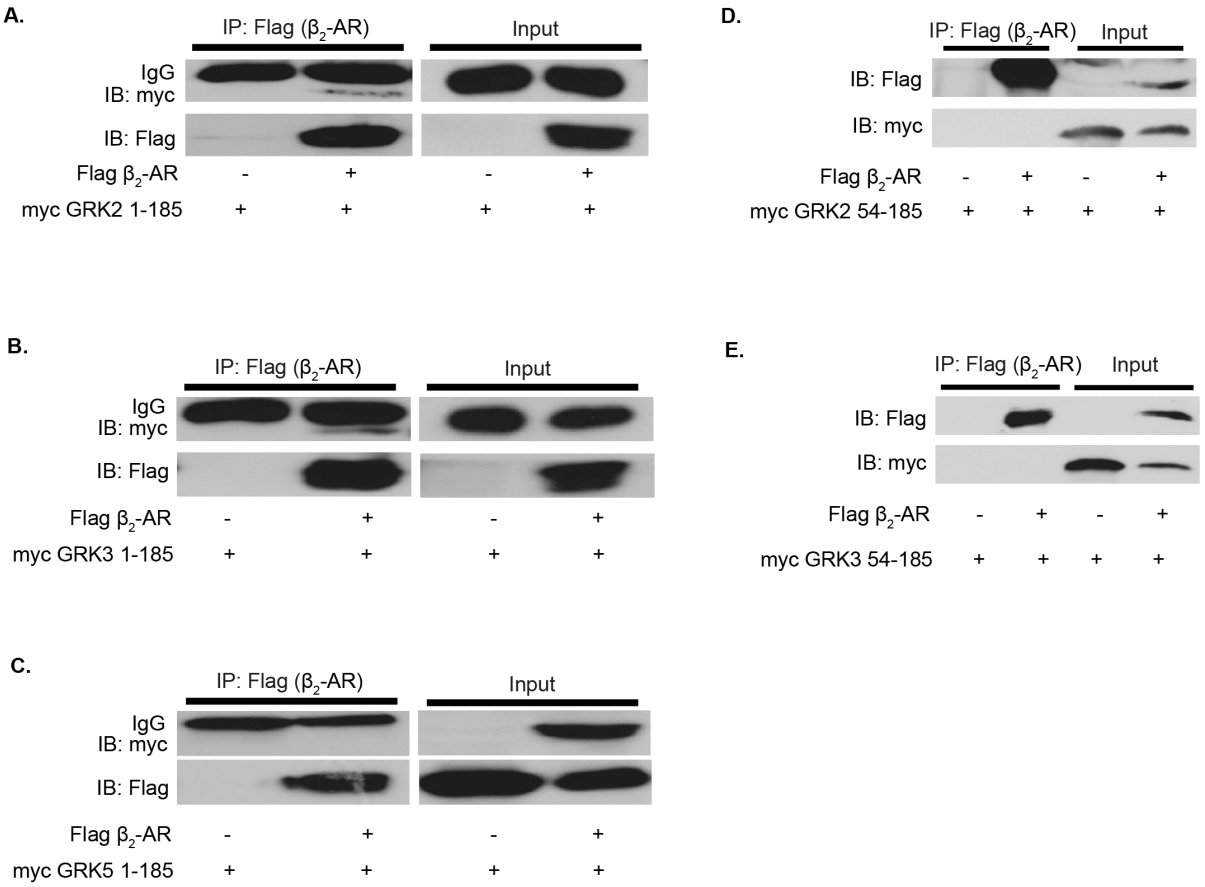

Figure 24: GRK2 1-185 and GRK3 1-185 bind β_2AR. HEK293 cells were transiently transfected with Flag-β_2AR or pcDNA$_3$ as control, and either myc-tagged A. GRK2 1-185, B. GRK3 1-185, C. GRK5 1-185, D. GRK2 54-185 or E. GRK3 54-185. Cell lysates (input) were incubated with Protein A sepharose coupled with Flag-M2 antibodies. Flag-β_2AR was immunoprecipitated (IP) and co- precipitated myc-tagged GRK2 1-185, GRK3 1-185, GRK5 1-185, GRK2 54-185 or GRK3 54-185 were detected via immunoblotting (IB) using antibodies directed against the myc-tag. n=4-5. IgG: immunoglobulin light chain.

6. Peptides' effect on isoproterenol induced hypertrophy.

Thus far, the experiments demonstrated that the N-termini (1-185) of GRK2 and GRK3 can reduce β_2-AR phosphorylation and internalization, increase PKA activity and that these results are due to a direct interaction between peptides and receptor. In view of their potential in modulating β-AR signaling and due to the fact that β-ARs play an important role in the development of hypertrophy, cardiac contractility, and heart failure, it was examined whether the peptides could be of relevance for the development of hypertrophy, although RKIP overexpressing mice developed cardiac hypertrophy comparable to wild type mice[138].

Hypertrophy (from Greek ὑπέρ "excess" + τροφή "nourishment") is the thickening of heart muscle due to cardiomyocyte enlargement, as a response to physiological or pathological events; at molecular level, it leads to alteration of cardiac cell signaling. If pathological, hypertrophy is associated with decreased contractility and is a risk factor for the development of heart failure[233].

To investigate the role of the peptides in β-AR mediated hypertrophy, neonatal mouse cardiomyocytes (NMCM) were used. Neonatal cardiomyocytes are extensively used in research since they are viable in cell culture for several days and can efficiently be transduced with adenoviral constructs[234,235].

Firstly, adenoviral myc-tagged peptides were constructed (Ad-myc GRK2 1-185, Ad-myc GRK3 1-185, Ad-myc GRK5 1-185) to achieve sufficient expression in NMCMs. To examine whether these constructs are indeed expressed in the NMCMs, cells were transduced, lysed and analyzed via western blotting for peptide expression (Fig.25).

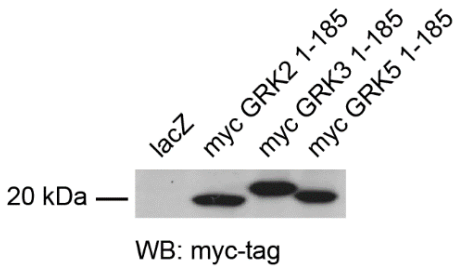

Figure 25: Expression of myc GRK2 1-185, myc GRK3 1-185 and myc GRK5 1-185 in NMCMs. NMCMs were transduced with the adenoviral myc-tagged constructs GRK2 1-185, GRK3 1-185 or GRK5 1-185 or lacZ (Ad-myc GRK2 1-185, Ad-myc GRK3 1-185, Ad-myc GRK5 1-185, Ad-lacZ), they were lysed after 48 hours and analyzed via western blotting using myc-tag antibodies. n=2

In order to elucidate the effect of the peptides under hypertrophic conditions, NMCMs were transduced with adenoviral myc-tagged constructs of GRK2 1-185 or GRK3 1-185, or GRK5 1-185 or adenoviral lacZ construct as control. The transduced cardiomyocytes were treated with isoproterenol, a β-AR agonist, which is known to cause cardiomyocyte hypertrophy[111] due to chronic activation of β-ARs. Isoproterenol stimulation took place for 24 hours. Subsequently, the cells were stained with Alexa Fluor 488-labeled phalloidin which binds to actin filaments enabling the visualization of NMCMs and their cross sectional area. Hoechst staining was used to visualize the cell nucleus. The cardiomyocyte size (cross sectional area) was determined via quantification with ImageJ.

In figure 26 A, representative images of transduced and stained NMCMs are illustrated. The pictures show that the cross sectional area is increased after isoproterenol stimulation in the control cells (lacZ).

As illustrated in figure 26 B, 26 C and 26 D, under basal conditions, the cardiomyocyte cross sectional area of cells expressing GRK2 1-185, GRK3 1-185 or GRK5 1-185 is slightly increased (non-significant) compared to control cells (lacZ). Under isoproterenol stimulation, cells expressing GRK2 1-185 (Fig.26 B) or GRK3 1-185 (Fig.26 C) present no significant increase in the cardiomyocyte cross sectional area in comparison to the unstimulated control cells, although the cross sectional area in both the stimulated and unstimulated samples is slightly increased in comparison to control. The stimulated control cells show a significant increase (*, $P < 0.05$) of the cross sectional area compared to unstimulated control cells. No significant difference in the cardiomyocyte cross sectional area between stimulated control cells and stimulated cells expressing GRK2 1-185, GRK3 1-185 or GRK5 1-185 was observed.

In contrast, in the presence of GRK5 1- 185 (Fig.26 D) a significant increase (*, $P < 0.05$) in the size of the stimulated cells in comparison to the unstimulated control lacZ is observed.

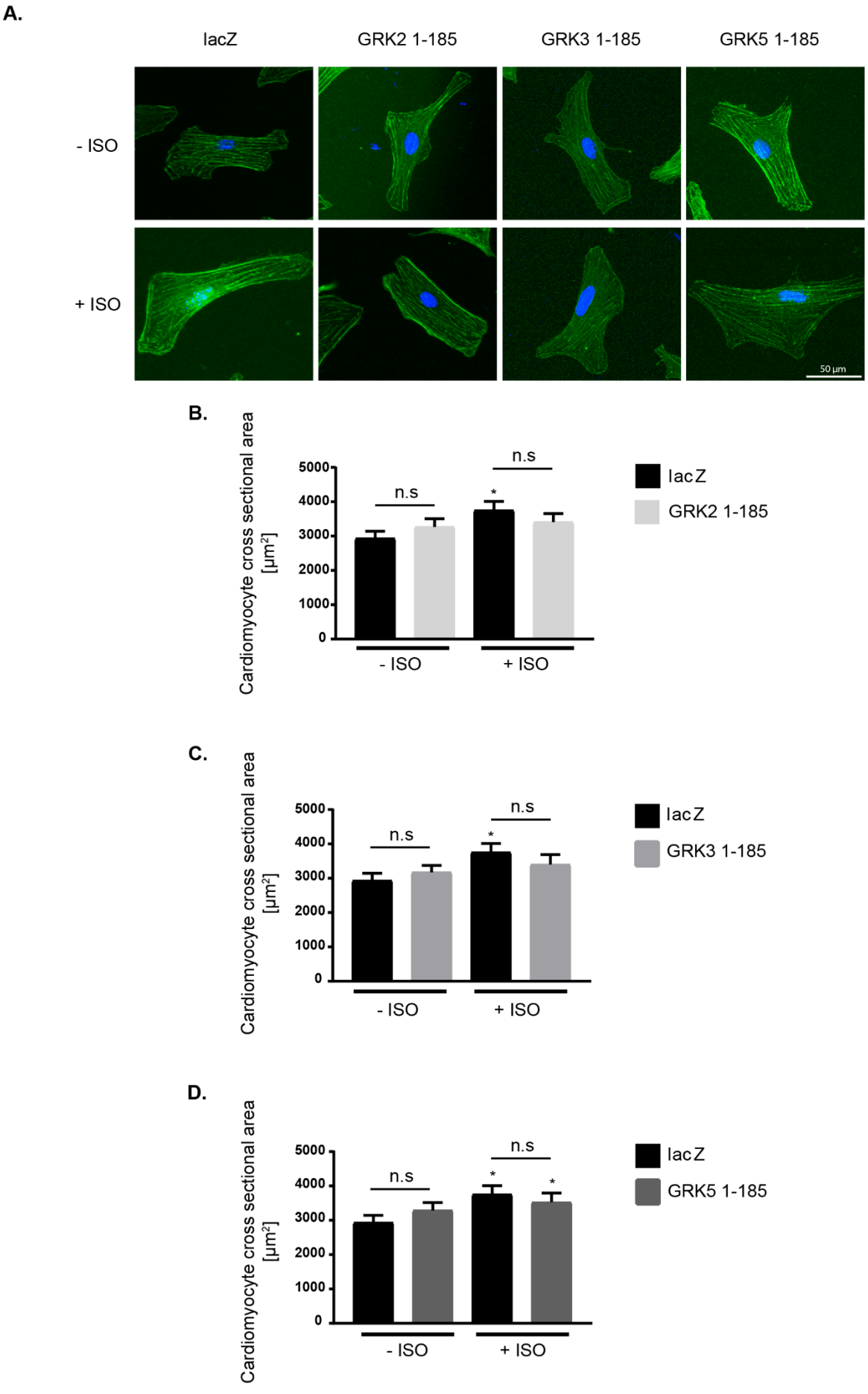
A.
lacZ
GRK2 1-185
GRK3 1-185
GRK5 1-185
- ISO
+ ISO
50 µm
B.
Cardiomyocyte cross sectional area [µm²]
5000
4000
3000
2000
1000
0
n.s
n.s
*
- ISO
+ ISO
lacZ
GRK2 1-185
C.
Cardiomyocyte cross sectional area [µm²]
n.s
n.s
*
- ISO
+ ISO
lacZ
GRK3 1-185
D.
Cardiomyocyte cross sectional area [µm²]
n.s
n.s
*
*
- ISO
+ ISO
lacZ
GRK5 1-185

Figure 26: Effect of the peptides on isoproterenol induced hypertrophy. A.: Representative images of NMCM stained with Alexa Fluor 488-labeled phalloidin and Hoechst. The scale is 50 µm. The cells were transduced with either lacZ (control) or Ad-myc GRK2 1-185 or Ad-myc GRK3 1-185 or Ad- myc GRK5 1-185 and were either stimulated with isoproterenol or were unstimulated (-/+ ISO; 5 µM; 24h). Brightness and contrast were modified for illustrative reasons. Images of the cells were recorded with a Leica DM6 B (20x/0.55 HC PL FLUOTAR objective) microscope. Hoechst was recorded at 435-485 nm and Alexa Fluor 488 at 520-550 nm. B., C., D.: Quantification of the cardiomyocyte cross sectional area of cells treated respectively with either Ad-myc GRK2 1-185 or Ad-myc GRK3 1-185 or Ad-myc GRK5 1-185 was performed using ImageJ (n=7; 50-60 cells per condition, per experiment). The values were normalized against unstimulated control (lacZ) and analyzed with repeated measurements one-way ANOVA. Results are means ± SEM. *, $P < 0.05$.

7. Contractility assessment in the presence of the peptides.

As mentioned above, maladaptive cardiac hypertrophy can be associated with depressed contractility[233]. Contractility is the inherent ability of the myocardium to contract and it can be enhanced by pharmacological agents and sympathetic autonomic activity. Considering the role of GRK2 1-185 and GRK3 1-185 in β-AR signaling, it would be expected that they might also affect cardiomyocyte contractility, especially since they seem to simulate RKIP's function, which was shown to enhance contractility[138]. NMCMs can spontaneously contract[236] and were therefore used to investigate if the peptides affect the rate of contraction.

To measure the beat rate of NMCMs in real time, the cells were seeded on Nanion CardioExcyte96 Sensor Plates (NSP-96) and were measured with the CardioExcyte96 system (Nanion Technologies). This system provides an impedance readout that serves as a correlate of cell contractility, generated by cellular action potentials of a cell monolayer[228,229] and is based on the mechanical movement of the spontaneously contracting cells. Furthermore, amplitude and base impedance that serves as a correlate of cell viability, were also evaluated. After the cells had reached a stable base impedance, namely they created cell-cell connections and a monolayer that facilitated spontaneous and synchronous beating, they were transduced; with adenoviral myc-tagged constructs of the N-termini (1-185) GRK2 or GRK3 or GRK5 or adenoviral lacZ construct, as negative control, or RKIP as positive control. Subsequently they were stimulated with isoproterenol. The effect of isoproterenol on contractility, amplitude and base impedance in the presence of the peptides was analyzed 2 minutes after stimulation to avoid pronounced receptor internalization.

As illustrated in figure 27 A-C, 28 A-C and 29 A-C, under basal conditions, the beat rate (A), base impedance (B) and amplitude (C) remain unchanged compared to the control cells.

The expression of GRK2 1-185, GRK3 1-185 and RKIP significantly increased the beat rate after isoproterenol stimulation, in comparison to isoproterenol-stimulated control cells which were transduced with lacZ (Figure 27 A, Figure 28 A and Figure 29 A respectively). Interestingly, the amplitude was slightly reduced, but not significantly in the presence of GRK2 1-185, GRK3 1-185 or RKIP (Figure 26C; Figure 27C; and Figure 28C respectively). When the cardiomyocytes contract faster, the free area between them is increased, the conductivity of the medium improves, the resistance decreases and therefor the amplitude also.

Neither GRK2 1-185, GRK3 1-185 nor RKIP had an effect on the base impedance (a correlate of viability) of the cells (Figure 27 B, Figure 28 B and Figure 29 B respectively), indicating that they had the same viability status at the point of analysis with the control cells. In addition, as shown in figures 27 E, 28 E

and 29 E the base impedance of the control cells and the cells transduced with either one of the peptides or RKIP, remained comparable throughout the whole experiment that lasted 4 to 5 days. This points out that all the cells had the same viability status during the experiment, therefore excluding the possibility of cell death affecting contractility and therefore, these experiments indeed show that GRK2 1-185 and GRK3 1-185 expression affect β-AR dependent contractile function, since β-AR stimulation with isoproterenol increased contractility in the presence of GRK2 1-185 and GRK3 1-185 compared to control cells.

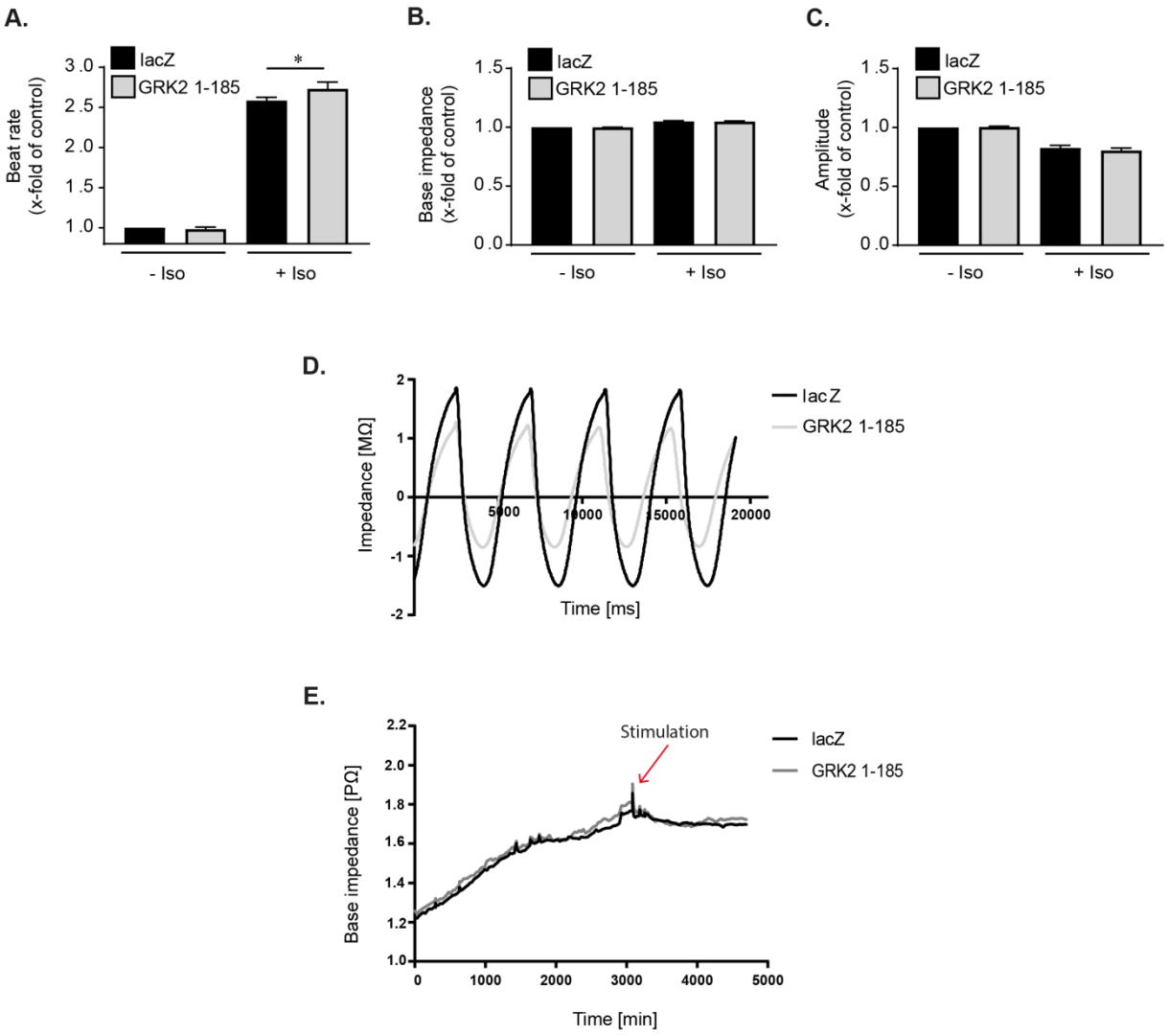

Figure 27: Evaluation of beat rate, amplitude and base impedance by impedance measurements in the presence of GRK2 1-185 in neonatal mouse cardiomyocytes. A. Beat rate, B. Base impedance, C. Amplitude, basal and after stimulation (±Iso; 50 nM, 2 min) of neonatal mouse cardiomyocytes transduced with viral construct of GRK2 1-185. The values were normalized against the control (lacZ; -Iso) and against the time point directly before stimulation, and analyzed with one-way ANOVA (n=8). D. Representative impedance pattern in one well, at a specific time point after stimulation. E. Representative base impedance diagram during a whole experiment. The red arrow indicates the time point at which the cells were stimulated. Results are means ± SEM. *, $P < 0.05$.

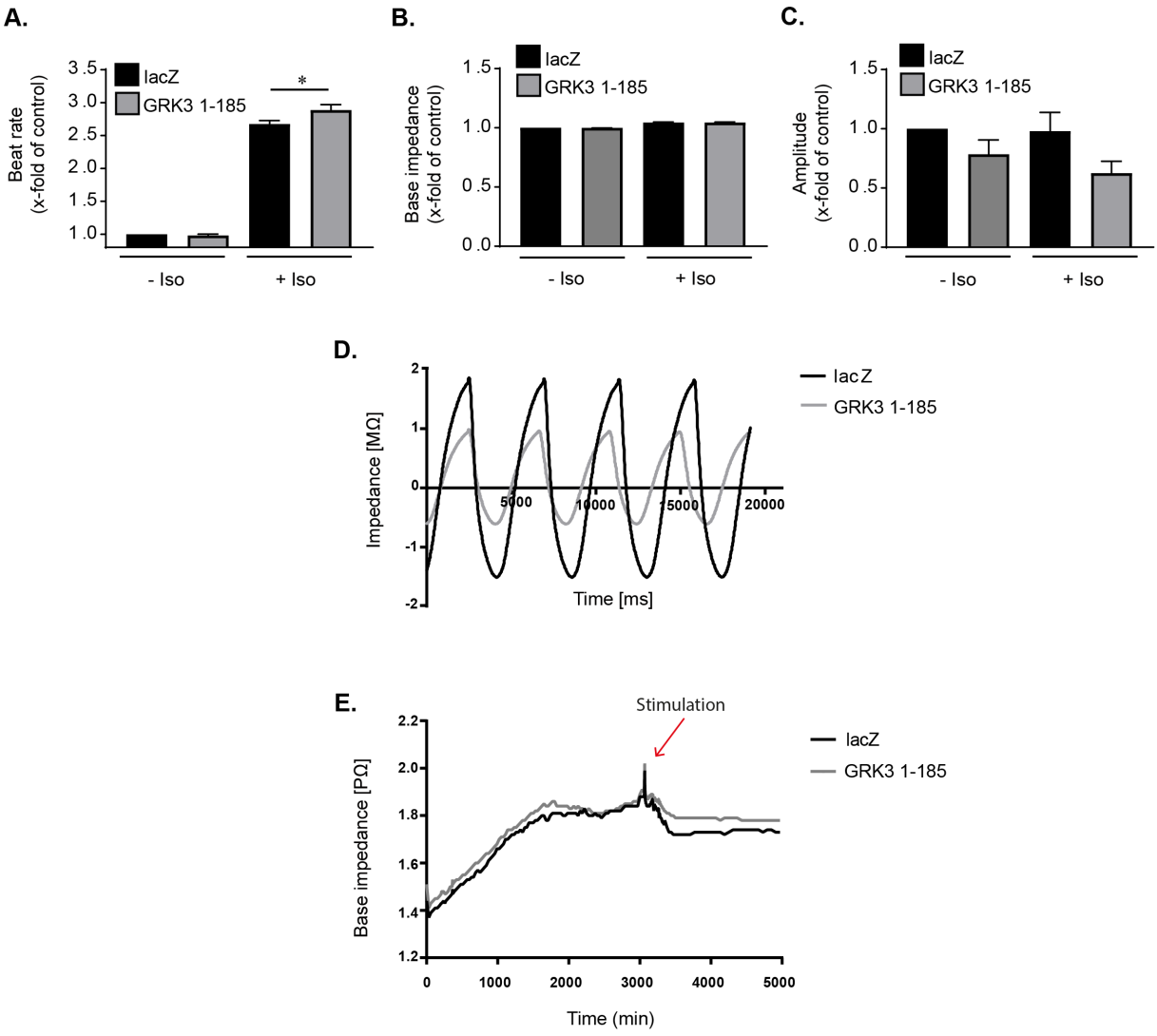

Figure 28: Evaluation of beat rate, amplitude and base impedance by impedance measurements in the presence of GRK3 1-185 in neonatal mouse cardiomyocytes. A. Beat rate, B. Base impedance, C. Amplitude, basal and after stimulation (±Iso; 50 nM, 2 min) of neonatal mouse cardiomyocytes transduced with viral construct of GRK3 1-185. The values were normalized against the control (lacZ; -Iso) and against the time point directly before stimulation, and analyzed with one-way ANOVA (n=13). D. Representative impedance pattern in one well, at a specific time point after stimulation. E. Representative base impedance diagram during a whole experiment. The red arrow indicates the time point at which the cells were stimulated. Results are means ± SEM. *, $P < 0.05$.

On the other hand, GRK5 1-185 did not show a significant effect on beat rate (Fig. 29 A), suggesting that this peptide does not have a comparable function as GRK2 1-185, GRK3 1-185 or RKIP. The base impedance (Fig. 29 B) was comparable between the control, GRK5 1-185 and RKIP. As mentioned above, the peptides that increased contractility as well as RKIP demonstrate a slightly lowered amplitude (non-significant), whereas this is not the case with GRK5 1-185 (Fig. 29 C).

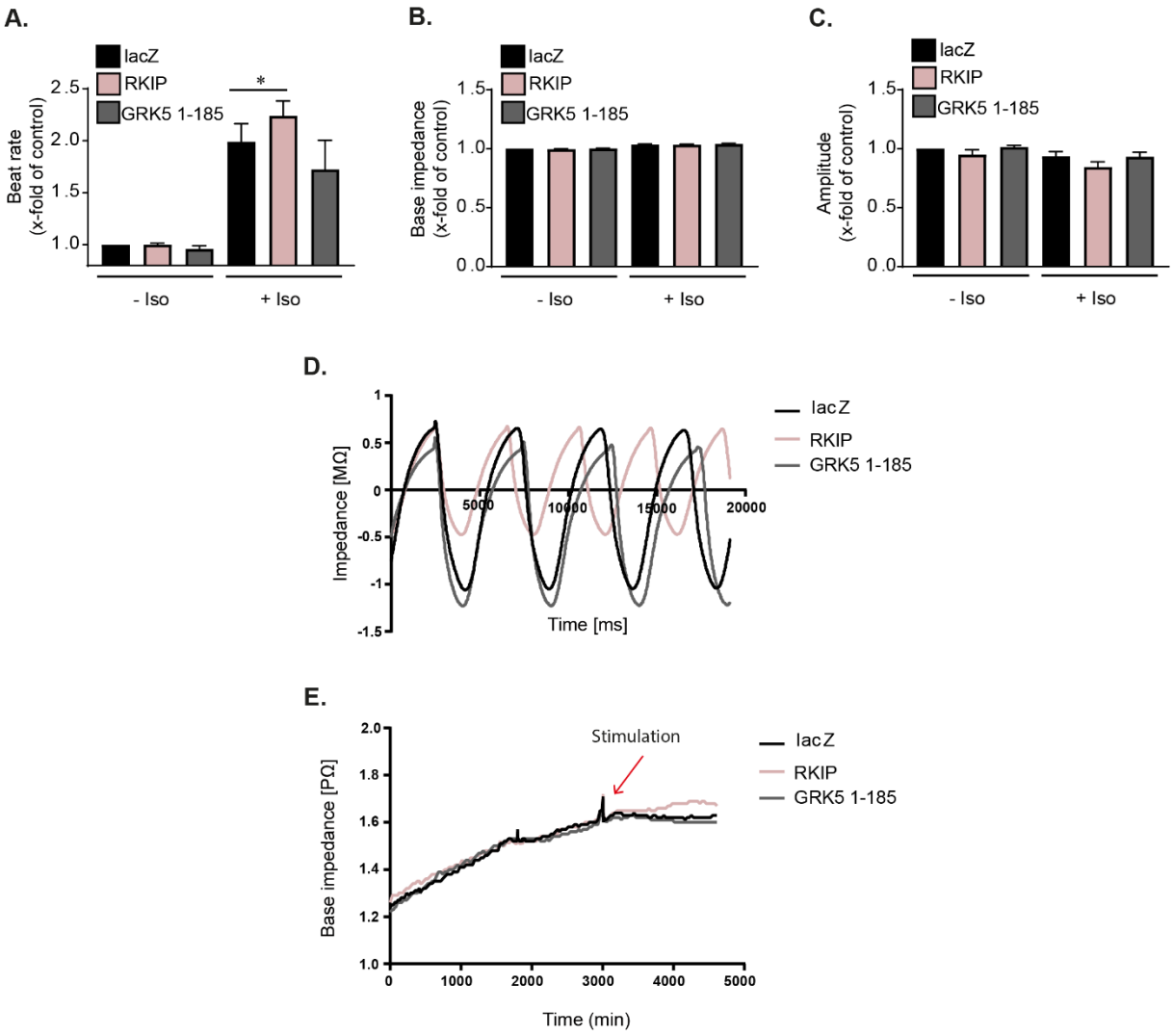

Figure 29: Evaluation of beat rate, amplitude and base impedance by impedance measurements in the presence of RKIP or GRK5 1-185 in neonatal mouse cardiomyocytes. A. Beat rate, B. Base impedance, C. Amplitude, basal and after stimulation (±Iso; 50 nM, 2 min) of neonatal mouse cardiomyocytes transduced with viral construct of RKIP or GRK5 1-185. The values were normalized against the control (lacZ; -Iso) and against the time point directly before stimulation, and analyzed with one-way ANOVA (n=9). D. Representative impedance pattern in one well, at a specific time point after stimulation. E. Representative base impedance diagram during a whole experiment. The red arrow indicates the time point at which the cells were stimulated. Results are means ± SEM. *, $P < 0.05$.

Altogether, it was demonstrated here, that GRK2 1-185 and GRK3 1-185 have a positive effect on contractility upon isoproterenol stimulation which is comparable with the already established effect of RKIP. Nonetheless, GRK5 1-185 does not seem to have an effect on contractility.

V. Discussion

In this project, the interaction interface of GRK/RKIP was investigated in order to define potential therapeutic strategies for heart failure that simulate the beneficial effects of RKIP. The N- termini of GRK2 and GRK3 had a significant influence on β_2AR phosphorylation and on its downstream signaling and internalization. Furthermore, at their presence, hypertrophy was not observed, and contractility was increased after stimulation. In addition, it was revealed that the peptides probably achieve these effects via direct binding to β_2AR. This result suggests a blockade of the binding and phosphorylation site of GRK2 on the receptor that hinders the GRK-mediated initiation of its desensitization and downregulation. Altogether, these results suggest that GRK2 1-185 and GRK3 1-185 could serve as a model for the generation of novel and more specific targeting strategies for receptor regulation in heart failure.

1. GPCR signaling in cardiovascular disease

GPCRs are a superfamily of membrane proteins that respond to a variety of extracellular signals thereby modulating a wide spectrum of cellular processes such as growth, differentiation, proliferation and death[237]. This renders GPCRs one of the most important targets for therapeutic drug development.

Upon stimulation of GPCRs, heterotrimeric G-proteins are activated, leading to their dissociation into Gα and Gβγ subunits, which are involved in the modulation of different effector systems. Furthermore, stimulation initiates regulatory mechanisms which lead to GPCR desensitization. Desensitization is triggered by receptor phosphorylation by specific G protein-coupled receptor kinases (GRKs). Upon receptor phosphorylation by GRKs, arrestins bind to the receptor, leading to uncoupling of GPCRs and G proteins and to mediation of internalization[121].

Adrenergic receptors are members of the GPCR family and are together with endothelin, angiotensin and adenosine receptors widely expressed in cardiovascular tissues. Their dysfunction has been shown to be involved in the onset and development of cardiovascular diseases, ultimately causing heart failure[237]. Heart failure is a leading cause of mortality and morbidity in the industrialized world. It is the condition when the ventricle cannot fill with or eject blood and its main characteristic is increased activation of the sympathetic nervous system (SNS). The SNS is involved in the regulation of cardiac function by means of releasing catecholamines which act on adrenergic receptors, eliciting increased myocardial contraction force. Under pathological conditions, elevated catecholamine levels can lead to cardiac deterioration and eventually to cardiomyocyte apoptosis and cardiac hypertrophy[238].

1.1 Pharmacological interventions

Current medication for treatment of heart failure consists mainly of β-adrenergic receptor (β-AR) antagonists and inhibitors of angiotensin II and aldosterone. In acute heart failure, β-adrenergic agonists are commonly used to stabilize patients. Although, the introduction of these pharmacotherapies has improved patients' survival, relief of symptoms and quality of life, prognosis and disease progression are not yet ideal[239–241]. Thus, novel targeting strategies for heart failure which prevent progression of cardiac dysfunction and improve cardiac contractility are mandatory.

2. Currently investigated strategies targeting cardiac β- adrenergic signaling

Adrenergic receptors are a major target of current cardiovascular pharmacotherapy. Consequently, they, and molecular components implicated in adrenergic signaling and involved in heart failure pathogenesis are intensively investigated, in order to further elucidate aspects of GPCR signaling that could contribute in the development of new therapy strategies.

2.1 GRK2 inhibitors

GRK2 recognizes and phosphorylates agonist-activated β-ARs, leading to their desensitization and downregulation. However, GRK2 has also non-receptor substrates[120]. The prevalence of GRK2 activity in cardiovascular disease and failing hearts has made it a major object of research over the past decades. Several studies have demonstrated that GRK2 expression levels and activity, both in humans and in animal models, play an important role in cardiac development[131] and hypertrophy[62,127,132], leading to the assumption that GRK2 inhibition could constitute a therapeutic approach for heart failure[242,243]. GRK2 and its therapeutic potential in cardiovascular disease has been extensively reviewed[64,110,111,244–247]. Nevertheless, due to the high similarity to other members of the GRK family and due to the fact that its catalytic mechanism is conserved among protein kinases[81], therapeutic targeting of GRK2 is challenging.

Over time, several inhibitors have been investigated, such as various chemical compounds (e.g. polyanions, polycations, and Takeda compounds), RNA-Aptamers[139], paroxetine[248–250], the physiological inhibitor RKIP[58,138] but also peptides such as βARKct[134,136,251,252], GRK2 RGS[137] and GRK5- NT[154,155].

Within the scope of defining the biological role of GRK2, polyanions and polycations such as heparin and dextran sulfate, were the first compounds tested for their ability to inhibit GRK2. The most potent inhibitor was proven to be heparin with an IC_{50} value of 0.15 μM[253]. However, it also targets other

kinases such as casein kinase II[254]. Moreover, these compounds are unable of crossing the cell membrane due to the fact that they are highly charged[253], therefore, their therapeutic potential is rather reduced.

The Takeda compounds are developed from Takeda Pharmaceuticals. Although they are highly selective and potent inhibitors of GRK2 (IC_{50} >2 μM), they have until now not advanced to clinical trials, suggesting undesirable effects such as low bioavailability[139,255,256].

RNA Aptamers are oligonucleotides that bind on a target. A highly specific and potent RNA-based inhibitor (C13) of GRK2 was identified *in vitro*[257,258]. However, these molecules have high molecular weight which affects their bioavailability and complicates their conversion to drug-molecules[139].

Paroxetine is a selective serotonin reuptake inhibitor which is approved by the FDA as an antidepressant. Although it is a moderately potent GRK2 inhibitor, it is selective and it was demonstrated in cells and in mice that it improves cardiac function and increases myocardial contractility[248,249,255]. Nevertheless, paroxetine is a drug used for depression treatment; in other words, it has effects independent of GRK2 inhibition.

The βARKct inhibitor consists of the GRK2 C-terminus which is responsible for Gβγ binding and membrane recruitment in order to phosphorylate the activated receptor[101]. βARKct scavenges Gβγ that dissociates from the receptor and thereby prevents it from binding GRK2, hindering this way its translocation to the membrane and subsequent receptor phosphorylation and desensitization. In a murine model of heart failure, βARKct overexpression prevented the development of cardiomyopathy[251] and in another it improved cardiac dilation, functionality and survival[134]. Moreover, in a porcine heart failure model, AAV6. βARKct treatment could ameliorate cardiac function, but could not completely restore it[259]. However, cardiac specific transgenic βARKct mice, developed hypertrophy to the same extent as wild type mice after transverse aorta constriction (TAC) operation[137]. Strikingly, it was demonstrated that the improved βAR responsiveness caused by βARKct, is actually achieved through Gβγ mediated L-type calcium current disinhibition[260]. In addition, Gβγ is involved in many signaling pathways, meaning that its scavenging could eventually lead to undesired effects. Altogether, besides the ambiguous role of βARKct in treating cardiac hypertrophy, its dimension exacerbates its clinical application due to the genetic tools necessary for its expression.

Raf kinase inhibitor protein (RKIP) was identified as a binding protein which can suppress Raf-1 kinase activity and Mitogen-Activated Protein (MAP) kinase signaling[170]. In addition, it was revealed that it can interact with the N-terminus of GRK2[58]. Later on, the mechanism of this interaction was elucidated: upon phosphorylation of RKIP at Ser153 by PKC, RKIP dissociates from Raf, dimerizes and binds GRK2 leading to its selective inhibition[172]. GRK2 inhibition prevents phosphorylation and desensitization of

βARs but its cytosolic substrates remain unaffected. Using transgenic mice overexpression and gene delivery approaches, it was demonstrated that RKIP enhances cardiac contractility in a well-tolerated manner and that it exerts anti-apoptotic, anti-fibrotic and anti-arrhythmic effects[261]. While GRK2 and its inhibition play an important role in heart failure, a chronic activation of the Raf/MEK/ERK pathway is observed in many tumors. Therefore, RKIP and its mechanism of action should be further investigated in order to set a starting point for the development of compounds or gene therapy for heart failure.

3. RKIP as a model for the development of new targeting strategies

Cardiovascular disease (CVD) accounts for 45% of all deaths in Europe and 37% of all deaths in the EU[262]. Hence, the development of effective therapeutics is essential to reduce morbidity and mortality. Aim of this project was to further investigate the interaction between GRK and RKIP in order to design novel therapeutic targeting strategies that simulate RKIP's beneficial effects in the heart.

3.1 RKIP/ GRK association

In the heart, the most abundant GRKs are GRK2, GRK3 and GRK5[129] and they are differentially expressed depending on heart failure etiology[130]. The critical role of GRKs and especially GRK2 and GRK5 in the regulation of cardiac function have been intensively studied since they are the predominant GRK isoforms localized in the heart.

GRK2 belongs to the same family as GRK3, they are both localized in the heart and they are highly homologous. The sequence alignment of GRK2 and GRK3 using CLUSTALW showed that they are to 85% similar to each other. Considering this, and the fact that they are both localized in the heart, the question arose whether RKIP interacts in the same way with GRK3 as with GRK2. For the interaction of RKIP with GRK2 to take place, PKC must be activated. PKC phosphorylates RKIP at Ser153 and triggers its dissociation from Raf and its association with GRK2. Through co-immunoprecipitation experiments it was investigated whether RKIP binds GRK3 and what the effect of PKC activation is. PMA is a diester of phorbol used to activate PKC. It was revealed that RKIP also binds GRK3 and that the binding is enhanced when PKA is stimulated with PMA. This suggests that RKIP interacts in a similar way with GRK3 as with GRK2.

GRK5 is as well found at high levels in the heart[54], however, in contrast to GRK3 it shows low homology to GRK2 (28%). In co-immunoprecipitation experiments performed with RKIP and GRK5, RKIP did not

bind GRK5 which is in accordance with the literature where it was already demonstrated that RKIP cannot bind and inhibit GRK5[58]. Stimulation of PKC had no effect.

When investigating protein interactions, the exact interaction site is of great significance. According to the literature, RKIP binds the N-terminus of GRK2 within the amino-terminus 1-185[58]. It consists of a short amino acids region and a regulator of G protein signaling (RGS) homology domain (RH). The N- terminal region of GRKs is conserved and unique in this group of kinases[54]. It interacts with the kinase domain to activate the kinase, thereby stabilizing the GRK active conformation and enhancing GRK activity[80,81]. Additionally, the N-terminus is involved in a direct interaction with GPCRs[76] and is necessary for receptor recognition[64]. After determining that RKIP interacts both with GRK2 and GRK3, the next step was to specify the exact binding region in the N-terminus. To investigate this, two new N- terminal peptides covering the amino acid region 1-185 of GRK2, GRK3 and GRK5 were generated: 1-53 and 54-185. Co-immunoprecipitation experiments including all the peptides 54-185 and 1-185 of GRK2, GRK3 and GRK5 were performed. The smallest peptide, 1-53, could not be used for these experiments due to inadequate expression/detection in HEK cells. In addition, pull down assays were performed with purified GST-tagged peptides in order to validate the results of the co-immunoprecipitations in a different setting. It was observed that all three peptides of GRK2 and GRK3 could bind RKIP, whereas as expected none of the GRK5 peptides could bind RKIP. This indicates that RKIP can bind to the whole N-terminal region of the GRKs.

4. Do the peptides have an effect on the process of receptor phosphorylation, internalization and downstream signaling?

4.1 Receptor phosphorylation

As previously described, RKIP inhibits the GRK2-mediated phosphorylation of β_2-AR[58]. Receptor phosphorylation inhibition prevents desensitization and downregulation and thereby receptor activity is enhanced. The ability to inhibit β- AR phosphorylation is important for a potential therapeutic, since it can lead to increased cardiac contractility.

To test whether the peptides 54-185 and 1-185 of GRK2, GRK3 and GRK5 are able to simulate the RKIP mediated interference of the GRK2/receptor interaction, we analyzed the β_2-AR phosphorylation in the absence and presence of the peptides and used RKIP as an internal positive control. It was revealed that the peptide 1-185 of GRK2 and GRK3 could reduce receptor phosphorylation to a similar extent as RKIP, whereas GRK5 1-185 had no significant effect. Among the smaller peptides, only GRK2 54-185 reduced significantly the receptor phosphorylation indicating that at least in case of GRK3 the full

length N-terminal peptide is necessary for receptor phosphorylation inhibition. On the other hand, neither GRK5 1-185 nor GRK5 54-185 significantly reduced receptor phosphorylation.

These results corroborate with the studies of *Pao et al.*[79] and *Noble et al.*[78] which demonstrated that a GRK2 peptide consisting of the amino acids 1-14 effectively inhibited isoproterenol stimulated GRK2 mediated β_2-AR phosphorylation[79], whereas the corresponding GRK5 peptide had no effect on GRK2 mediated β_2-AR phosphorylation[78]. In this study, the 1-185 peptides that were used included the amino acids 1-14 and it was demonstrated that GRK2 1-185 and GRK3 1-185 as well, had an effect on GRK2 mediated β_2-AR phosphorylation. GRK2 and GRK3 are highly homologous and belong to the same subfamily of GRKs which could explain why GRK3 1-185 also shows specificity for GRK2 mediated β_2- AR phosphorylation. Why GRK2 54-185 which does not contain the initial 1-14 amino acids also significantly reduced receptor phosphorylation remains unclear. After this point, only the 1-185 peptides of all GRKs were used.

In addition, the peptides seem to mimic RKIP's function, since it was shown that RKIP can inhibit β_2- AR phosphorylation[58].

4.2 Receptor internalization

GRK-mediated receptor phosphorylation is a well-characterized mechanism for GPCR desensitization. Upon agonist binding, conformational changes are triggered which in combination with post-translational modifications enable the binding of β-arrestin proteins on the receptor[263]. β-arrestin facilitates homologous desensitization by disabling its coupling to G proteins[48,49]. Furthermore, β- arrestin binding, targets the receptor to clathrin coated pits which leads to receptor internalization/endocytosis[50], a process that serves to resensitize the receptor or target it to lysosomes for degradation[52]. Since the peptides of GRK2 and GRK3 reduced receptor phosphorylation it was hypothesized that they would also have an effect on receptor internalization, which is a process triggered by receptor phosphorylation.

Live cell fluorescence imaging and radioligand binding assays were employed to determine receptor internalization in the presence of the peptides. As expected, and mimicking RKIP[58], GRK2 1-185 and GRK3 1-185 reduced receptor internalization; GRK5 1-185 also reduced it but not significantly. These results are in line with the observed reduced phosphorylation in the presence of GRK2 1-185 and GRK3 1-185 and confirm the dogma that dictates correlation between receptor phosphorylation and internalization, which has been often reviewed since its discovery about three decades ago[264]. Furthermore, a study performed with another N-terminal GRK2 domain, named β-ARKnt and consisting of amino acids 50-145, showed that this peptide attenuates cardiac β-AR downregulation in transgenic mice expressing β-ARKnt 50- 145 in the heart, when treated with isoproterenol in

comparison to control mice[265]. This is in agreement with the observed reduced internalization in this project, although the peptides do not cover exactly the same sequence.

4.3 Receptor downstream signaling

When β-ARs are stimulated, $G\alpha_s$ activates adenylate cyclase (AC) which generates the second messenger cyclic adenosine monophosphate (cAMP); increased cAMP levels activate cAMP-dependent protein kinase A (PKA) which in turn can phosphorylate various cell proteins such as phosducin[173,178,232]. To study the effect of the peptides on β_2AR downstream signaling, kinase activity of PKA was investigated by determining phosducin phosphorylation.

As expected, since reduced receptor phosphorylation and internalization lead to enhanced receptor signaling, it was observed that GRK2 1- 185 and GRK3 1-185 cause a significant increase in PKA activity, indicated by increased phosducin phosphorylation. A study performed by *Keys et al.* using the previously mentioned β-ARKnt transgenic mice, demonstrated that β-AR signaling in response to isoproterenol was not enhanced which is the contrary of what was observed in this project and it is not in line with the fact that they did observe attenuated β-AR downregulation[265]. Although GRK2 and GRK3 are isozymes and they are mostly found in the same tissues, GRK3 is much less investigated than GRK2 regarding β- adrenergic signaling. In contrast to GRK3 1-185, which as shown here enhances PKA activity, allowing the assumption that cAMP signaling is enhanced, full-length GRK3 has no effect on adenylyl cyclase activity as shown in a study from *Iaccarino et al.*[101]. In order to assess β-adrenergic signaling in mouse cardiomyocytes, they performed adenylyl cyclase assays with isoproterenol stimulation and showed that receptor desensitization in GRK3 transgenic animals was at the same level as in the control animals[101]. In addition, another study investigating among others the adenylyl cyclase activity in mice overexpressing GRK2, demonstrated lower isoproterenol-stimulated adenylyl cyclase activities in comparison to control, probably due to increased GRK2-mediated receptor phosphorylation[136]. Altogether, it can be pointed out that GRK2 1-185 and GRK3 1-185 have the opposite effect regarding β- adrenergic signaling than their respective full-length proteins.

Despite the fact that GRK5 1-185 had no significant effect neither on receptor phosphorylation nor on receptor internalization, it was revealed that it as well increased phosducin phosphorylation and therefore cAMP signaling and PKA activation. A similar observation regarding cAMP signaling was made by *Sorriento et al.* when they tested the effect of GRK5-NT 45- 150 on CREB (cAMP response element-binding protein), a transcription factor activated by cAMP. They demonstrated that the GRK5 N-terminal peptide did not inhibit CREB activation, but slightly increased it at the basal state and significantly increased it when stimulated with phenylephrine (PE)[154]. Taken together, although

GRK5 1-185 seems to be implicated in PKA signaling, it is probably through another pathway and not through the activation of β_2-AR.

Altogether, the effects of GRK2 1-185 and GRK3 1-185 seem to simulate the function of RKIP as described from *Lorenz et al.*[58], who showed that RKIP inhibits phosphorylation of the β_2-AR, attenuates agonist-stimulated receptor internalization and enhances receptor signaling[58].

5. The potential mechanism behind the effects of the peptides on β_2-AR regulation and signaling.

To this point, it was revealed that the peptides had a significant influence on β_2AR phosphorylation and internalization, and β_2AR downstream signaling. However, the mechanism by which this is achieved remained unclarified. One could hypothesize either, that the peptides simulate RKIP's function and bind directly GRK2 like RKIP, thus preventing it from phosphorylating the receptor, or that they bind the receptor and indirectly hinder its phosphorylation by GRK2 by binding the GRK2/receptor interaction domain. Due to the fact that to the present no dimer formation of GRK2 or GRK3 has been reported in the literature, it was hypothesized that the peptides bind directly to the intracellular part of the receptor, where the GRK2/receptor interaction and receptor phosphorylation take place[119,266]. As a consequence of a direct interaction between receptor and peptide, GRK2 would not be able to bind the receptor and phosphorylate it; thereby receptor downregulation and desensitization would be prevented. To examine whether this hypothesis was valid, co-immunoprecipitation experiments with β_2AR and the peptides were performed.

It was revealed that GRK2 1-185 and GRK3 1-185 bind the receptor, suggesting that the previously observed peptide mediated effects take place due to a direct interaction between receptor and peptide which prevents GRK2 from binding and phosphorylating the receptor. In contrast, GRK2 54-185 and GRK3 54-185 did not bind the receptor. As previously described, the N-terminus of the GRKs is essential for the direct interaction with GPCRs and for their recognition as well[64,76,267]. Considering this, and that the GRK2 surface responsible for the interaction with the receptor is located at the beginning of the N-terminus[267], it was to be expected that GRK2 1-185 would bind the receptor. Regarding GRK3, which has been studied in a lesser extent than GRK2, most of the available literature describes its role in α- adrenergic, in endothelin (ET) and odorant receptor signaling[104,142,144,268,269]. However, a study from *Iaccarino et al.*[101] demonstrated that myocardial overexpression of GRK3 leads to unaltered β-AR signaling. Revealing here, that GRK3 1-185 can associate with the β_2-AR and influence β-AR signaling is a rather new and interesting finding.

Although full-length GRK5 has been shown to interact with β-ARs[106,270–272], here, GRK5 1-185 did not demonstrate consistent binding on the receptor, which could be an explanation for the previous results, where GRK5 1-185 did not significantly reduce receptor phosphorylation or internalization. Furthermore, this suggests that the N-terminus of GRK5, in contrast to the N-termini of GRK2 and GRK3 and despite the fact that all three kinases belong to the same family, has a different signaling modus which engenders other effects.

6. The physiological effect of the peptides

β-ARs are important regulators of myocardial function. Therefore, their dysregulation has been characterized as a precursor for the development of heart failure[176,177]. Heart failure is the end stage of many cardiovascular diseases and remains one of the most common causes of death worldwide. Its main characteristic is increased activation of the sympathetic nervous system (SNS) due to increased load or stress on the heart like acute injury, which results in elevated catecholamine release. Catecholamine levels regulate cardiac contractility. At the molecular level, this causes stimulation and increased activation of β-ARs in the heart, which initially serves as a compensatory mechanism in order to increase cardiac output[179]. Activation of β-ARs triggers their phosphorylation from GRKs, leading to receptor desensitization and downregulation. This is initially considered a protective mechanism; however, chronic receptor activation has deleterious effects on the heart. Nevertheless, in the failing heart this triggers a vicious cycle of persistent SNS activation and subsequent desensitization and downregulation of the receptor[182]. This leads eventually to contractility attenuation and progressive cardiac remodeling.

Considering the role of β-ARs in the development of heart failure and that until this point, it was shown that GRK2 1-185 and GRK3 1-185 can favorably influence β-AR signaling, as next, it was examined whether these peptides also had an effect on hypertrophy and contractility.

6.1 Hypertrophy

Cardiac hypertrophy (from Greek ὑπέρ "excess" + τροφή "nourishment") is the thickening of heart muscle due to cardiomyocyte enlargement, but in the absence of cell division, as a response to physiological or pathological events; at molecular level, it leads to alteration of cardiac cell signaling. If pathological, hypertrophy is associated with decreased contractility and is a risk factor for the development of heart failure[233].

To study hypertrophy, isolated neonatal mouse cardiomyocytes were transduced with adenoviral constructs of the peptides and were either not stimulated or stimulated with the hypertrophic stimulus

isoproterenol. After evaluating their cell surface and comparing the stimulated peptide cardiomyocytes with the unstimulated control cardiomyocytes, it was revealed that the cardiomyocytes treated either with GRK2 1-185 or GRK3 1-185 were not significantly hypertrophic compared with the unstimulated control, whereas the cells with GRK5 1-185 showed increased cell surface compared to the unstimulated control.

To date, the effects of the N-terminus of GRK2 on hypertrophy are rather discordant. The previously mentioned study performed by Keys et al.[265] *in vivo,* using the β- ARKnt also investigated the effect of β-ARKnt on hypertrophy. They concluded, due to increased heart size, that expression of β-ARKnt in mice induces cardiac hypertrophy both in an isoproterenol and in a transverse aortic constriction (TAC) model. However, echocardiography and histology showed no difference between the models and the control animals[265]. Later on, another study by *Schumacher et al.* was performed using a slightly different peptide of GRK2 to investigate hypertrophy in mice, namely the β-ARKrgs, which consists of the RGS domain and amino acids 50-145. Here it was demonstrated via echocardiography and histology that β-ARKrgs transgenic mice exhibit an antihypertrophic effect after TAC. They postulate that β-ARKrgs serves as a noncanonical inhibitor of Gαq-mediated hypertrophic signaling since they could observe that the β-ARKrgs peptide interacts with Gαq[137]; enhanced Gαq signaling has been shown to induce cardiac hypertrophy[273–275]. Although all three peptides share overlapping residues, neither the outcome of the study of *Keys et al.*[265] nor of *Schumacher et al.*[137] entirely corresponds with that of this project, probably due to differences in the sequence, which can lead to mechanistic discrepancies. In addition, different methods and models were used. In the current project it was revealed that GRK2 1-185 and GRK3 1-185 modulate β-AR signaling. Nevertheless, the cardiomyocyte size is slightly increased (not significantly) and there is no significant size difference between the stimulated control cardiomyocytes and the stimulated peptide cardiomyocytes. The mechanistic difference possibly relies on the fact that the β- ARKrgs peptide consists only of the RGS domain of GRK2 which can inhibit Gαq signaling[276], however, the extreme N-terminus which is responsible for interaction with the receptor is absent. Of note, RKIP overexpressing mice developed cardiac hypertrophy that was comparable to wild type control mice but was not associated to heart failure onset[138].

Regarding the effect of the N-terminus of GRK5 on hypertrophy, two studies have been thus far published that try to address it; both were performed by the same group of scientists. In both studies, an adenoviral construct of GRK5 1-170 was used, named AdGRK5-NT. In the first study, they demonstrated that in cardiomyoblasts (H9c2) AdGRK5-NT modulates the NF-κB transcriptional activity and thereby, it regulates the expression of hypertrophic genes. In the *in vivo* experiments, they performed intracardiac injection of AdGRK5-NT in normotensive and hypertensive rats and they observed that AdGRK5-NT inhibits left ventricular hypertrophy (LVH)[154]. The subsequent study using

the same peptide and as well cardiomyoblasts and rats, showed that GRK5-NT inhibits cardiac hypertrophy through the binding and sequestration of calmodulin, a messenger protein necessary for the regulation of calcium-calmodulin dependent transcription factors such as NFAT (Nuclear factor of activated T-cells), which regulate the transcription of hypertrophic genes[155]. Each of these studies suggests a different mechanistic pathway for the inhibition of cardiac hypertrophy: by protein-protein interaction in the RH domain for inhibition of NF-κB[154] or calmodulin binding at the N-terminus and inhibition of NFAT[155]. However the authors claim that GRK5-NT can act simultaneously on both pathways. Noticeably, GRK5-NT expression was never confirmed, neither *in vitro* nor *in vivo* in none of these studies. In this project, the contrary was demonstrated than what is reported in the studies of *Sorriento et al.*[154,155], namely that GRK5 1-185 does not prevent the development of hypertrophy, an effect comparable to that of RKIP, which does not inhibit cardiac hypertrophy in RKIP transgenic mice in comparison to control mice[138]. The discordancy observed between this project and *Sorriento et al.*[154,155] regarding the effect of GRK5 N-terminus on hypertrophy could be ascribed to the different models and different hypertrophic stimuli used. Here, the hypertrophic effect was investigated in neonatal mouse cardiomyocytes under the influence of isoproterenol, whereas they used a cardiomyoblasts cell line and rat models (hypertension-induced LVH, phenylephrine induced hypertrophy). Isoproterenol and phenylephrine both target the adrenergic system, but have different receptors as targets: isoproterenol is a non-selective β-AR agonist[277] and phenylephrine is a selective α1-AR agonist[278], thus they are implicated in the modulation of distinct signaling pathways.

6.2 Contractility

In the heart, β-ARs comprise the majority of cardiac adrenergic receptors, with β_1-AR being the predominant subtype that induces contractility; however, chronic β_1-AR stimulation is detrimental for the heart. On the contrary, long-term increased activity of β_2-AR seems to be better tolerated than chronic β_1-AR stimulation[138,279–281]. Therefore, β- adrenergic signaling is suited as a target for improving contractility.

To measure contractility (beat rate) of NMCMs, the cardiomyocytes were seeded on Nanion CardioExcyte 96 Sensor Plates (NSP-96) and were measured with the CardioExcyte96 system (Nanion Technologies). This system provides an impedance readout (a correlate of cell contractility) generated by cellular action potentials of a cell monolayer[228,229] and is based on the mechanical movement of the spontaneously contracting cells. The cardiomyocytes were transduced with the adenoviral constructs of GRK2 1-185, GRK3 1-185, GRK5 1-185 and lacz as control. Beat rate, amplitude and base impedance were determined before and after isoproterenol stimulation.

The peptides GRK2 1-185 and GRK3 1-185 and RKIP increased beat rate after isoproterenol stimulation in comparison to control. These results are controversial to the results from the two studies, which used β-ARKnt or β-ARKrgs and determined their effect on cardiac contractility, in isolated cardiomyocytes and mice respectively. They both demonstrated that the presence of those peptides does not cause cardiac contractility alterations neither at baseline nor in response to isoproterenol[137,265]. In this project, GRK2 1-185 and GRK3 1-185 seem to mimic the function of RKIP in regard to contractility, since neonatal rat cardiomyocytes transduced with RKIP had increased contractility in comparison to control as well[261]. This discrepancy could rely on the fact that *Keys et al.*[265] used adult mouse cardiomyocytes to investigate the effect of β- ARKnt, and *Schumacher et al.*[137] transgenic mice and terminal hemodynamics to study the effect of β-ARKrgs on contractility. Isolated neonatal and adult mouse cardiomyocytes are physiologically different, especially in matters of contractility; neonatal cardiomyocytes can contract spontaneously, whereas adult cardiomyocytes need pacing to induce contraction[236]. Furthermore, the analysis of contractions *in vivo* performed by *Schumacher et al.*[137], comprises a decidedly different model than the *ex vivo* analysis performed with isolated neonatal mouse cardiomyocytes in this project.

In contrast to GRK2 1-185 and GRK3 1-185, GRK5 1-185 did not induce contractility. However, *Sorriento et al.* showed that GRK5-NT ameliorates cardiac contractility in spontaneously hypertensive rats (SHR)[154], which contradicts the results obtained in this project. To be taken into consideration, is the fact that the SHR model used in that study is an entirely different model than the NMCMs used in this project, which could explain the observed discordancy.

However, after stimulation contractility increased in comparison to control and amplitude decreased, although not significantly. Nevertheless, in a study using the alternative technology to CardioExcyte 96, xCELLigence RTCA, and mouse embryonic stem cells it was observed after isoproterenol stimulation that the beat rate increased and the amplitude was decreased in comparison to baseline[282]. The principle of the impedance recording mode of CardioExcyte 96, via which parameters such as beat rate, amplitude and base impedance are calculated, is applying an excitation voltage between the sensing and reference electrode and picking up the resulting current. Two current paths contribute to the impedance readout: a path across the cell layer and a path through the intermediate spaces (through the electrolytic medium). Electrical capacitance and resistance caused by the cell monolayer and the cell morphology are two determinants of the both current paths[228]. So, based on the principle of the impedance readout and Ohm's law ($R_{resistance}=V_{voltage}/I_{current}$), when cells contract, the intermediate space between the cells grows leading to an increased electrical resistivity of the medium, which in turn causes resistance reduction. When resistance is reduced, the amplitude is also reduced. In other words, when the contractility increases, the cell intermediate space increases, leading to improved electrical resistivity and reduced resistance, hence reduced amplitude.

7. Proposed mechanism of action

Taking into consideration all the results of this project, a mechanism of action of the two peptides could be proposed. In contrast to RKIP, which binds GRK2 and leads to its inhibition, GRK2 1-185 and GRK3 1-185 peptides seem to modulate β-adrenergic signaling by directly binding to the receptor and thereby acting as competitors for GRK2, thus preventing it from phosphorylating and desensitizing the receptor (Fig. 30), leading to increased downstream signaling and increased contractility.

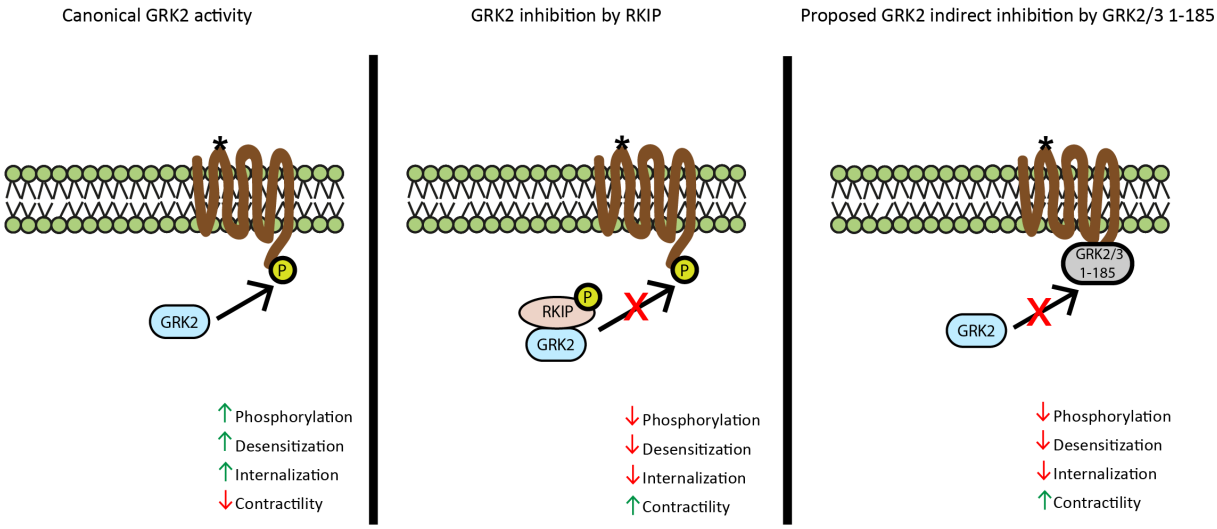

Figure 30: GRK2 modes of action. Canonical GRK2 activity, where GRK2 phosphorylates the receptor leading to increased desensitization and internalization and decreased contractility. Newly discovered GRK2 inhibition by RKIP that leads to reduced phosphorylation and therefore reduced desensitization and internalization, and increased contractility. Proposed mechanism of action of the peptides via indirect GRK2 inhibition, through binding at the receptor, thus preventing GRK2-receptor association leading to reduced phosphorylation, desensitization and internalization and increased contractility.

8. Outlook

In this project, it was shown that GRK2 1-185 and GRK3 1-185 can modulate β_2-AR signaling by binding the receptor and thereby reduce the GRK2 mediated phosphorylation and internalization, and increase downstream signaling mimicking RKIP's function. Moreover, GRK2 1-185 and GRK3 1-185 were proven to have a physiological relevance since they do not induce cardiomyocyte hypertrophy, but they increase the beat rate after isoproterenol stimulation.

Furthermore, it was possible to show that GRK2 1- 185 and GRK3 1-185 bind β_2-AR hence provide a mechanistic explanation for the observed effects: A hypothesis is that the two peptides bind at the third intracellular loop and/or carboxyl terminal tail of β_2-AR which is where the GRK2 mediated phosphorylation takes place and thereby hinder GRK2 from binding and phosphorylating the receptor; so they prevent the initiation of internalization and downregulation. Concerning this, it still remains to be clarified where exactly GRK2 1- 185 and GRK3 1-185 bind and if the binding region corresponds with the GRK2-binding and -phosphorylation site on the β_2-AR. The interaction between β_2-AR C-terminal peptides and GRK2 1- 185 or GRK3 1-185 tagged with fluorophores could be analyzed using Förster resonance energy transfer (FRET). Moreover, a crystal of the complex of β_2-AR with GRK2 1- 185 or GRK3 1-185 would be of great interest in order to determine the molecular structure of the interaction interface and create a 3-dimensional model of the interaction interface.

All the experiments in this project were performed either *in vitro* or *ex-vivo* with immortalized cell lines or isolated neonatal mouse cardiomyocytes respectively. These models often respond to a variety of stimuli differently than the heart as a whole organ in a living organism. After a detailed investigation and characterization of GRK2 1- 185 and GRK3 1-185 using *in vitro* and *ex-vivo* models, *in vivo* experiments are essential to advance the understanding of the role of GRK2 1- 185 and GRK3 1-185 in the modulation of β_2-AR signaling and further examine their physiological effects in regard to cardiovascular diseases. In addition, it would be compelling to investigate whether a targeting strategy based on GRK2 1- 185 and GRK3 1-185 would differentiate between physiological and pathological β-AR activation.

Studies over the past decades have explored the functions and consequences of several GRK2 inhibitors; however none of them has made it to clinical trials. GRK2 1-185 and GRK3 1-185 seem to mimic the beneficial effects of RKIP in the heart. Nonetheless, even if the effects of GRK2 1-185 and GRK3 1- 185 are proven *in vivo*, they are probably not suitable to be therapeutically utilized as such, due to their biochemical features and size of approximately 21 kDa. Viral delivery of therapeutic molecules in humans is still at early stages of research and development, is ethically debatable and has many hurdles to overcome such as the immune system response and high costs. Therefore, in order

to devise innovative pharmacological therapies for cardiovascular diseases, GRK2 1-185 and GRK3 1-185 could be used as a prototype for designing smaller molecules with the hope to pave the way in novel therapeutic strategies for heart failure.

VI. Summary

G protein coupled receptor kinases (GRK) phosphorylate and thereby desensitize G protein coupled receptors (GPCR) including β-adrenergic receptors (βAR), which are critical regulators of cardiac function. We identified the Raf kinase inhibitor protein (RKIP) as an endogenous inhibitor of GRK2 that leads to increased cardiac contractility via βAR activation. RKIP binds to the N-terminus (aa1-185) of GRK2, which is important for the GRK2/receptor interaction. Thereby it interferes with the GRK2/receptor interaction without interference with cytosolic GRK2 target activation. In this project, the RKIP/GRK interface was investigated to develop strategies that simulate the effects of RKIP on βAR.

RKIP binding to different isoforms of GRK expressed in the heart was analyzed by protein interaction assays using full-length and N-termini of GRK2, GRK3 and GRK5: 1-53, 54-185 and 1-185. Co-immunoprecipitation (Co-IPs) and pull-down assays revealed that RKIP binds to the peptides of GRK2 and GRK3 but not to the ones of GRK5, which suggests the existence of several binding sites of RKIP within the N-termini of GRK2 and GRK3. To analyze whether the peptides of GRK2 and GRK3 are able to simulate the RKIP mediated interference of the GRK2/receptor interaction, we analyzed the β_2-AR phosphorylation in the absence and presence of the peptides. Interestingly, N-termini (aa1-185) of GRK2 and GRK3 reduced β_2AR phosphorylation to a comparable extent as RKIP. In line with reduced receptor phosphorylation, the peptides also reduced isoproterenol-stimulated receptor internalization as shown by [^{3}H] CGP-12177 radioligand binding assay and fluorescence microscopy compared to control cells. Subsequently, these peptides increased downstream signaling of β_2AR, *i.e.* the phosphorylation of the PKA substrate phosducin. In an attempt to elucidate the mechanism behind the observed effects, Co-IPs were performed in order to investigate whether the peptides bind directly to the β_2-AR and block its phosphorylation by GRK2. Indeed, GRK2 1-185 and GRK3 1-185 could bind the receptor, suggesting that this way GRK2 is prevented from inhibiting the receptor. To investigate the physiological effect of GRK2 1-185, GRK3 1-185 and GRK5 1-185, their effect on neonatal mouse cardiomyocyte contractility and hypertrophy was analyzed. After long-term isoproterenol stimulation**,** in the presence of GRK2 1-185 and GRK3 1-185 the cross-sectional area of the cardiomyocytes showed no significant increase in comparison to the unstimulated control cells. In addition, upon isoproterenol stimulation, GRK2 1-185 and GRK3 1-185 increased the beat rate in cardiomyocytes, mimicking RKIP while the base impedance, an indicator of viability, remained stable.

The N-termini (1-185) of GRK2 and GRK3 simulated RKIP's function and had a significant influence on β_2AR phosphorylation, on its downstream signaling and internalization, could bind β_2-AR, increased beat rate and did not significantly induce hypertrophy, suggesting that they may serve as a model for the generation of new and more specific targeting strategies for GRK mediated receptor regulation.

VII. Zusammenfassung

G-Protein gekoppelte Rezeptorkinasen (GRK) phosphorylieren und desensitisieren G-Protein gekoppelte Rezeptoren (GPCR), einschließlich β-adrenerge Rezeptoren (βAR), welche wichtige Regulatoren der Herzfunktion sind. Raf Kinase Inhibitor Protein (RKIP) ist ein endogener Inhibitor von GRK2, der zur Aktivierung von βAR führt und dadurch zur Steigerung der Herzkontraktilität. RKIP bindet N-terminal (1-185) an GRK2; der GRK2 N-Terminus ist wichtig für die GRK2/Rezeptor Interaktion. Durch diese Bindung wird GRK2 inhibiert und derer Interaktion mit den Rezeptor gestört, allerdings bleiben die zytosolische GRK2 Substrate unbeeinflusst. In diesem Projekt wurde die Interaktion zwischen RKIP und GRK untersucht, um neue *Targeting* Strategien zu entwickeln, die die positiven Effekte von RKIP auf βAR Signalwege simulieren.

Die Bindung von RKIP an verschiedene, im Herzen lokalisierte GRK-Isoformen wurde über *protein interaction assays* untersucht: mit GRK2, GRK3 und GRK5 und mit deren N-terminalen Peptiden 1-53, 54-185, 1-185. Die Co-Immunopräzipitationen (Co-IPs) und die *pull-down* Versuche haben gezeigt, dass RKIP sowohl GRK2 und GRK3 als auch deren N-Termini bindet, GRK5 und dessen N-termini hingegen nicht. Daraus lässt sich schlussfolgern, dass sich mehrere RKIP Bindungsstellen an dem GRK2 N-Terminus befinden. Um zu analysieren, ob die GRK2- und GRK3-Peptide eine ähnliche Wirkung wie RKIP auf die Interaktion von GRK2 und Rezeptor aufweisen, wurde die Rezeptorphosphorylierung ermittelt. Es konnte gezeigt werden, dass GRK2 1-185 und GRK3 1-185 die Phosphorylierung des βAR reduzieren können. Radioligandbindungsassays mit [^{3}H] CGP-12177 und Fluoreszenzmikroskopie zeigten zudem, dass GRK2 1-185 und GRK3 1-185 auch die Internalisierungsrate des βAR senken können. Anschließend hatten GRK2 1-185 und GRK3 1-185 einen positiven Effekt auf einem βAR *downstream* Signalmolekül. Hierbei handelte es sich um die Phosphorylierung von Phosducin, was ein PKA-Substrat ist. Um die Wirkungsweise der N-termini zu erläutern, wurde untersucht, ob diese direkt den β_2AR binden und somit die GRK2 vermittelte Phosphorylierung hindern. Interessanterweise konnte gezeigt werden, dass GRK2 1-185 und GRK3 1- 185 den β_2AR binden und dementsprechend einen Einfluss auf die Phosphorylierung haben. Des Weiteren, wurden die Effekte der Peptide auf Kontraktilität und Hypertrophie in neonatalen Mauskardiomyozyten analysiert. In Anwesenheit von GRK2 1-185 und GRK3 1-185 war die Querschnittsfläche der Mauskardiomyozyten nicht signifikant größer im Vergleich zu den unstimulierten Kontrollzellen. Außerdem wurde eine signifikante Erhöhung der Kontraktilität in den Mauskardiomyozyten mit GRK2 1-185 und GRK3 1-185 beobachtet.

Insgesamt, konnten GRK2 1-185 und GRK3 1-185 RKIPs Funktion simulieren: sie hatten einen signifikanten Effekt auf β_2AR-Phosphorylierung, Internalisierung und downstream Signaling. Zudem konnten sie die Kontraktilität erhöhen und hatten keinen Einfluss auf Hypertrophie. Somit könnten sie

als Prototyp für die Entwicklung neuer Targeting Strategien für die GRK-vermittelte Rezeptor Regulation, genutzt werden.

VIII. Abbreviations

AAV	Adeno-associated virus
AC	Adenylate Cyclase
AGC	Protein kinase A, G and C
AR	Adrenergic receptor
BAEC	Bovine aorta endothelial cells
BBS	N,N-Bis(2-hydroxyethyl)-2-aminoethanesulfonic acid
BSA	Bovine Serum Albumin
CA	Catecholamines
CA1	Cornu Ammonis 1
cAMP	Cyclic adenosine monophosphate
Co-IP	Co-immunoprecipitation
CPM	Counts per minute
CREB	cAMP response element-binding protein
cSrc	Tyrosine protein kinase
CVD	Cardiovascular disease
DC	Dilated cardiomyopathy
DMEM	Dulbecco's Modified Eagle Medium
DMSO	Dimethyl sulfoxide
DTT	Dithiothreitol
EDTA	Ethylenediaminetetraacetic acid
ERK1/2	Extracellular signal–regulated kinase
ET-R	Endothelin receptor
FCS	Fetal Calf Serum
Fig.	Figure
FVB/N	Friend Virus B NIH
GAP	GTPase-activating protein
GDP	Guanosine diphosphate
GEF	Guanine nucleotide exchange factor
GPCR	G-protein coupled receptor kinase
GRK	G-protein coupled Receptor Kinase
GSK3	Glycogen synthase kinase-3
GTP	Guanosine triphosphate
Gα	G alpha

Gβγ	G beta gamma
HCNP	Hippocampal cholinergic neurostimulating peptide
HDAC5	Histone Deacetylase 5
HDX-MS	hydrogen/deuterium exchange mass spectrometry
HF	Heart Failure
HRF-MS	hydroxyl radical mediated protein footprinting mass spectrometry
IBMX	3-isobutyl-1-methylxanthine
IBX	2-Iodoxybenzoic acid
IC	Ischemic cardiomyopathy
IgG	Immunoglobulin G
IKK	IκB kinase
Iso	Isoproterenol
IκB	Inhibitory κB
LB	Lysogeny broth
LID	L-DOPA-induced dyskinesia
LV	Left ventricle
LVH	Left ventricular hypertrophy
M1AChR	M1 muscarinic acetylcholine receptor
MAPK	Mitogen-Activated Protein Kinase
Mdm2	Mouse double minute 2 homolog
MEF2	Myocyte Enhancer Factor 2
MEK	MAPK/ERK kinase
MWCO	Molecular Weight Cut Off
NFAT	Nuclear factor of activated T-cells
NFH	Non-failing heart
NF-κB	Nuclear factor κB
NIK	NFκB inducing kinase
NINDC	Non-ischemic non-dilated cardiomyopathy
NLS	Nuclear Localization Sequence
NMCM	Neonatal mouse cardiomyocytes
NP-40	Nonidet P-40
NT	N-terminus
PAFR	Platelet-activating factor receptor
PBS	Phosphate-buffered saline
PDE	Phosphodiesterase

PE	Phenylephrine
PEBP1	Phosphatidylethanolamine-binding protein 1
PFA	Paraformaldehyde
PH	Pleckstrin Homology
PI	Protease Inhibitor
PI3K	Phosphoinositide 3-kinase
PIP2	Phosphatidylinositol 4,5-bis-phosphate
PKA	Protein Kinase A
PKC	Protein Kinase C
PLB	Phospholamban
PLC	Phospholipase C
PMA	Phorbol 12-myristate 13-acetate
PMSF	Phenylmethylsulfonyl fluoride
PVDF	Polyvinylidene difluoride
RAAS	Renin angiotensin aldosterone system
Raf	Rapidly accelerated fibrosarcoma
Raf-1	Rapidly accelerated fibrosarcoma
RGS	Regulator of G protein signaling
RH	RGS Homology
RKIP	Raf Kinase Inhibitor Protein
ROS	Reactive oxygen species
RTK	Receptor tyrosine kinase
SDS	Sodium dodecyl sulfate
Ser	Serine
Ser/Thr	Serine/Threonine
SHR	Spontaneously hypertensive rats
SNS	Sympathetic Nervous System
TAC	Transverse aortic constriction
TAE	Tris base, acetic acid EDTA
TAK1	Transforming growth factor beta (TGFβ)-activated kinase 1
TEMED	Tetramethylethylendiamine
Tg	Transgene
Thr	Threonine
TSE	Tris/Saline/EDTA buffer
Tyr	Tyrosine

βARKct	β-adrenergic receptor kinase carboxyl-terminus
β-ARKnt	β-adrenergic receptor kinase amino-terminus
β-ARKrgs	β-adrenergic receptor kinase regulator of G protein signaling

IX. References

1. Fredriksson, R., Lagerström, M. C., Lundin, L.-G. & Schiöth, H. B. The G-protein-coupled receptors in the human genome form five main families. Phylogenetic analysis, paralogon groups, and fingerprints. *Mol. Pharmacol.* **63**, 1256–72 (2003).

2. Venkatakrishnan, A. J. *et al.* Molecular signatures of G-protein-coupled receptors. *Nature* **494**, 185–194 (2013).

3. Hu, G. M., Mai, T. L. & Chen, C. M. Visualizing the GPCR Network: Classification and Evolution. *Sci. Rep.* **7**, 1–15 (2017).

4. Schulte, G. & Wright, S. C. Frizzleds as GPCRs – More Conventional Than We Thought! *Trends Pharmacol. Sci.* **39**, 828–842 (2018).

5. Buck, L. & Axel, R. A novel multigene family may encode odorant receptors: A molecular basis for odor recognition. *Cell* **65**, 175–187 (1991).

6. Mombaerts, P. Seven-transmembrane proteins as odorant and chemosensory receptors. *Science (80-.).* **286**, 707–711 (1999).

7. Matsunami, H., Montmayeur, J. P. & Buck, L. B. A family of candidate taste receptors in human and mouse. *Nature* **404**, 601–4 (2000).

8. Howard, A. D. *et al.* Orphan G-protein-coupled receptors and natural ligand discovery. *Trends Pharmacol. Sci.* **22**, 132–140 (2001).

9. Bang, I. & Choi, H.-J. Structural Features of ß2 Adrenergic Receptor: Crystal Structures and Beyond. *Mol. Cells* **38**, 105–111 (2015).

10. Heifetz, A. *et al.* GPCR structure, function, drug discovery and crystallography: report from Academia-Industry International Conference. *Naunyn. Schmiedebergs. Arch. Pharmacol.* **388**, 883–903 (2015).

11. Chan, H. C. S., Li, Y., Dahoun, T., Vogel, H. & Yuan, S. New Binding Sites, New Opportunities for GPCR Drug Discovery. *Trends Biochem. Sci.* 1–19 (2019). doi:10.1016/J.TIBS.2018.11.011

12. Gurevich, V. V. & Gurevich, E. V. Molecular mechanisms of GPCR signaling: A structural perspective. *Int. J. Mol. Sci.* **18**, 1–17 (2017).

13. Manglik, A. *et al.* Structural insights into the dynamic process of β2 -adrenergic receptor signaling. *Cell* **161**, 1101–1111 (2015).

14. Kauk, M. & Hoffmann, C. Intramolecular and Intermolecular FRET Sensors for GPCRs – Monitoring Conformational Changes and Beyond. *Trends Pharmacol. Sci.* **39**, 123–135 (2018).

15. Oldham, W. M. & Hamm, H. E. Heterotrimeric G protein activation by G-protein-coupled receptors. *Nat. Rev. Mol. Cell Biol.* **9**, 60–71 (2008).

16. Neves, S. R., Prahland, T. R. & Iyengar, R. G Protein Pathways. *Science (80-.).* **296**, 1636–1639 (2002).

17. Syrovatkina, V., O.Alegre, K., Dey, R. & Huang, X.-Y. Regulation, Signaling and Physiological Functions of G-proteins. *J Mol Biol* **428**, 3850–3868 (2016).

18. Holbrook, S. R. & Kim, S. H. Molecular model of the G protein alpha subunit based on the crystal structure of the HRAS protein. *Proc. Natl. Acad. Sci. U. S. A.* **86**, 1751–5 (1989).

19. Gilman, A. G. G Proteins : Transducers of Receptor-Generated Signals. *Proteins* (1987).

20. Schmidt, C. J., Thomas, T. C., Levine, M. A. & Neer, E. J. Specificity of G protein beta and gamma subunit interactions. *J Biol Chem* **267**, 13807–13810 (1992).

21. Huang, C. C. & Tesmer, J. J. G. Recognition in the face of diversity: Interactions of heterotrimeric G proteins and G protein-coupled receptor (GPCR) kinases with activated GPCRs. *J. Biol. Chem.* **286**, 7715–7721 (2011).

22. Onrust, R. *et al.* Receptor and betagamma binding sites in the alpha subunit of the retinal G protein transducin. *Science* **275**, 381–4 (1997).

23. Milligan, G. & Kostenis, E. Heterotrimeric G-proteins: A short history. *Br. J. Pharmacol.* **147**, (2006).

24. Wedegaertner, P. B., Wilson, P. T. & Bourne, H. R. Lipid Modifications of Trimeric G Proteins. *J. Biol. Chem.* **270**, 503–506 (1995).

25. Pierce, K. L., Premont, R. T. & Lefkowitz, R. J. Signalling: Seven-transmembrane receptors. *Nat. Rev. Mol. Cell Biol.* **3**, 639–650 (2002).

26. Biesen, T. Van *et al.* Go -protein α-Subunits Activate Kinase via a Novel Protein Kinase C-dependent Mechanism. *J. Biol. Chem.* **271**, 1266–1269 (1996).

27. Logothetis, D. E., Kurachi, Y., Galper, J., Neer, E. J. & Clapham, D. E. The beta gamma subunits of GTP-binding proteins activate the muscarinic K+ channel in heart. *Nature* **325**, 321–6 (1987).

28. Meir, A., Bell, D. C., Stephens, G. J., Page, K. M. & Dolphin, A. C. Calcium channel beta subunit promotes voltage-dependent modulation of alpha 1B by G beta gamma. *Biophys. J.* **79**, 731–

746 (2000).

29. Park, D., Jhon, D. Y., Lee, C. W., Lee, K. H. & Rhee, S. G. Activation of phospholipase C isozymes by G protein beta gamma subunits. *J Biol Chem* **268**, 4573–4576 (1993).

30. Daaka, Y. *et al.* Receptor and G betagamma isoform-specific interactions with G protein-coupled receptor kinases. *Proc. Natl. Acad. Sci. U. S. A.* **94**, 2180–2185 (1997).

31. Ballesteros, J. A. *et al.* Activation of the β2-Adrenergic Receptor Involves Disruption of an Ionic Lock between the Cytoplasmic Ends of Transmembrane Segments 3 and 6. *J. Biol. Chem.* **276**, 29171–29177 (2001).

32. Farahbakhsh, Z. T., Ridge, K. D., Gobind Khorana, H. & Hubbell, W. L. Mapping Light-Dependent Structural Changes in the Cytoplasmic Loop Connecting Helices C and D in Rhodopsin: A Site-Directed Spin Labeling Study. *Biochemistry* **34**, 8812–8819 (1995).

33. Ablohr, N.-A. D. & Thomas, D. D. Phospholamban phosphorylation, mutation, and structural dynamics: a biophysical approach to understanding and treating cardiomyopathy. *Biophys Rev* **7**, 63–76 (2015).

34. Khan, S. M., Sung, J. Y. & Hébert, T. E. Gβγ subunits—Different spaces, different faces. *Pharmacol. Res.* **111**, 434–441 (2016).

35. Rasmussen, S. G. F. *et al.* Crystal structure of the β2 adrenergic receptor-Gs protein complex. *Nature* **477**, 549–557 (2011).

36. Andhirka, S. K., Vignesh, R. & Aradhyam, G. K. The nucleotide-free state of heterotrimeric G proteins α-subunit adopts a highly stable conformation. *FEBS J.* **284**, 2464–2481 (2017).

37. Du, Y. *et al.* Assembly of a GPCR-G Protein Complex. *Cell* **177**, 1–11 (2019).

38. Liu, X. *et al.* Structural Insights into the Process of GPCR-G Protein Complex Formation. *Cell* **177**, 1–9 (2019).

39. Krupnick, J. G. & Benovic, J. L. The Role of Receptor Kinases and Arrestins in G Protein–Coupled Receptor Regulation. *Annu. Rev. Pharmacol. Toxicol.* **38**, 289–319 (2002).

40. Pitcher, J. A., Freedman, N. J. & Lefkowitz, R. J. G Protein – Coupled Receptor Kinases. *Annu. Rev. Biochem.* **67**, 653–692 (1998).

41. Hausdorff, W. P., Caron, M. G. & Lefkowitz, J. Turning off the signal: desensitization of beta-adrenergic receptor function. *FASEB* **4**, 2881–2889 (1990).

42. Lohse, M. J., Benovic, J. L., Caron, M. G. & Lefkowitz, R. J. Multiple Pathways of Rapid Receptor

Desensitization their contributions. *Biol. Chem.* **265**, 3202–3209 (1990).

43. Lohse, M. J. Molecular mechanisms of membrane receptor desensitization. *BBA - Mol. Cell Res.* **1179**, 171–188 (1993).

44. Premont, R. T., Inglese, J. & Lefkowitz, R. J. Protein kinases that phosphorylate activated G protein-coupled receptors. *FASEB J.* **9**, 175–182 (1995).

45. Ferguson, S., Barak, L. S., Zhang, J. & Caron, M. G. G-protein-coupled receptor regulation: role of G-protein-coupled receptor kinases and arrestins. *Can. J. Physiol. Pharmacol.* **74**, 1095–1110 (1996).

46. Tobin, A. B. G-protein-coupled receptor phosphorylation: where, when and by whom. *Br. J. Pharmacol.* **153**, S167–S176 (2009).

47. Alfonzo-Méndez, M. A., Carmona-Rosas, G., Hernández-Espinosa, D. A., Romero-Ávila, M. T. & García-Sáinz, J. A. Different phosphorylation patterns regulate α1D-adrenoceptor signaling and desensitization. *Biochim. Biophys. Acta - Mol. Cell Res.* **1865**, 842–854 (2018).

48. Lohse, M. J. *et al.* β-Arrestin : A Protein That Regulates β-Adrenergic Receptor Function. *Science (80-.).* **248**, 1547–1550 (1990).

49. Gurevich, V. V. *et al.* Arrestin interactions with G protein-coupled receptors: Direct binding studies of wild type and mutant arrestins with rhodopsin, b2-adrenergic, and m2 muscarinic cholinergic receptors. *Journal of Biological Chemistry* **270**, 720–731 (1995).

50. Goodman, O. B. *et al.* β-Arrestin acts as a clathrin adaptor in endocytosis of the β2-adrenergic receptor. *Nature* **383**, 447–450 (1996).

51. Von Zastrow, M. & Kobilka, B. K. Ligand-regulated internalization and recycling of human β2-adrenergic receptors between the plasma membrane and endosomes containing transferrin receptors. *J. Biol. Chem.* **267**, 3530–3538 (1992).

52. Ribas, C. *et al.* The G protein-coupled receptor kinase (GRK) interactome: Role of GRKs in GPCR regulation and signaling. *Biochim. Biophys. Acta - Biomembr.* **1768**, 913–922 (2006).

53. Mushegian, A., Gurevich, V. V. & Gurevich, E. V. The origin and evolution of G protein-coupled receptor kinases. *PLoS One* **7**, 1–12 (2012).

54. Sato, P. Y., Chuprun, J. K., Schwartz, M. & Koch, W. J. The Evolving Impact of G Protein-Coupled Receptor Kinases in Cardiac Health and Disease. *Physiol. Rev.* **95**, 377–404 (2015).

55. Diviani, D. *et al.* Effect of Different G Protein-coupled Receptor Kinases on Phosphorylation and

Desensitization of the α1B -Adrenergic Receptor. *J. Biol. Chem.* **271**, 5049–5058 (1996).

56. Willets, J. M., Challiss, R. a J. & Nahorski, S. R. Non-visual GRKs: Are we seeing the whole picture? *Trends Pharmacol. Sci.* **24**, 626–633 (2003).

57. Schumacher, S. M. & Koch, W. J. Non-canonical roles of GRKs in cardiovascular signaling. *J. Cardiovasc. Pharmacol.* **70**, 129–141 (2017).

58. Lorenz, K., Lohse, M. J. & Quitterer, U. Protein kinase C switches the Raf kinase inhibitor from Raf-1 to GRK-2. *Nature* **426**, 574–579 (2003).

59. Sallese, M., Mariggiò, S., D'Urbano, E., Iacovelli, L. & De Blasi, A. Selective Regulation of Gq Signaling by G Protein-Coupled Receptor Kinase 2: Direct Interaction of Kinase N Terminus with Activated Gαq. *Mol. Pharmacol.* **57**, 826–831 (2000).

60. Penela, P., Murga, C., Ribas, C., Lafarga, V. & Mayor, F. The complex G protein-coupled receptor kinase 2 (GRK2) interactome unveils new physiopathological targets. *Br. J. Pharmacol.* **160**, 821–832 (2010).

61. Ruiz-Gomez, A. *et al.* Phosphorylation of phosducin and phosducin-like protein by G protein-coupled receptor kinase 2. *J. Biol. Chem.* **275**, 29724–29730 (2000).

62. Ungerer, M., Bohm, M., Elce, J. S., Erdmann, E. & Lohse, M. J. Altered expression of beta-adrenergic receptor kinase and beta 1- adrenergic receptors in the failing human heart. *Circulation* **87**, 454–463 (1993).

63. Huang, Z. M., Gao, E., Chuprun, J. K. & Koch, W. J. GRK2 in the Heart: A GPCR Kinase and Beyond. *Antioxid. Redox Signal.* **00**, 1–12 (2014).

64. Hullmann, J., Traynham, C. J., Coleman, R. C. & Koch, W. J. The expanding GRK interactome: Implications in cardiovascular disease and potential for therapeutic development. *Pharmacol. Res.* **110**, 52–64 (2016).

65. Obrenovich, M. E., Palacios, H. H., Gasimov, E., Leszek, J. & Aliev, G. The GRK2 Overexpression Is a Primary Hallmark of Mitochondrial Lesions during Early Alzheimer Disease. *Cardiovasc. Psychiatry Neurol.* **2009**, (2009).

66. Cruces-Sande, M. *et al.* Involvement of G protein-coupled receptor kinase 2 (GRK2) in the development of non- alcoholic steatosis and steatohepatitis in mice and humans . *Biochim. Biophys. Acta Mol Basis Dis.* **1864**, 9–10 (2018).

67. Li, W. *et al.* GRK3 is essential for metastatic cells and promotes prostate tumor progression. *Proc. Natl. Acad. Sci. U. S. A.* **111**, 1521–1526 (2014).

68. Billard, M. J. *et al.* G protein coupled receptor kinase 3 regulates breast cancer migration, invasion, and metastasis. *PLoS One* **11**, 1–23 (2016).

69. Ahmed, M. R., Bychkov, E., Li, L., Gurevich, V. V & Gurevich, E. V. GRK3 suppresses L-DOPA-induced dyskinesia in the rat model of Parkinson's disease via its RGS homology domain. *Sci. Rep.* **5**, 10920 (2015).

70. Dzimiri, N., Muiya, P., Andres, E. & Al-Halees, Z. Differential functional expression of human myocardial G protein receptor kinases in left ventricular cardiac diseases. *Eur. J. Pharmacol.* **489**, 167–177 (2004).

71. Traynham, C. J., Hullmann, J. & Koch, W. J. "canonical and non-canonical actions of GRK5 in the heart". *J. Mol. Cell. Cardiol.* (2016). doi:10.1016/j.yjmcc.2016.01.027

72. Zhao, J. *et al.* GRK5 influences the phosphorylation of tau via GSK3 β and contributes to Alzheimer ' s disease. *Cell. Physiol.* 1–10 (2018). doi:10.1002/jcp.27709

73. Jiang, L. *et al.* GRK5 functions as an oncogenic factor in non-small-cell lung cancer. *Cell Death Dis.* **9**, 1–12 (2018).

74. Carman, C. V *et al.* Selective Regulation of Galpha q/11 by an RGS Domain in the G Protein-coupled Receptor Kinase, GRK2. *J. Biol. Chem.* **274**, 34483–34492 (1999).

75. Homan, K. T. & Tesmer, J. J. G. Structural insights into G protein-coupled receptor kinase function. *Curr. Opin. Cell Biol.* **27**, 25–31 (2014).

76. Boguth, C. A., Singh, P., Huang, C. C. & Tesmer, J. J. G. Molecular basis for activation of G protein-coupled receptor kinases. *EMBO J.* **29**, 3249–3259 (2010).

77. Yu, Q. M. *et al.* The amino terminus with a conserved glutamic acid of G protein-coupled receptor kinases is indispensable for their ability to phosphorylate photoactivated rhodopsin. *J. Neurochem.* **73**, 1222–1227 (1999).

78. Noble, B., Kallal, L. a., Pausch, M. H. & Benovic, J. L. Development of a yeast bioassay to characterize G protein-coupled receptor kinases: Identification of an NH2-terminal region essential for receptor phosphorylation. *J. Biol. Chem.* **278**, 47466–47476 (2003).

79. Pao, C. S., Barker, B. L. & Benovic, J. L. Role of the amino terminus of G protein-coupled receptor kinase 2 in receptor phosphorylation. *Biochemistry* **48**, 7325–7333 (2009).

80. Huang, C. C., Orban, T., Jastrzebska, B., Palczewski, K. & Tesmer, J. J. G. Activation of G Protein-Coupled Receptor Kinase 1 Involves Interactions between Its N-Terminal Region and Its Kinase Domain. *Biochemistry* **50**, 1940–1949 (2011).

81. Huang, C. C., Yoshino-Koh, K. & Tesmer, J. J. G. A surface of the kinase domain critical for the allosteric activation of G protein-coupled receptor kinases. *J. Biol. Chem.* **284**, 17206–17215 (2009).

82. Stoffel, R. H., Pitcher, J. A. & Lefkowitz, R. J. Targeting G protein-coupled receptor kinases to their receptor substrates. *J. Membr. Biol.* **157**, 1–8 (1997).

83. Xu, H., Jiang, X., Shen, K., Fischer, C. C. & Wedegaertner, P. B. The regulator of G protein signaling (RGS) domain of G protein-coupled receptor kinase 5 (GRK5) regulates plasma membrane localization and function. *Mol. Biol. Cell* **25**, 2105–15 (2014).

84. Day, P. W., Wedegaertner, P. B. & Benovic, J. L. Analysis of G-protein-coupled receptor kinase RGS homology domains. *Methods Enzymol.* **390**, 295–310 (2004).

85. Hepler, J. R. Emerging roles for RGS proteins in cell signalling. *Trends Pharmacol. Sci.* **20**, 376–382 (1999).

86. Sterne-Marr, R. *et al.* G protein-coupled receptor kinase 2/Gαq/11 interaction: A novel surface on a regulator of G protein signaling homology domain for binding Gα subunits. *J. Biol. Chem.* **278**, 6050–6058 (2003).

87. Carman, C. V *et al.* Selective regulation of G alpha(q/11) by an RGS domain in the G protein-coupled receptor kinase, GRK2. *J. Biol. Chem.* **274**, 34483–34492 (1999).

88. Sterne-Marr, R., Dhami, G. K., Tesmer, J. J. G. & Ferguson, S. S. G. Characterization of GRK2 RH domain-dependent regulation of GPCR coupling to heterotrimeric G proteins. *Methods Enzymol.* **390**, 310–336 (2004).

89. Tesmer, J. J. G. *Chapter 4 Structure and Function of Regulator of G Protein Signaling Homology Domains*. *Progress in Molecular Biology and Translational Science* **86**, (Elsevier Inc., 2009).

90. Inglese, J., Freedman, N. J., Koch, W. J. & Lefkowitz, R. J. Structure and mechanism of the G protein-coupled receptor kinases. *J. Biol. Chem.* **268**, 23735–23738 (1993).

91. Thiyagarajan, M. M. *et al.* A Predicted Amphipathic Helix Mediates Plasma Membrane Localization of GRK5. *J. Biol. Chem.* **279**, 17989–17995 (2004).

92. Pitcher, J. *et al.* Role of beta gamma subunits of G proteins in targeting the beta-adrenergic receptor kinase to membrane-bound receptors. *Science (80-.).* **257**, 1264–1267 (1992).

93. Homan, K. T., Glukhova, A. & Tesmer, J. J. G. Regulation of G Protein-Coupled Receptor Kinases by Phospholipids. *Curr. Med. Chem.* **20**, 39–46 (2012).

94. Johnson, L. R., Scott, M. G. H. & Pitcher, J. A. G Protein-Coupled Receptor Kinase 5 Contains a DNA-Binding Nuclear Localization Sequence. *Mol. Cell. Biol.* **24**, 10169–10179 (2004).

95. Xian, P. Y. *et al.* Myocardial expression and redistribution of GRKs in hypertensive hypertrophy and failure. *Anat. Rec. - Part A Discov. Mol. Cell. Evol. Biol.* **282**, 13–23 (2005).

96. Jiang, X., Benovic, J. L. & Wedegaertner, P. B. Plasma Membrane and Nuclear Localization of G Protein–coupled Receptor Kinase 6A. *Mol. Biol. Cell* **18**, 2960–2969 (2007).

97. Johnson, L. R., Robinson, J. D., Lester, K. N. & Pitcher, J. A. Distinct Structural Features of G Protein-Coupled Receptor Kinase 5 (GRK5) Regulate Its Nuclear Localization and DNA-Binding Ability. *PLoS One* **8**, (2013).

98. Waldschmidt, H. V *et al.* Utilizing a structure-based docking approach to develop potent G protein-coupled receptor kinase (GRK) 2 and 5 inhibitors. *Bioorg. Med. Chem. Lett.* **5**, 1–9 (2018).

99. Osawa, S. & Weiss, E. R. A Tale of Two Kinases in Rods and Cones. *Adv Exp Med Biol* **723**, 821–827 (2012).

100. Evron, T., Daigle, T. L. & Caron, M. G. GRK2: multiple roles beyond G protein-coupled receptor desensitization. *Trends Pharmacol Sci.* **33**, 154–164 (2012).

101. Iaccarino, G., Rockman, H. a, Shotwell, K. F., Tomhave, E. D. & Koch, W. J. Myocardial overexpression of GRK3 in transgenic mice: evidence for in vivo selectivity of GRKs. *Am J Physiol* **275**, H1298-306. (1998).

102. Premont, R. T. *et al.* Characterization of the G Protein-coupled Receptor Kinase GRK4 recently identified by positional cloning in the search. *J. Biol. Chem.* **271**, 6403–6410 (1996).

103. Voigt, C., Hp, H., Meyer, S. & Paschke, R. Increased expression of G-protein-coupled receptor kinases 3 and 4 in hyperfunctioning thyroid nodules . *J Endocrinol.* **182**, 2004 (2004).

104. Vinge, L. E. *et al.* Cardiac-restricted expression of the carboxyl-terminal fragment of GRK3 uncovers distinct functions of GRK3 in regulation of cardiac contractility and growth: GRK3 Controls cardiac alpha1-adrenergic receptor responsiveness. *J. Biol. Chem.* **283**, 10601–10610 (2008).

105. Dautzenberg, F., Wille, S., Braun, S. & Hauger, R. GRK3 regulation during CRF- and urocortin-induced CRF1 receptor. *Biochem. Biophys. Res. Commun.* **298**, 303–8 (2002).

106. Komolov, K. E. *et al.* Structural and Functional Analysis of a β 2 -Adrenergic Receptor Complex with GRK5. *Cell* **169**, 407-421.e16 (2017).

107. Walker, J. K. L. *et al.* G protein-coupled receptor kinase 5 regulates airway responses induced by muscarinic receptor activation. *Am J Physiol Lung Cell Mol Physiol* **286**, 312–319 (2004).

108. Watari, K., Nakaya, M. & Kurose, H. Multiple functions of G protein-coupled receptor kinases. *J. Mol. Signal.* **9**, 1 (2014).

109. Li, L. *et al.* G Protein-coupled Receptor Kinases of the GRK4 Protein Subfamily Phosphorylate Inactive G Protein-coupled Receptors (GPCRs). *J. Biol. Chem. VOL.* **290**, 10775–10790 (2015).

110. Huang, Z. M., Gold, J. I. & Koch, W. J. G protein-coupled receptor kinases in normal and failing myocardium. *Front. Biosci. (Landmark Ed.* **16**, 3047–60 (2011).

111. Lieu, M. & Koch, W. J. GRK2 and GRK5 as therapeutic targets and their role in maladaptive and pathological cardiac hypertrophy. *Expert Opin. Ther. Targets* **23**, 201–214 (2019).

112. Buczyłko, J., Gutmann, C. & Palczewski, K. Regulation of rhodopsin kinase by autophosphorylation. *Proc. Natl. Acad. Sci. U. S. A.* **88**, 2568–72 (1991).

113. Chen, C.-K., Inglese, J., Lefkowitz, R. J. & Hurley, J. B. Ca2+ dependent Interaction of Recoverin with Rhodopsin Kinase. *J. Biol. Chem.* **270**, 18060–18066 (1995).

114. Torisawa, A., Arinobu, D., Tachibanaki, S. & Kawamura, S. Amino acid residues in GRK1/GRK7 responsible for interaction with S-modulin/recoverin. *Photochem. Photobiol.* **84**, 823–830 (2008).

115. Cong, M. *et al.* Regulation of Membrane Targeting of the G Protein-coupled Receptor Kinase 2 by Protein Kinase A and Its Anchoring Protein AKAP79. *J. Biol. Chem.* **276**, 15192–15199 (2001).

116. Chuang, T. T., LeVine, H. & De Blasi, A. Phosphorylation and Activation of β-Adrenergic Receptor Kinase by Protein Kinase C. *J. Biol. Chem.* **270**, 18660–18665 (1995).

117. Sarnago, S., Elorza, A. & Mayor, F. Agonist-dependent phosphorylation of the G protein-coupled receptor kinase 2 (GRK2) by Src tyrosine kinase. *J. Biol. Chem.* **274**, 34411–34416 (1999).

118. Mariggiò, S. *et al.* Tyrosine phosphorylation of G-protein-coupled-receptor kinase 2 (GRK2) by c-Src modulates its interaction with Gαq. *Cell. Signal.* **18**, 2004–2012 (2006).

119. Fredericks, Z. L., Pitcher, J. A. & Lefkowitz, R. J. Identification of the G Protein-coupled Receptor Kinase Phosphorylation Sites in the Human β2 -Adrenergic Receptor. *J Biol Chem* **271**, 13796–13803 (1996).

120. Gurevich, E. V, Tesmer, J. J. G., Mushegian, A. & Gurevich, V. V. G protein-coupled receptor kinases: more than just kinases and not only for GPCRs. *Pharmacol Ther* **133**, 40–69 (2012).

121. Penela, P., Ribas, C. & Mayor, F. Mechanisms of regulation of the expression and function of G protein-coupled receptor kinases. *Cell. Signal.* **15**, 973–981 (2003).

122. Penela, P. *Chapter Three - Ubiquitination and Protein Turnover of G-Protein-Coupled Receptor Kinases in GPCR Signaling and Cellular Regulation*. *Progress in Molecular Biology and Translational Science* **141**, (Elsevier Inc., 2016).

123. Finley, D. & Chau, V. Ubiquitination. *Annu. Rev. Cell Biol.*. **7**, 25–69 (1991).

124. Penela, P., Ruiz-Gómez, A., Castaño, J. G. & Mayor, F. Degradation of the G protein-coupled receptor kinase 2 by the proteasome pathway. *J. Biol. Chem.* **273**, 35238–35244 (1998).

125. Penela, P., Elorza, A., Sarnago, S. & Mayor F., J. β-arrestin- and c-Src-dependent degradation of G-protein-coupled receptor kinase 2. *EMBO J.* **20**, 5129–5138 (2001).

126. Salcedo, A., Mayor, F. & Penela, P. Mdm2 is involved in the ubiquitination and degradation of G-protein-coupled receptor kinase 2. *EMBO J.* **25**, 4752–4762 (2006).

127. Choi, D. J., Koch, W. J., Hunter, J. J. & Rockman, H. A. Mechanism of β-adrenergic receptor desensitization in cardiac hypertrophy is increased β-adrenergic receptor kinase. *J. Biol. Chem.* **272**, 17223–17229 (1997).

128. Gros, R., Tan, C. M., Benovic, J. L. & Feldman, R. D. G-protein-coupled receptor kinase expression in hypertension. *J Clin Invest.* **99**, 2087–2093 (1997).

129. Brinks, H. & Koch, W. J. Targeting G protein-coupled receptor kinases (GRKs) in Heart Failure. *Drug Discov Today Dis Mech* **7**, 1–10 (2010).

130. Monto, F. *et al.* Different expression of adrenoceptors and GRKs in the human myocardium depends on heart failure ethiology and correlates to clinical variables. *AJP Hear. Circ. Physiol.* **303**, H368–H376 (2012).

131. Jaber, M. *et al.* Essential role of ß-adrenergic receptor kinase 1 in cardiac development and function. *Proc. Natl. Acad. Sci.* **93**, 12974–12979 (1996).

132. Schlegel, P. *et al.* G protein-coupled receptor kinase 2 promotes cardiac hypertrophy. *PLoS One* **12**, 1–19 (2017).

133. Rockman, H. A. *et al.* Receptor-specific in vivo desensitization by the G protein-coupled receptor kinase-5 in transgenic mice. *Proc. Natl. Acad. Sci. U. S. A.* **93**, 9954–9959 (1996).

134. Harding, V. B., Jones, L. R., Lefkowitz, R. J., Koch, W. J. & Rockman, H. A. Cardiac βARK1 inhibition prolongs survival and augments blocker therapy in a mouse model of severe heart failure. *Proc.*

Natl. Acad. Sci. **98**, 5809–5814 (2001).

135. Sorriento, D., Ciccarelli, M., Cipolletta, E., Trimarco, B. & Iaccarino, G. "Freeze, Don't Move": How to Arrest a Suspect in Heart Failure – A Review on Available GRK2 Inhibitors. *Front. Cardiovasc. Med.* **3**, 48 (2016).

136. Koch, W. J. *et al.* Cardiac Function in Mice Overexpressing the β-Adrenergic Receptor Kinase or a βARK Inhibitor. *Science (80-.).* **268**, 1350–1354 (1995).

137. Schumacher, S. M. *et al.* A peptide of the RGS domain of GRK2 binds and inhibits Gαq to suppress pathological cardiac hypertrophy and dysfunction. *Sci. Signal.* **9**, (2016).

138. Schmid, E. *et al.* Cardiac RKIP induces a beneficial β-adrenoceptor-dependent positive inotropy. *Nat. Med.* **21**, 1298–1306 (2015).

139. Guccione, M. *et al.* G Protein-coupled Receptor Kinase 2 (GRK2) Inhibitors: Current Trends and Future Perspectives. *J. Med. Chem.* **2**, 9277–9294 (2016).

140. Aguero, J. *et al.* Myocardial G protein receptor-coupled kinase expression correlates with functional parameters and clinical severity in advanced heart failure. *J. Card. Fail.* **18**, 53–61 (2012).

141. Arnett, D. K. *et al.* Linkage of left ventricular contractility to chromosome 11 in humans: The hyperGEN study. *Hypertension* **38**, 767–772 (2001).

142. Peppel, K. *et al.* G protein-coupled receptor kinase 3 (GRK3) gene disruption leads to loss of odorant receptor desensitization. *J. Biol. Chem.* **272**, 25425–25428 (1997).

143. von Lueder, T. G. *et al.* Cardiomyocyte-restricted inhibition of G protein-coupled receptor kinase-3 attenuates cardiac dysfunction after chronic pressure overload. *AJP Hear. Circ. Physiol.* **303**, H66–H74 (2012).

144. Vinge, L. E. *et al.* Substrate specificities of g protein-coupled receptor kinase-2 and -3 at cardiac myocyte receptors provide basis for distinct roles in regulation of myocardial function. *Mol. Pharmacol.* **72**, 582–91 (2007).

145. Belmonte, S. L. & Blaxall, B. C. GRK5 : Exploring its hype in cardiac hypertrophy. *Circ Res* **111**, 957–958 (2012).

146. Gainetdinov, R. R. *et al.* Muscarinic supersensitivity and impaired receptor desensitization in G protein-coupled receptor kinase 5-deficient mice. *Neuron* **24**, 1029–1036 (1999).

147. Martini, J. S. *et al.* Uncovering G protein-coupled receptor kinase-5 as a histone deacetylase

kinase in the nucleus of cardiomyocytes. *Proc. Natl. Acad. Sci. U. S. A.* **105**, 12457–12462 (2008).

148. Gold, J. I. *et al.* Nuclear Translocation of Cardiac G Protein-Coupled Receptor Kinase 5 Downstream of Select Gq-Activating Hypertrophic Ligands Is a Calmodulin-Dependent Process. *PLoS One* **8**, (2013).

149. Karin, M., Cao, Y., Greten, F. R. & Li, Z.-W. NF-κB in cancer: from innocent bystander to major culprit. *Nat. Rev. Cancer* **2**, 301–310 (2002).

150. Jane Dyson, H. & Komives Elizabeth A. Role of disorder in IκB-NFκB interaction. *IUBMB Life* **64**, 499–505 (2013).

151. Hoesel, B. & Schmid, J. A. The complexity of NF-κB signaling in inflammation and cancer. *Mol. Cancer* **12**, 1 (2013).

152. Sorriento, D. *et al.* The G-protein-coupled receptor kinase 5 inhibits NFκB transcriptional activity by inducing nuclear accumulation of IκB. *Proc. Natl. Acad. Sci.* **105**, 17818–17823 (2008).

153. Higuchi, Y. *et al.* Involvement of Nuclear Factor-κB and Apoptosis Signal-Regulating Kinase 1 in G-Protein–Coupled Receptor Agonist–Induced Cardiomyocyte Hypertrophy. *Circulation* **105**, 509–515 (2002).

154. Sorriento, D. *et al.* Intracardiac injection of AdGRK5-NT reduces left ventricular hypertrophy by inhibiting NF-κB-Dependent hypertrophic gene expression. *Hypertension* **56**, 696–704 (2010).

155. Sorriento, D. *et al.* The Amino-Terminal Domain of GRK5 Inhibits Cardiac Hypertrophy through the Regulation of Calcium-Calmodulin Dependent Transcription Factors. *Int. J. Mol. Sci.* **19**, (2018).

156. Traynham, C. J. *et al.* Differential Role of G Protein-Coupled Receptor Kinase 5 in Physiological Versus Pathological Cardiac Hypertrophy. *Circ Res* **117**, 1001–1012 (2015).

157. Rajkumar, K., Nichita, A., Anoor, P. K., Raju, S. & Singh, S. S. Understanding perspectives of signalling mechanisms regulating PEBP1 function. *Cell Biochem Funct* (2016).

158. Granovsky, A. E. & Rosner, M. R. Raf kinase inhibitory protein: A signal transduction modulator and metastasis suppressor. *Cell Res.* **18**, 452–457 (2008).

159. Granovsky, A. E. *et al.* Raf Kinase Inhibitory Protein Function Is Regulated via a Flexible Pocket and Novel Phosphorylation-Dependent Mechanism. *Mol. Cell. Biol.* **29**, 1306–1320 (2009).

160. Al-Mulla, F., Bitar, M. S., Taqi, Z. & Yeung, K. C. RKIP: Much more than Raf Kinase inhibitory protein. *J. Cell. Physiol.* **228**, 1688–1702 (2013).

161. Lorenz, K., Rosner, M. R., Brand, T. & Schmitt, J. P. Raf kinase inhibitor protein: lessons of a better way for β-adrenergic receptor activation in the heart. *J. Physiol.* **595**, 4073–4087 (2017).

162. Jing, S.-H., Gao, X., Yu, B. & Qiao, H. Raf Kinase Inhibitor Protein (RKIP) Inhibits Tumor Necrosis Factor-α (TNF-α) Induced Adhesion Molecules Expression in Vascular Smooth Muscle Bells by Suppressing (Nuclear Transcription Factor-κB (NF-kappaB) Pathway. *Med. Sci. Monit.* **23**, 4789–4797 (2017).

163. Woodgett, J. R. Judging a Protein by More Than Its Name: GSK-3. *Sci. Signal.* **2001**, re12 (2003).

164. Maqbool, M. & Hoda, N. GSK3 Inhibitors in the Therapeutic Development of Diabetes, Cancer and Neurodegeneration: Past, Present and Future. *Curr. Pharm. Des.* **23**, 4332–4350 (2017).

165. Al-Mulla, F. *et al.* Raf kinase inhibitor protein RKIP enhances signaling by glycogen synthase kinase-3β. *Cancer Res.* **71**, 1334–1343 (2011).

166. Pearson, G. *et al.* Mitogen-Activated Protein (MAP) Kinase Pathways: Regulation and Physiological Functions 1. *Endocr. Rev.* **22**, 153–183 (2001).

167. Ferrell, J. E. MAP Kinases in Mitogenesis and Development. *Curr. Top. Dev. Biol.* **33**, 1–60 (1996).

168. Zeng, L., Imamoto, A. & Rosner, M. R. Raf kinase inhibitory protein (RKIP): a physiological regulator and future therapeutic target. *Expert Opin. Ther. Targets* **12**, 1275–1287 (2008).

169. Downward, J. Targeting RAS signalling pathways in cancer therapy. *Nat. Rev. Cancer* **3**, 11–22 (2003).

170. Yeung, K. *et al.* Suppression of Raf-1 kinase activity and MAP kinase signalling by RKIP. *Nature* **401**, 173–177 (1999).

171. Yeung, K. *et al.* Mechanism of Suppression of the Raf/MEK/Extracellular Signal-Regulated Kinase Pathway by the Raf Kinase Inhibitor Protein. *Mol. Cell. Biol.* **20**, 3079–3085 (2000).

172. Deiss, K., Kisker, C., Lohse, M. J. & Lorenz, K. Raf kinase inhibitor protein (RKIP) dimer formation controls its target switch from Raf1 to G protein-coupled receptor kinase (GRK) 2. *J. Biol. Chem.* **287**, 23407–23417 (2012).

173. Madamanchi, A. Beta-adrenergic receptor signaling in cardiac function and heart failure. *MJM* **10**, 99–104 (2007).

174. Wachter, S. B. & Gilbert, E. M. Beta-adrenergic receptors, from their discovery and characterization through their manipulation to beneficial clinical application. *Cardiology* **122**, 104–112 (2012).

175. Zheng, M., Zhu, W., Han, Q. & Xiao, R. P. Emerging concepts and therapeutic implications of β-adrenergic receptor subtype signaling. *Pharmacol. Ther.* **108**, 257–268 (2005).

176. Feldman, D. S., Carnes, C. a, Abraham, W. T. & Bristow, M. R. Mechanisms of disease: beta-adrenergic receptors--alterations in signal transduction and pharmacogenomics in heart failure. *Nat. Clin. Pract. Cardiovasc. Med.* **2**, 475–483 (2005).

177. Agüero, J. *et al.* Correlation Between Beta-Adrenoceptors and G-Protein-Coupled Receptor Kinases in Pretransplantation Heart Failure. *Transplant. Proc.* **40**, 3014–3016 (2008).

178. Wallukat, G. The β-adrenergic receptors. *Herz* **27**, 683–690 (2002).

179. Huang, Z. M., Gao, E., Chuprun, J. K. & Koch, W. J. GRK2 in the Heart: A GPCR Kinase and Beyond. *Antioxid. Redox Signal.* **21**, 2032–2043 (2014).

180. Nobles, K. N. *et al.* Distinct Phosphorylation Sites on the β2 -Adrenergic Receptor Establish a Barcode That Encodes Differential Functions of β- Arrestin. *Sci Signal* **4**, (2011).

181. Fan, X. *et al.* Cardiac β2-Adrenergic receptor phosphorylation at Ser355/356 Regulates receptor internalization and functional resensitization. *PLoS One* **11**, 1–15 (2016).

182. Kamal, F. A., Travers, J. G. & Blaxall, B. C. G Protein-Coupled Receptor Kinases in Cardiovascular Disease: Why 'Where' Matters. *Trends Cardiovasc. Med.* **22**, 213–219 (2012).

183. Azevedo, P. S., Polegato, B. F., Minicucci, M. F., Paiva, S. A. R. & Zornoff, L. A. M. Cardiac Remodeling: Concepts, Clinical Impact, Pathophysiological Mechanisms and Pharmacologic Treatment. *Arq. Bras. Cardiol.* 62–69 (2016). doi:10.5935/abc.20160005

184. Bristow, M. R. Beta-Adrenergic Receptor Blockade in Chronic Heart Failure. *Circulation* **101**, 558–69 (2000).

185. Yesilkanal, A. E. & Rosner, M. R. Targeting raf kinase inhibitory protein regulation and function. *Cancers (Basel).* **10**, (2018).

186. Zaravinos, A., Bonavida, B., Chatzaki, E. & Baritaki, S. RKIP: A Key Regulator in Tumor Metastasis Initiation and Resistance to Apoptosis: Therapeutic Targeting and Impact. *Cancers (Basel).* **10**, 287 (2018).

187. Mattson, M. P. Pathways Towards and Away from Alzheimer's Disease. *Nature* **430**, 631–639 (2004).

188. Klysik, J., Theroux, S. J., Sedivy, J. M., Moffit, J. S. & Boekelheide, K. Signaling Crossroads: The function of Raf Kinase Inhibitory Protein in Cancer, the Central Nervous System and

Reproduction. *Cell Signal* **20**, 1–9 (2009).

189. Tohdoh, N., Tojo, S., Agui, H. & Ojika, K. Sequence homology of rat and human HCNP precursor proteins, bovine phosphatidylethanolamine-binding protein and rat 23-kDa protein associated with the opioid-binding protein. *Mol. Brain Res.* **30**, 381–384 (1995).

190. K., O., S., M., T., K., N., K. & M., T. Two different molecules, NGF and free-HCNP, stimulate cholinergic activity in septal nuclei in vitro in a different manner. *Dev. Brain Res.* **79**, 1–9 (1994).

191. Ojika, K. *et al.* Hippocampal cholinergic neurostimulating peptides (HCNP). *Prog. Neurobiol.* **60**, 37–83 (2000).

192. Maki, M. *et al.* Decreased expression of hippocampal cholinergic neurostimulating peptide precursor protein mRNA in the hippocampus in Alzheimer disease. *J. Neuropathol. Exp. Neurol.* **61**, 176–185 (2002).

193. Keller, E. T., Fu, Z. & Brennan, M. The role of Raf kinase inhibitor protein (RKIP) in health and disease. *Biochem. Pharmacol.* **68**, 1049–1053 (2004).

194. Palczewski, K., Buczylko, J., Lebioda, L., Crabb, J. W. & Polans, A. S. Identification of the N-terminal region in rhodopsin kinase involved in its interaction with rhodopsin. *J. Biol. Chem.* **268**, 6004–6013 (1993).

195. Saiki, R. *et al.* Primer-directed enzymatic amplification of DNA with a thermostable DNA polymerase. *Science (80-.).* **239**, 487–491 (1988).

196. life technologies. Gateway ® Technology A universal technology to clone DNA sequences for functional analysis and expression in multiple systems. *Invitrogen* **70**, 1–60 (2003).

197. M.Solioz & D. Bienz. Bacterial genetics by electric shock. *Trends Biochem Sci* **15**, 175–177 (1990).

198. Hanahan, D. Studies on transformation of Escherichia coli with plasmids. *J. Mol. Biol.* **166**, 557–580 (1983).

199. Desjardins, P. R. & Conklin, D. S. Microvolume quantitation of nucleic acids. *Curr. Protoc. Mol. Biol.* 1–5 (2011). doi:10.1002/0471142727.mba03js93

200. Wold, W. S. M. & Gooding, L. R. Region E3 of adenovirus: A cassette of genes involved in host immunosurveillance and virus-cell interactions. *Virology* **184**, 1–8 (1991).

201. Strober, W. Trypan Blue Exclusion Test of Cell Viability. *Curr. Protoc. Immunol.* **111**, 1–3 (2015).

202. Kielberg, V. Cryopreservation of Mammalian Cells – Protocols. *Thermo Sci. Tech Note No. 14* 1–2 (2010). doi:10.1016/j.joms.2017.02.020

203. Mazia, D., Schatten, G. & Sale, W. Adhesion of cells to surfaces coated with polylysine: Applications to electron microscopy. *J. Cell Biol.* **66**, 198–200 (1975).

204. Haas, R., Banerji, S. S. & Culp, L. A. Adhesion site composition of murine fibroblasts cultured on gelatin-coated substrata. *J. Cell. Physiol.* **120**, 117–125 (1984).

205. Bradford, M. M. A rapid and sensitive method for the quantitation of microgram quantities of protein utilizing the principle of protein-dye binding. *Anal. Biochem.* **72**, 248–254 (1976).

206. Laemmli, U. K. Cleavage of structural proteins during the assembly of the head of bacteriophage T4. *Nature* **227**, 680–685 (1970).

207. de St.Groth, S. ., Webster, R. G. & Datyner, A. Two new staining procedures for quantitative estimation of proteins on electrophoretic strips. *Biochim. Biophys. Acta* **71**, 377–391 (1963).

208. Towbin, H., Staehelin, T. & Gordon, J. Electrophoretic transfer of proteins from polyacrylamide gels to nitrocellulose sheets: procedure and some applications. *Proc. Natl. Acad. Sci.* **76**, 4350–4354 (1979).

209. Burnette, W. N. Western Blotting: Electrophoretic Transfer of Proteins from Sodium Dodecyl Sulfate-Polyacrylamide Gels to Unmodified Nitrocellulose and Radiographic Detection with Antibody and Radioiodinated Protein A. *Anal. Biochem.* **112**, 195–203 (1981).

210. Ogata, K., Arakawa, M., Kasahara, T., Shioiri-Nakano, K. & Hiraoka, K. ichi. Detection of toxoplasma membrane antigens transferred from SDS-polyacrylamide gel to nitrocellulose with monoclonal antibody and avidin-biotin, peroxidase anti-peroxidase and immunoperoxidase methods. *J. Immunol. Methods* **65**, 75–82 (1983).

211. Legocki, R. P. & Verma, D. P. S. Multiple immunoreplica technique: Screening for specific proteins with a series of different antibodies using one polyacrylamide gel. *Anal. Biochem.* **111**, 385–392 (1981).

212. Firestone, G. L. & Winguth, S. D. Immunoprecipitation of proteins. *Immunol. Proced.* **182**, 688–700 (1990).

213. Louche, A., Salcedo, S. P. & Bigot, S. Protein–Protein Interactions: Pull-Down Assays. *Bact. Protein Secret. Syst. Methods Protoc. Methods Mol. Biol.* **1615**, 257–275 (2017).

214. Rosenberg, A. H. *et al.* Vectors for selective expression of cloned DNAs by T7 RNA polymerase. *Gene* **56**, 125–135 (1987).

215. Studier, F. W. & Moffatt, B. A. Use of Bacteriophage T7 RNA Polymerase to Direct Selective High-level Expression of Cloned Genes. *J. Mol. Biol.* **189**, 113–130 (1986).

216. Studier, F. W. & Moffatt, B. A. Use of T7 RNA Polymerase to Direct Expression of Cloned Genes. *Methods Enzymol.* **185**, 60–89 (1990).

217. Dubendorff, J. W. & Studier, F. W. Creation of a T7 autogene. Cloning and expression of the gene for bacteriophage T7 RNA polymerase under control of its cognate promoter. *J. Mol. Biol.* **219**, 61–68 (1991).

218. Smith, D. B. & Johnson, K. S. Single-step purification of polypeptides expressed in Escherichia coli as fusions with glutathione S-transferase. *Gene* **67**, 31–40 (1988).

219. Rebay, I. & Fehon, R. G. Preparation of soluble GST fusion proteins. *Cold Spring Harb. Protoc.* **4**, (2009).

220. Lohse, M. J., Benovic, J. L., Codina, J., Caron, M. G. & Lefkowitz, R. J. beta-Arrestin: a protein that regulates beta-adrenergic receptor function. *Science (80-.).* 1574–1550 (1990).

221. Werner, M., Chott, A., Fabiano, A. & Battifora, H. Effect of formalin tissue fixation and processing on immunohistochemistry. *Am. J. Surg. Pathol.* **24**, 1016–1019 (2000).

222. Mason, J. T. & O'Leary, T. J. Effects of Formaldehyde Structure: A Calorimetric Investigation'. *J. Histochem. Soc.* **39**, 225–229 (1991).

223. Cooper, J. A. Effects of Cytochalasin and Phalloidin on Actin. *J. Cell Biol.* **105**, 1473–1478 (1987).

224. Jamur, M. C. & Oliver, C. Permeabilization of Cell Membranes. *Methods Mol. Biol.* **588**, 63–66 (2010).

225. Atale, N., Gupta, S., Yadav, U. C. S. & Rani, V. Cell-death assessment by fluorescent and nonfluorescent cytosolic and nuclear staining techniques. *J. Microsc.* **255**, 7–19 (2014).

226. Dunigan, C. D., Curran, P. K. & Fishman, P. H. Detection of beta-adrenergic receptors by radioligand binding. *Methods Mol. Biol.* **126**, 329–43 (2000).

227. Baker, J. G., Hall, I. P. & Hill, S. J. Pharmacological characterization of CGP 12177 at the human β2-adrenoceptor. *Br. J. Pharmacol.* **137**, 400–408 (2002).

228. Doerr, L. *et al.* New Easy-to-Use Hybrid System for Extracellular Potential and Impedance Recordings. *J. Lab. Autom.* **20**, 175–188 (2015).

229. Obergrussberger, A. *et al.* Safety pharmacology studies using EFP and impedance. *J. Pharmacol. Toxicol. Methods* **81**, 223–232 (2016).

230. Upadhyay, P. & Bhaskar, S. Real time monitoring of lymphocyte proliferation by an impedance method. *J. Immunol. Methods* **244**, 133–137 (2000).

231. Katamay, R. & Nussenblatt, R. B. Blood-Retinal Barrier, Immune Privilege, and Autoimmunity. *Retin. Fifth Ed.* **1**, 579–589 (2012).

232. Bauer, P. H. *et al.* Phosducin is a PKA-regulated G-protein regulator. *Nature* **358**, 73–76 (1992).

233. Bernardo, B. C., Weeks, K. L., Pretorius, L. & McMullen, J. R. Molecular distinction between physiological and pathological cardiac hypertrophy: Experimental findings and therapeutic strategies. *Pharmacol. Ther.* **128**, 191–227 (2010).

234. Louch, W. E., Sheehan, K. A. & Wolska, B. M. Methods in Cardiomyocyte Isolation, Culture, and Gene Transfer. *J Mol Cell Cardiol.* **51**, 288–298 (2011).

235. Woodcock, E. A. & Matkovich, S. J. Cardiomyocytes structure, function and associated pathologies. *Int. J. Biochem. Cell Biol.* **37**, 1746–1751 (2005).

236. Ehler, E., Moore-Morris, T. & Lange, S. Isolation and Culture of Neonatal Mouse Cardiomyocytes. *J. Vis. Exp.* 1–10 (2013). doi:10.3791/50154

237. Rengo, G. *et al.* Targeting the β-adrenergic receptor system through g-protein-coupled receptor kinase 2: A new paradigm for therapy and prognostic evaluation in heart failure from bench to bedside. *Circ. Hear. Fail.* **5**, 385–391 (2012).

238. de Lucia, C., Eguchi, A. & Koch, W. J. New insights in cardiac β-Adrenergic signaling during heart failure and aging. *Front. Pharmacol.* **9**, 1–14 (2018).

239. Vinge, L. E., Raake, P. W. & Koch, W. J. Gene Therapy in Heart Failure. *Circ Res* **102**, 1458–1470 (2008).

240. Stanley, W. W. C., Recchia, F. a & Lopaschuk, G. D. Myocardial Substrate Metabolism in the Normal and Failing Heart. *Physiol. …* **85**, 1093–1129 (2005).

241. Voors, A. A. *et al.* ESC Guidelines for the diagnosis and treatment of acute and chronic heart failure 2012: The Task Force for the Diagnosis and Treatment of Acute and Chronic Heart Failure 2012 of the European Society of Cardiology. Developed in collaboration with the Heart. *Eur. Heart J.* **33**, 1787–1847 (2012).

242. Lymperopoulos, A. *et al.* Reduction of sympathetic activity via adrenal-targeted GRK2 gene deletion attenuates heart failure progression and improves cardiac function after myocardial infarction. *J. Biol. Chem.* **285**, 16378–16386 (2010).

243. Raake, P. W. *et al.* G Protein-Coupled Receptor Kinase 2 Ablation in Cardiac Myocytes Before or After Myocardial Infarction Prevents Heart Failure. *Circ Res* **103**, 413–422 (2008).

244. Hansen, J. L., Theilade, J., Aplin, M. & Sheikh, S. P. Role of G-Protein-Coupled Receptor Kinase 2 in the Heart-Do Regulatory Mechanisms Open Novel Therapeutic Perspectives? *Trends Cardiovasc. Med.* **16**, 169–177 (2006).

245. Cannavo, A., Liccardo, D. & Koch, W. J. Targeting cardiac b-adrenergic signaling via GRK2 inhibition for heart failure therapy. *Front. Physiol.* **4**, 1–7 (2013).

246. Woodall, M. C., Ciccarelli, M., Woodall, B. P. & Koch, W. J. G Protein–Coupled Receptor Kinase 2 A Link Between Myocardial Contractile Function and Cardiac Metabolism. *Circ. Res.* **114**, 1661–1670 (2014).

247. Alessandro Cannavo, Klara Komici, Leonardo Bencivenga, Maria Loreta D'amico, Giuseppina Gambino, Daniela Liccardo, N. F. & G. R. GRK2 as a therapeutic target for heart failure. *Expert Opin. Ther. Targets* **22**, 75–83 (2018).

248. Thal, D. M. *et al.* Paroxetine Is a Direct Inhibitor of G Protein-Coupled Receptor Kinase 2 and Increases Myocardial Contractility. *ACS Chem. Biol.* **7**, 1830–1839 (2012).

249. Schumacher, S. M. *et al.* Paroxetine-mediated GRK2 inhibition reverses cardiac dysfunction and remodeling after myocardial infarction. *Sci. Transl. Med.* **7**, ra31 (2015).

250. Guo, S., Carter, R. L., Grisanti, L. A., Koch, W. J. & Tilley, D. G. Impact of paroxetine on proximal β -adrenergic receptor signaling. *Cell. Signal.* **38**, 127–133 (2017).

251. Rockman, H. A. *et al.* Expression of a beta-adrenergic receptor kinase 1 inhibitor prevents the development of myocardial failure in gene-targeted mice. *Proc. Natl. Acad. Sci. U. S. A.* **95**, 7000–5 (1998).

252. Salazar, N. C. *et al.* GRK2 blockade with βARKct is essential for cardiac β2-adrenergic receptor signaling towards increased contractility. *Cell Commun. Signal.* **11**, 64 (2013).

253. Benovic, J. L., Stone, W. C., Caron, M. G. & Lefkowitz, R. J. Inhibition of the β-Adrenergic Receptor Kinase by Polyanions. *J Biol Chem* **264**, 6707–6710 (1989).

254. Hathaway, G. M., Lubben, T. H. & Traugh, J. A. Inhibition of casein kinase II by heparin. *J. Biol. Chem.* **255**, 8038–8041 (1980).

255. Homan, K. T. & Tesmer, J. J. G. Molecular Basis for Small Molecule Inhibition of G Protein-Coupled Receptor Kinases. *ACS Chem. Biol.* **10**, 246–256 (2015).

256. Waldschmidt, H. V. *et al.* Structure-Based Design, Synthesis, and Biological Evaluation of Highly Selective and Potent G Protein-Coupled Receptor Kinase 2 Inhibitors. *J. Med. Chem.* **59**, 3793–3807 (2016).

257. Mayer, G. *et al.* An RNA molecule that specifically inhibits G-protein-coupled receptor kinase 2 in vitro. *RNA* **14**, 524–534 (2008).

258. Tesmer, V., Lennarz, S., Mayer, G. & Tesmer, J. J. G. Molecular mechanism for inhibition of G protein-coupled receptor kinase 2 by a selective RNA aptamer. *Structure* **20**, 1300–1309 (2012).

259. Raake, P. W. J. *et al.* AAV6.βARKct cardiac gene therapy ameliorates cardiac function and normalizes the catecholaminergic axis in a clinically relevant large animal heart failure model. *Eur. Heart J.* **34**, 1437–1447 (2013).

260. Völkers, M. *et al.* The inotropic peptide βARKct improves βAR responsiveness in normal and failing cardiomyocytes through Gßγ -mediated L-type calcium current disinhibition. *Circ Res* **108**, 27–39 (2011).

261. Schmid, E. *et al.* Supplements.Cardiac RKIP induces a beneficial β-adrenoceptor-dependent positive inotropy. *Nat. Med.* **21**, 1298–1306 (2015).

262. Wilkins, E. *et al.* European Cardiovascular Disease Statistics. *Eur. Hear. Network, Brussels* 192 (2017). doi:978-2-9537898-1-2

263. Violin, J. D., Ren, X. R. & Lefkowitz, R. J. G-protein-coupled receptor kinase specificity for b-arrestin recruitment to the b2-adrenergic receptor revealed by fluorescence resonance energy transfer. *J. Biol. Chem.* **281**, 20577–20588 (2006).

264. Drake, M. T., Shenoy, S. K. & Lefkowitz, R. J. Trafficking of G protein-coupled receptors. *Circ. Res.* **99**, 570–582 (2006).

265. Keys, J. R. *et al.* Cardiac hypertrophy and altered β -adrenergic signaling in transgenic mice that express the amino terminus of β -ARK1. *Am J Physiol Hear. Circ Physiol* **285**, 2201–2211 (2003).

266. Benovic, J. *et al.* Synthetic peptides of the hamster beta 2-adrenoceptor as substrates and inhibitors of the beta-adrenoceptor kinase. *Br. J. Clin. Pharmacol.* **30**, 3S-12S (1990).

267. Beautrait, A. *et al.* Mapping the putative G protein-coupled receptor (GPCR) docking site on GPCR kinase 2: Insights from intact cell phosphorylation and recruitment assays. *J. Biol. Chem.* **289**, 25262–25275 (2014).

268. Eckhart, A. D. *et al.* Hybrid transgenic mice reveal in vivo specificity of G protein-coupled receptor kinases in the heart. *Circ. Res.* **86**, 43–50 (2000).

269. Kato, A., Reisert, J., Ihara, S., Yoshikawa, K. & Touhara, K. Evaluation of the role of G protein-coupled receptor kinase 3 in desensitization of mouse odorant receptors in a mammalian cell line and in olfactory sensory neurons. *Chem. Senses* **39**, 771–780 (2014).

270. Premont, R. T., Koch, W. J., Inglese, J. & Lefkowitz, R. J. Identification, purification, and characterization of GRK5, a member of the family of G protein-coupled receptor kinases. *J. Biol. Chem.* **269**, 6832–6841 (1994).

271. Tran, T. M., Jorgensen, R. & Clark, R. B. Phosphorylation of the β2-adrenergic receptor in plasma membranes by intrinsic GRK5. *Biochemistry* **46**, 14438–14449 (2007).

272. Wayne, C. H. W., Mihlbachler, K. a., Bleecker, E. R., Weiss, S. T. & Liggett, S. B. A Polymorphism of GRK5 Alters Agonist-Promoted Desensitization of β2-Adrenergic Receptors. *Pharmacogenes Genomics* **18**, 729–732 (2009).

273. D'Angelo, D. D. *et al.* Transgenic Gαq overexpression induces cardiac contractile failure. *Proc. Natl. Acad. Sci.* **94**, 8121–8126 (1997).

274. Adams, J. W. *et al.* Enhanced Gαq signaling: A common pathway mediates cardiac hypertrophy and apoptotic heart failure. *Proc. Natl. Acad. Sci. U. S. A.* **95**, 10140–5 (1998).

275. Wiesen, K. *et al.* Cardiac remodeling in Gαq and Gα11 knockout mice. *Int. J. Cardiol.* **202**, 836–845 (2016).

276. Usui, H. *et al.* RGS domain in the amino-terminus of G protein-coupled receptor kinase 2 inhibits Gq-mediated signaling. *Int. J. Mol. Med.* **5**, 335–340 (2000).

277. Bristow, M. R., Hershberger R E, Minobe, W. & Rasmussen, R. Beta 1- and beta 2-adrenergic receptor-mediated adenylate cyclase stimulation in nonfailing and failing human ventricular myocardium. *Mol. Pharmacol.* **35**, 295–303 (1989).

278. Landzberg, J. S., Parker, J. D., Gauthier, D. F. & Colucci, W. S. Effects of myocardial α1-adrenergic receptor stimulation and blockade on contractility in humans. *Circulation* **84**, 1608–1614 (1991).

279. Lohse, M. J., Engelhardt, S. & Eschenhagen, T. What Is the Role of β-Adrenergic Signaling in Heart Failure? *Circ. Res.* **93**, 896–906 (2003).

280. Ahmet, I. *et al.* Cardioprotective and Survival Benefits of Long-Term Combined Therapy with β2 Adrenoreceptor (AR) Agonist and β1 AR Blocker in Dilated Cardiomyopathy Postmyocardial Infarction. *J. Pharmacol. Exp. Ther.* **325**, 491–499 (2008).

281. O'Connell, T. D., Jensen, B. C., Baker, A. J. & Simpson, P. C. Cardiac Alpha1-Adrenergic Receptors: Novel Aspects of Expression, Signaling Mechanisms, Physiologic Function, and Clinical Importance. *Pharmacol. Rev.* **66**, 308–333 (2013).

282. Abassi, Y. A. *et al.* Dynamic monitoring of beating periodicity of stem cell-derived

cardiomyocytes as a predictive tool for preclinical safety assessment. *Br. J. Pharmacol.* **165**, 1424–1441 (2012).

283. Invitrogen. pAd/CMV/V5-DEST ™ and pAd/PL-DEST ™ Gateway ® Vectors. *life Technol.* (2012).

Publications

Journal articles

Maimari, T., Krasel, C., Bünemann, M., Lorenz, K. *The N-termini of GRK2 and GRK3 simulate the stimulating effects of RKIP on β-adrenoceptors.* Biochem Biophys Res Commun. 2019 Oct 8 pii: S0006-291X(19)31873-X. doi: 10.1016/j.bbrc.2019.09.135. [Epub ahead of print]

Faustmann G, Tiran B, **Maimari T**, Kieslinger P, Obermayer-Pietsch B, Gruber HJ, Roob JM, Winklhofer-Roob BM. *Circulating leptin and NF-κB activation in peripheral blood mononuclear cells across the menstrual cycle.* Biofactors. 8;42(4):376-87 (2016).

Abstracts for conferences:

Maimari, T., Krasel, C., Bünemann, M., Lorenz, K. *Analysis of Raf kinase inhibitor protein (RKIP) binding to different isoforms of G protein receptor kinases (GRK).* 22nd Joint Meeting "Signal Transduction – Receptors, Mediators and Genes". Weimar, Germany 05.11.2018-07.11.2018 (Poster)

Maimari, T., Krasel, C., Bünemann, M., Lorenz, K. *Investigation of the Raf kinase inhibitor protein (RKIP) and G protein coupled receptor kinases (GRK) interaction interface*. EUREKA! 2018. Würzburg, Germany 10.10.2018-11.10.2018 (Poster)

Maimari, T., Krasel, C., Bünemann, M., Lorenz, K. *Characterization of the interaction of RKIP with GRK.* 3rd German Pharm-Tox Summit: 84th Annual Meeting of the German Society for Experimental and Clinical Pharmacology and Toxicology and 20th Annual Meeting of clinical Pharmacology with contribution of AGAH. Göttingen, Germany 26.02.18-01.03.18 (Poster)

Acknowledgements

During this dissertation I have received a lot of support and assistance.

I would first like to express my gratitude to my supervisor, Prof. Dr. Lorenz, for all of the opportunities I was given to conduct my research and whose expertise and guidance were invaluable throughout my time as a PhD student.

Furthermore, I would like to thank my co-supervisors Prof. Dr. Schlosser and Prof. Dr. Kisker for being in my thesis committee and for providing interesting feedback and insightful comments during our annual meetings.

My sincere thanks also go to Prof. Dr. Krasel from the University of Marburg for his scientific advice and knowledge in this research field.

I would like to acknowledge my colleagues from the Institute of Pharmacology and Toxicology in Würzburg and from ISAS in Dortmund for their wonderful collaboration and excellent technical assistance especially Martina Fischer from Würzburg and Edeltraut Hoffmann-Posorske and Ann-Katrin Weiss from Dortmund. You supported me greatly and were always willing to help me. My appreciation goes to Dr. El Magraoui for his meticulous comments and optimism. I also want to thank Julia Fender, whom I supervised and who was an immense help during the last stages of my thesis.

In addition, I would like to thank my parents and sister for their wise counsel and sympathetic ear, and my husband for supporting me in his own special way. Finally, there are my friends and the rest of my family, who provided cheerful distraction and encouragement to rest my mind outside of my research.